Investigating Critical Parameters of Dissolved Air Flotation for Solid-Liquid Separation with Different Influents

Master's Thesis

Tavishi Guleria

TU Delft

LOTUS HR

Investigating Critical Parameters of Dissolved Air Flotation for Solid-Liquid Separation with Different Influents

Master's Thesis

submitted in partial fulfillment of the requirements for the degree of

MASTER OF SCIENCE

in

CIVIL ENGINEERING

at the Delft University of Technology
Faculty of Civil Engineering and Geosciences

By

Tavishi Guleria

Student id: 4743202
Email: tavishiguleria93@gmail.com

Thesis duration: February, 2019 – October, 2019

Thesis Committee:

Dr. Ir. Ralph Lindeboom (Chair)	(TU Delft)
Prof. Dr. Ir. Merle de Kreuk	(TU Delft)
Dr. Luis Portela	(TU Delft)

TU Delft

LOTUS HR
Local Treatment of Urban Sewage and Streams for Healthy Reuse

Preface

This report culminates an exhilarating 2 years of my master's education in Environmental Engineering at TU Delft. Looking back now, it has been one of the most challenging and enriching experiences of my life. For the last 9 months, I have been immersed in laboratory and field research on Dissolved Air Flotation (DAF) as part of the LOTUS^{HR} project, resulting in this report. Due to the collaborative nature of the project, from the beginning it had many experimental and logistical challenges. Many days were a struggle, but all in all, I look back at the whole process really fondly. I am deeply grateful to everyone who has helped and guided me during this period both professionally and personally. Appendix M shows some photographic glimpses of my experience throughout this project.

Firstly, I would like to thank my thesis committee - Ralph Lindeboom, Merle de Kreuk and Luis Portela for giving me this unique opportunity to pursue my master's thesis within the LOTUS project. As New Delhi is my hometown, I have grown up around these drains and like many other residents of the city, have always wished to find solutions to clean them up. I am truly grateful for this opportunity. Thank you Ralph for you unconditional encouragement, creativity and kindness throughout the entire project. I really enjoyed our discussions, learnt a lot from you and sincerely thank you for making me a better researcher. Professor Merle, thank you for your support and invaluable feedback during this project, and for everything you have done for us throughout the course of the master. I consider myself very lucky to have had the opportunity to learn from you. Thank you Professor Portela for your critical feedback and suggestion throughout the course of this thesis. Our meetings really helped me look at the research from a different perspective and encouraged me to take the thesis work up a notch.

A big thank you to my project PhD supervisor - Antonella Piaggio. This whole project would not have been possible without you. Even though our time together was short, I had an amazing time working with you and have learnt so much from you. Thank you for guiding me with the DAF set up, lab work and report writing, and for your support and understanding during the tough times. A special thank to Laís Américo Soares for her time and patience in helping me with designing the experiments and lab work. I can not thank you enough for all your guidance and warmth. There was a time when I was really struggling with parts of this project and your support got me through it. A big thank you to Bruno Bicudo Perez for his technical guidance and support which helped me conduct all the pathogen experiments in Delhi. I really enjoyed working with you and it would not have been possible to get this data without your support. Thank you Steef de Valk for helping out with the DAF set up. Your energy is contagious and our nice LOTUS project discussions always made me feel positive about the research. I would also like to thank Sarthak Chaturvedi for helping me with the DAF sludge experiments. Thank you for your enthusiasm and I really appreciate the hard work you put in. Thank you Armand Middeldorp for all the support in the Water Lab especially with the packing and logistics of the DAF set up. One of the most nerve-racking parts of the project for me was shipping the DAF set-up from Delft to India and you made it so easy and enjoyable. Thanks a lot for all your help.

A big chunk of the experiments for this thesis were performed at the LOTUS site laboratory and The Energy and Resources Institute (TERI) at New Delhi. I am very grateful for the help and guidance I received by everyone working at the site and at TERI. I would like to express my sincere

gratitude to Professor Malini Balakrishnan and her team at TERI for their amazing support during my time in Delhi. Thank you Professor Malini for your time and feedback during the experimental work in Delhi. I have learnt a lot about field projects from you and I really enjoyed all our discussions. Thank you everyone at TERI - Aditi Ma'am, Ravi ji, Sushila ji, Sachin, Nimisha Ma'am, Praksh ji and Professor Vidya for all the support and good times. One of the most challenging and exciting parts of this project was setting up and conducting site experiments literally next to the Barapullah drain. I would like to thank everyone at the site - Mr. Rawat, Mr. Lalchand and the site guards for their help in tackling the numerous problems faced during site experiments. Working at the smelly drain in Delhi's extreme weather conditions is not easy, so thank you for all your hard work and for your support during my time there. A special thank you to Dr. Arti Kapil and her team, especially Ms. Neelam for their support with the pathogen experiments in Delhi. Thank you for your time and I really enjoyed our stimulating discussions.

A lot of this thesis would not have been possible without the support of my family and friends. A huge thank you to my fellow amazing environmental engineers from whom I've learnt a lot and have shared such wonderful memories. Thanks to the GVR committee - Kelly, Fabian and Fabian, and everyone on the trip to Peru last year. I loved every minute of planning and going on the trip with you guys. Kelly and Judith, you guys are so special to me. Thank you for your friendship and always being there for me. Looking forward to holidays in India, Taiwan and USA in the future. Manoj Uncle, Kavita Aunty, Mehek and Vasu, thank you for being such wonderful local guardians so far away from home. My Indian family here - Dhruv, Kanav, Sanjeev, Arka, Sumi, Gouri, Nirmal, Rahul, Bhati, Vaidehi and Vysali and Sasha, thank you for deciding to do a master's here at the same time. Life in TU Delft would not be the same without you. At the beginning of the master, I had quite a tough time because of my ankle injury. If it wasn't for you guys I would not have been able to finish my thesis on time. I am truly very grateful for all that you guys have done for me. Dhruv, it's pretty impossible to imagine the last 2 years without you. Thank you for making this journey so special and for always being so patient and encouraging during the thesis time. Thank you Vartika Ma'am and Ashu for taking out the time to review the report and for teaching me so many things about research and writing. Lastly, to my family - thank you for your unconditional love and support, and for helping me during the site work in Delhi as well. Dadu, thank you for all you do for us. You will always be my biggest inspiration. Mom, Dad and Karan, well, we all know I might need a pep talk once in a while. Thank you for being my biggest teachers and supporters throughout the ups and downs.

Working at the TU Delft lab and Barapullah site were 2 very different and unique experiences. While the time I spent in the TU Delft lab was intellectually stimulation, the site experience was extremely challenging, eye-opening and motivating. A lot of work still needs to be done to solve Delhi's wastewater woes, but working with the LOTUS project showed me that it is possible to find innovative solutions to such complex problems. I envision this project as a world class treatment plant and truly wish this project breaks the glass ceiling.

Tavishi Guleria
Delft
October 24, 2019

Abstract

Many rapidly expanding cities around the world including India's capital New Delhi face increasing potable water quality and health risks due contaminated open drains carrying the cities untreated wastewater into the adjoining river, which is also the city's water source. To tackle this problem in a practical and holistic way, innovative wastewater treatment solutions are needed. This is the goal of LOTUS^{HR} project - to research and build a holistic and resource oriented wastewater treatment plant (wwtp) to treat the Barapullah drain water in New Delhi, India. To achieve this goal, Dissolved air Flotation (DAF), due to its ability to withstand fluctuating flows and low area requirements was identified as a possible technology in the LOTUS wwtp scheme. This research is focused on identifying and investigating critical operating parameters of a bench scale DAF column set up with various influents for a comparative and deeper understanding. To achieve this, different influent at the site - Barapullah drain water and anaerobic sludge from a Delhi wwtp, and their counterparts in the laboratory - canal water and anaerobic sludge from a Delft wwtp were tested with the DAF. As there were potentially many critical factors which could have an impact on the DAF performance, experiments were conducted based on the Plackett-Burman experimental design. Furthermore, to understand the effect of particle characteristics and morphology on the DAF performance, microscopic images of the influent and clean effluent samples were analysed using ImageJ-Fiji. Finally, Particle Image Velocitimetry (PIV) analysis was done to gain insight into the characteristics and behaviour of the particle-bubble agglomerate and its relation to the DAF performance. Additionally, pathogen (*E-coli* and *C. Perfringens*) removal potential of the DAF was studied with Barapullah drain water.

The results obtained suggest that for canal water the critical parameters are Time of Coagulation prior to the DAF, Retention Time and Influent TSS Concentration. Whereas, for drain water it was only the Influent TSS Concentration. For anaerobic sludge from the wwtp in Delft the most significant parameter was found to be Pressure and a similar trend with higher removal was observed for anaerobic sludge from Delhi. Image analysis with canal water, drain water and sludge samples showed that for higher TSS removal runs, a general trend of average influent particle sizes of 12 µm, 3-5 µm and 80-100 µm respectively was observed. And, clean effluent particle sizes were found to be 2-3 µm for drain water and canal water. Furthermore, for drain water runs with high removal, the particle-bubble agglomerate rise velocities were found similar to the theoretically calculated values of 1.69E-03 m/s. Bubble to particle ratio for high TSS removal runs was calculated to be 34 bubbles/-particle for drain water and 50 times more for sludge. In terms of pathogen removal, *E-coli* removal for drain was found as high as 1.65 log for higher influent TSS runs. No significant correlation was found between the TSS removal and *E-coli* removal by the DAF.

It is recommended that for future research further optimization (with experimental designs such as CCDR) of the significant parameters identified should be done. More extensive research in addition to results found in this study is suggested to be done on the effect of different coagulants and coagulation conditions on the DAF performance. To further understand the differences observed in the significant parameters of the influents, research on the influent properties such as hydrophobicity and density are recommend. More experiments with adequate site equipment are suggested to be done to understand the removal of *Giardia* and *Cryptosporidium* to further understand their relation to the TSS removal by the DAF.

List of Figures

List of Tables

Contents

Abbreviations

LOTUSHR	Local Treatment of Urban Sewage for Healthy Reuse
DAF	Dissolved Air Flotation
AD	Anaerobic Digestion
WWTP	Wastewater Treatment plant
MLD	Million Liters per Day
PSD	Particle Size Distribution
PIV	Particle Image Velocimetry
TSS	Total Suspended Solids
DOE	Design of Experiments
A/S	Air to Solids ratio

1 Introduction

1.1. Delhi's looming (waste)water crisis

Water scarcity and poor water quality are glaring problems faced by many cites today, especially by the rapidly growing cities of the world. "Dangerously Low on Water, Cape Town Now Faces 'Day Zero'" (New York Times, 2018), "As Chennai Runs Out Of Water, 9 Million Pray For Rain" (NDTV, 2019), "10 crore people drinking contaminated water in India" (Economic Times, 2017) and many more such headlines have become front page news (refer Appendix A for more details, numbers and forecasts about India's water scarcity). In recent years, due to unprecedented population growth, rapid urbanization and climate change, coupled with growing economic aspirations many developing cities, especially in India can be found at the forefront of numerous studies citing severe water stressed regions and low water quality (WWAP, 2019) (WorldBank, 2018). It is predicted that by 2030, a number of Indian cities', including it's capital, New Delhi would face high to extreme water stress with potable water demand outstripping supply and mortality numbers reaching 2,00,000 annually due to lack of access to safe water. Around 70% of water in India is contaminated, with India ranking 120 out of 122 countries in water quality index. (NITIAayog, 2018)

For the last few years, Delhi has consistently been one of the most polluted cities in the world (Cherian, 2004). A major reason for inadequate water supply and low water quality can be attributed to the inability of the cities infrastructure to cope up with the growing population, migration and rapid development, especially when it comes to water supply and wastewater treatment systems. As a result, there is stress on water availability and at the same time many drains are severely polluted as large volumes of untreated wastewater is discharged into them creating health risks for society. Even though industrial, residential, vehicular and water pollution monitoring capacity has increased over time, contamination and health issues have continued to rise (T K Gadhok, 2014).

One of the biggest victims of this onslaught has been and continues to be the Yamuna river (connected with many tributaries including the Barapullah drain). More than 1400 MLD (million liters per day) of sewage and 1900 MLD wastewater from the city is discharged into the river reducing it to a black, smelly drain. Furthermore, nitrates and fluorides of high concentration (up to 100 mg/l) have been found in the groundwater, with many hospitals and small industries discharging untreated waste into Delhi's streams and

rivers. (T K Gadhok, 2014) (Cherian, 2004) Consequently, to alleviate water scarcity, manage wastewater as well as potentially recover resources, holistic solutions for wastewater treatment and innovative methods for resource recovery are need of the hour.

1.2. The LOTUS^{HR} project

LOTUS^{HR} (Local Treatment of Urban Sewage for Healthy Reuse) aims to assess, research and build a resource oriented wwtp at the Barapullah drain in New Delhi, India (refer to Appendix B for more historical and geographical information about the drain). The overall goal of the project is to investigate and implement novel, holistic (waste)water management strategies that will treat and reuse water, recover nutrients and produce energy from the Barapullah drain (LOTUSHR, 2018).

The Barapullah along with the other drains of Delhi were considered a tributary of the mighty River Yamuna till the 19^{th} century. Over the years, due to rapid development in Delhi and lack of water management, this historical drain which used to carry rain water has been polluted with wastewater, sewage and solid waste. (NURI, 2018) About 1.6 million liters of wastewater pass through the 20 km long Barapullah drain making it heavily polluted. This untreated wastewater then flows into the Yamuna River which is a one of the main water sources of New Delhi, contributing to water scarcity and treatment costs (LOTUSHR, 2018). Thus, considering parameters such as high population density, water scarcity and large fluctuating wastewater flow for this area, the project research lines were defined and the project site at the end of the drain was set up.

To achieve this goal, the entire project is divided into 3 main research lines; each related to one of the treatment steps of the drain. Figure 1.1 gives an overview of all the 3 research lines which make up the project.

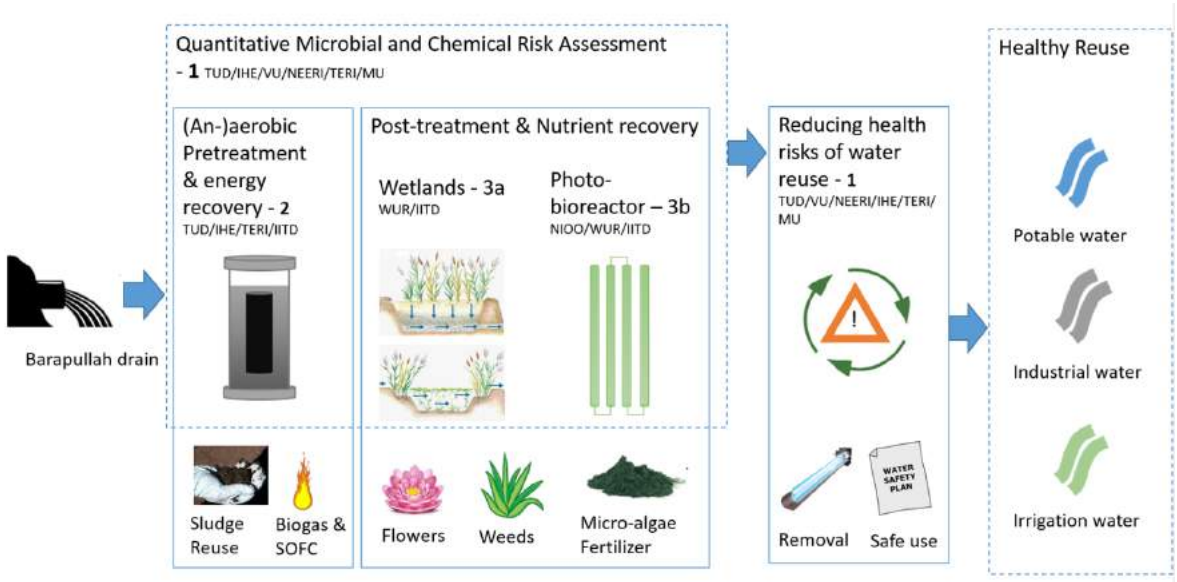

Figure 1.1: Schematic representation of the LOTUS^{HR} project research lines (source: (LOTUSHR, 2018).

Research line 1 focuses on reducing the health risks of water reuse and comprises of a microbial and chemical risk assessment of the treated wastewater. **The second research line corresponds to the sewage pre-treatment and energy recovery within which this masters thesis is framed.** This research line conducts research on sewage pre- treatment and also looks into sludge reuse and biogas utilization via SOFCs (solid-oxide fuel cells). Finally, research line 3 corresponds to the post-treatment and nutrient recovery by investigating wetlands and photo-bioreactor technology. (LOTUSHR, 2018)

1.3. Problem Description

The overarching objectives of research line 2 in the LOTUS^{HR} project are to develop stable and robust process to remove organic material and convert it to biogas, as well as reliable reuse of wastewater. Furthermore, this system should be resilient against variations in flux and pollutant concentrations which are typical to monsoon climates such as New Delhi, at the same time ensuring superior effluent quality which can be subjected to additional treatment. For this, anaerobic treatment was identified coupled either by dissolved air flotation (AD-DAF) or by membrane filtration (Anaerobic Membrane Bio Reactor (AnMBR)). Even though membrane filtration produces higher quality effluent, for the high fluctuating hydraulic flows and composition of the Barapullah drain, DAF is known to cope better with such fluctuations. Moreover, DAF is generally a primary treatment technology and a potential application of the DAF could be as a stand alone solids separation system to pre-treat the complex drain water directly from the drain.

DAF works on the principle of buoyancy by micro-bubbles which attach and remove suspended particles by forming bubble-particle agglomerates and float to the surface of the flotation tank. In literature, a design for a continuous DAF system, or a blueprint for a laboratory DAF or even consistent theory for the design and operation of the DAF is lacking (Benjamin, 2013). Thus, to gain insight into the working, operating parameters and performance of this technology, its long term effects on water quality and its feasibility as a part of the LOTUS^{HR} project (as a pre-treatment for drain water or as a coupled technology with Anaerobic Digestion (DAF-AD), it is essential to investigate the DAF further at the laboratory scale and with real wastewater from the LOTUS^{HR} site.

1.4. Research Objective

It can be concluded from the discussions above that DAF is a promising technology as a pre-treatment solids separation system or as a combined technology with the AD-DAF configuration within the LOTUS^{HR} project. However, due to the complex and erratic nature of the Barapullah drain water and the uncertain composition of the AD sludge being fed into the DAF, its performance and operating parameters with these different influents (the drain water itself and anaerobic sludge as part of the AD-DAF treatment process) need to be investigated in order to achieve optimum DAF performance. Furthermore, for similar type of drains, further understanding of the DAF performance with drain wastewater can widen it's application scope. Considering these points, the following research objective was formulated:

"Identifying and investigating critical operating parameters of a bench-scale DAF column system to achieve optimum solids-liquid separation for different influents: canal water and anaerobic sludge in a controlled laboratory setup, and with real wastewater and anaerobic sludge from the Barapullah drain site as part of the LOTUS^{HR} project"

1.5. Research Questions and Approach

As per the aforementioned objective, the research questions constructed were as follows:

1. What are the critical operating parameters for DAF based on different influents (canal water, anaerobic sludge from Harnaschpolder wwtp in Delft, Barapullah drain water and anaerobic sludge from Okhla wwtp in Delhi) and how do they compare in terms of TSS (Total Suspended Solids) removal efficiency?

2. What is the maximum efficiency that can be reached by the DAF in terms of TSS removal with these influents and operating parameters?

3. How do the physical characteristics of particles in these influents affect DAFs TSS removal efficiency?

4. How do the size, behaviour, flow pattern and velocity of the bubbles and bubble-particle agglomerates in the DAF column affect the TSS removal efficiency?

5. How effective is the DAF as a pre-treatment in removing pathogens such as *E-coli*, *Cryptosporidium* and *Giardia*?

To achieve the research objective and answer the research questions, this thesis was further divided into the following parts:

1. **Literature review:** In the first section a detailed literature review is presented. This is given in chapter 2 which first briefly touches upon flotation technologies and then elaborates on the fundamental principles of the DAF, its background theory, key parameters, design considerations and DAF applications. It further describes the background and fundamentals of the Design of Experiments (DOE) approach adopted to analyze the DAF's performance for each influent. Then the background about image analysis by ImageJ-Fiji and Particle Image Velocitimetry (PIV) is discusses followed by literature about the pathogen removal potential of the DAF.

2. **DAF experiments:** Based on information on the DAF gathered from Chapter 2 and the previous data available on the Barapullah drain (see Appendix C) the experiments were designed. Design of Experiments (Plackett Burman) approach was used to build a framework for the experiments in order to gain maximum information from a minimum number of experiments. These experiments were then conducted in 2 parts - laboratory experiments and site experiments to gather comparative data for investigation. Canal water and anaerobic sludge from Harnaschpolder wwtp in Delft was used as influents for part 1 and Barapullah Drain water and anaerobic sludge from Okhla wwtp in Delhi were used for part 2. The experimental setup and analytic methodologies followed to understand and explain the DAF performance for the different influents are given in Chapter 3.

3. **Results and discussion:** Lastly Chapter 4 analyzes, discusses and compares the DAF TSS removal performance, significant operating parameters, influent characteristics and particle-bubble flow behaviour for the different influents studies in this thesis, to gain insight about optimum operating conditions. Furthermore, it investigates the pathogen removal performance of DAF for the Barapullah drain water. The detailed calculation and analysis for the results obtained are given in the appendix.

4. **Conclusion and Recommendations:** The conclusions obtained from the analysis and results are given in Chapter 5 followed by recommendation for future work in Chapter 6.

2

Literature Review

This chapter first briefly touches upon the background of flotation technology in wastewater treatment. Then it goes on to give an overview of the literature studied to gain understanding of the DAF process and its design and operational parameters. Furthermore, it talks about the experimental methods researched and adopted to design the experimental framework for scientifically analyzing the DAF. Finally, literature about the TSS removal performance, bubble particles interaction and PIV are discussed followed by background on the application of the DAF for pathogen removal.

2.1. Flotation Technology

Physically flotation is when particles, aggregates or flocs move in an upward motion as a result of a net buoyant force. (Shammas et al., 2010). Flotation technology has its origins in the mineral processing industry and is an extremely popular method for the recovery of many important minerals ores. For mineral separation, traditionally stable froth is used for selective separation of different minerals as a solid-solid separation. (Kitchener, 1984) Nowadays, it finds its application in many industries ranging from minerals, to biotechnology, to plastic, and even the fruit juice industry (Kitchener, 1984)(Schügerl, 2000)(Rubio et al., 2002). The flotation process can be broadly described in 4 steps (Shammas and Bennett, 2010):

1. Generation of bubbles in the waste water
2. Contact between the suspended particle in water and the gas bubbles
3. Attachment or entrapment of the particle and the gas bubble
4. Rise of the particle-bubble agglomerate to the surface of the water for removal/recovery.

In the flotation process, solid phase is separated from the liquid phase by injecting a gaseous phase (in the form of bubbles) into the liquid phase. These bubbles are lighter and rise in the liquid phase attaching to solid particles along the way. This in turn forms a bubble-particle agglomerate which has an apparent density lighter than water causing this agglomerate to rise to the surface, where it can be removed or recovered. Although, in

general the mechanism of flotation is the same, however, there can be significant difference as the area of application diversifies. (Bondelind et al., 2013)

As per the flotation process, based on the method of forming the bubbles, flotation technology can be further classified into 6 possible variants as follows:

1. Dissolved gas flotation: gas bubbles are formed in a pressurized super-saturated liquid/gas solution due to release of pressure. When this gas is air, the process is referred to Dissolve Air Flotation (DAF) (Shammas, 2010).

2. Dispersed gas flotation: generation of gas bubbles by mechanical mixing of gas and liquid. This can be achieved by dispersing gas through a porous medium or by the the shear created by mixing with the propeller action at atmospheric pressure. When this gas is air, the system is called as Dispersed Air Flotation (Ata and Jameson, 2005).

3. Froth flotation: A sparger is applied to inject the gas directly into the liquid (Gelinas and Finch, 2005).

4. Electrolytic flotation: Fine oxygen and hydrogen bubbles are produced as a result of electrolysis of water (Shammas and Bennett, 2010).

5. Vacuum flotation: bubbles are generated by using gas to saturate the liquid at atmospheric temperature followed applying negative pressure using a vacuum mechanism (Rohlich, 1954).

6. Biological flotation: Due to the biological systems like nitrification and de-nitrification, nitrogen and carbon dioxide gas bubbles are produced (Shammas and Bennett, 2010).

When it comes to the waste water industry, only the first 4 variants have been applied to a certain extent (Shammas and Bennett, 2010). Out of these, dispersed air flotation is known to be much more researched and commercially applied for the mineral industry, whereas dissolved air flotation is adopted more for water treatment (Bondelind et al., 2013). Considering this and as discussed in the introduction, this research focuses on investigating DAF in the context of the LOTUS^{HR} project.

2.2. Dissolved Air Flotation

Dissolved Air Flotation (DAF) has been used for many years for separating liquid particulate matter. The first DAFs were used in the 1920's, for recovering ores and valuable materials from water suspensions for exploitation in industries (Kiuri, 2001). Of all the flotation technologies, DAFs are essentially used for separation of suspended solids and colloidal material from the liquid phase, by suspension (flotation) of these compounds. The system comprises of four main components: air supply, air injection mechanism, pressurizing pump, pressure regulator/pressure release valve, retention tank/saturation vessel, chemical addition unit and flotation chamber (Vigneswaran, 2009) (Shammas, 2010). This process is achieved by adding saturated-pressurized water, also known as 'whitewater', at the bottom of the DAF unit. Whitewater is water that appears white because of the presence of pressurized micro-bubbles in it (USGC, 2016). By allowing the whitewater to enter the floating tank at atmospheric pressure, fine micro-scaled air bubbles are created nucleating from the

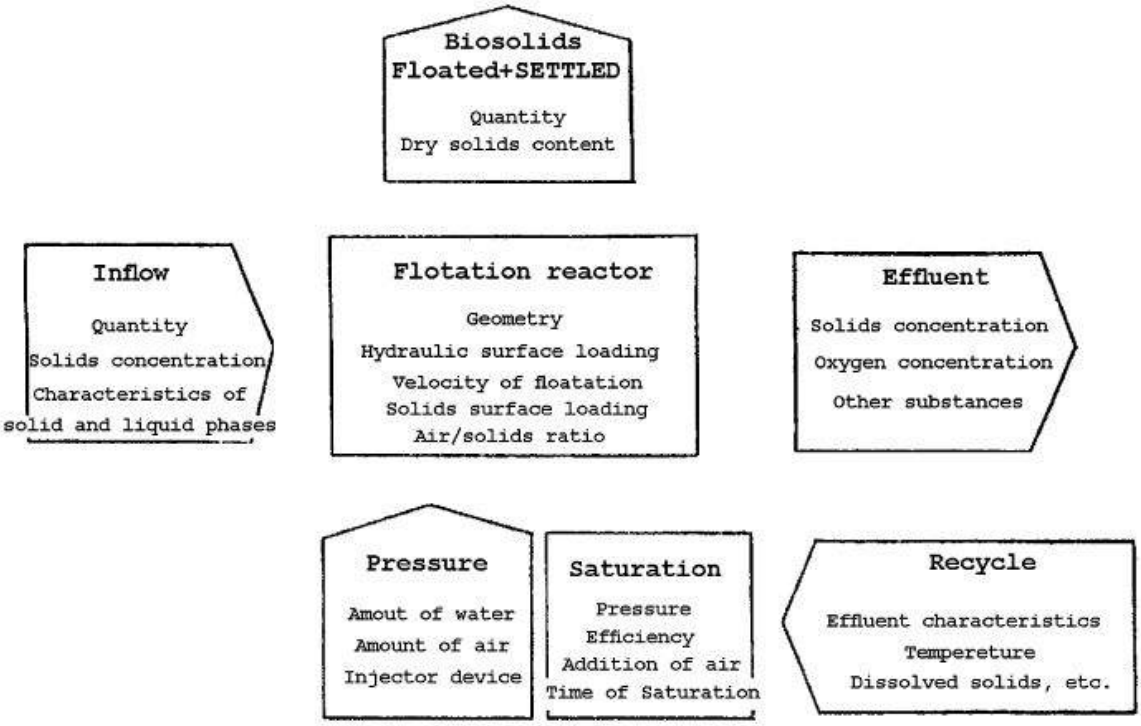

Figure 2.1: Process scheme of the DAF (Shammas, 2010).

supersaturated solution. The micro-bubbles rush upwards and adhere with the suspended matter of the effluent, bringing these particles to the surface. Here, all the adhered matter accumulates and therefore is easily removed. (Wang et al., 2005) Generally air is the most common gas applied to this process, how verve in recent times nitrogen, methane and carbon dioxide have also been used (Shammas, 2010). Figure 2.2 shows the scheme of the DAF process.

In terms of application in the waste water field, DAF is known to have first been applied to separate suspended solids, fibers and solids with low density (Wang, 2006). It is also used as a process to thicken activated sludge and chemically flocculated sludge (Wang et al., 2007). Out of all the floatation methods the DAF is known to be the most efficient in treating municipal wastewater (Shammas et al., 2010). In recent years, DAF has also started being used to remove oil and grease compounds from waste water (Melo et al., 2006). In the early 1900s, DAF started to find its feet in the water industry. 1st generation DAF systems were developed as tanks capable of a basic flotation mechanism with low flow rates of 2-3 m/h, and not any higher than 5 m/h. Around the 1960s the 2nd generation of DAFs were introduced which are even widely used till even today which have surface loading rates below 57 m/h and time recorded for flocculation more than 45 minutes. More advances were seen in the late 1960s where in-filter DAF processes known as dissolved air filtration/notation (DAFT) were developed. Inspired from the DAFT process more recently the 3rd generation of DAFs have been developed. These include technologies like counter current dissolved air flotation (COCODAFF) where a recycle flow is introduced special high volume high flow nozzles which disperse bubbles above the filter medium. Some other new technologies include AquaDAF and DAFRapide. (Vigneswaran, 2009)

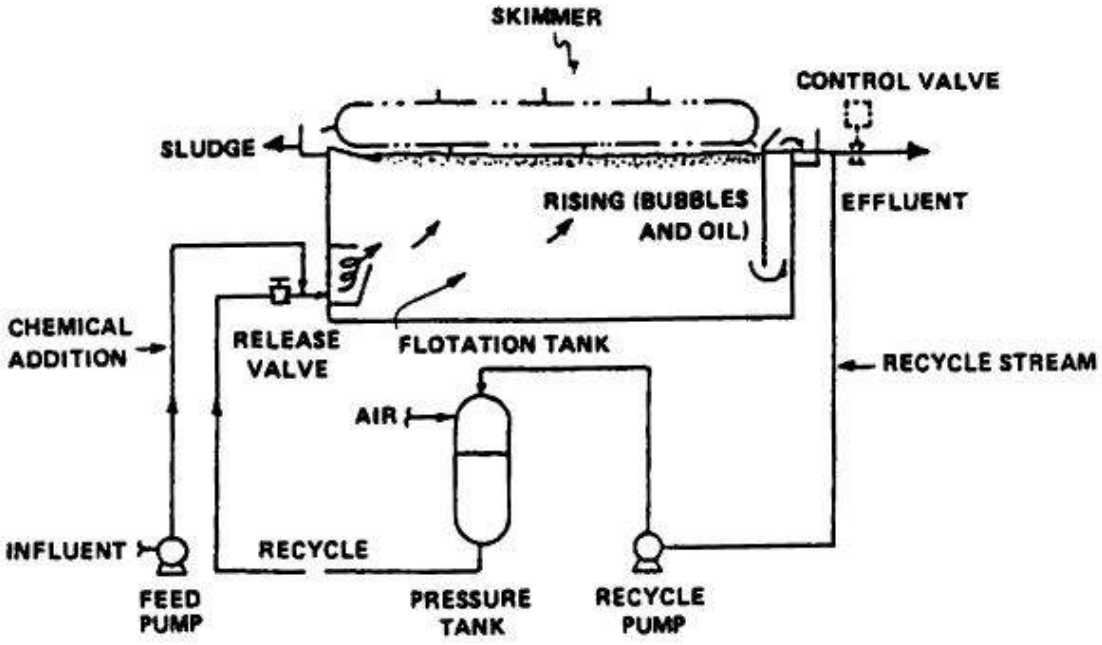

Figure 2.2: Schematic representation of DAF system (Shammas, 2010).

In wastewater treatment, a majority of the concerning contaminants are in the form of particulate matter or related to particles. These include silts, clay, inorganic metals, biological pollutants such as bacteria, viruses, protozoa and algae (Wiesner and Mazounie, 1989). Along with polluting water, particles have been known to shield harmful organisms from treatment (Lawler, 1997). Along with the removal of TSS some fraction of COD/BOD might be removed as well since a part of the suspension as organic matter or dissolved organic substances which may adsorb to solids and are removed by flotation (Shammas et al., 2010) (Wang et al., 2005). Therefore, removing particulate matter from wastewater is imperative in maintaining water discharge and preventing public health epidemics. In physical separation treatment removal of constituents is achieved by a physical transformation from diluted to a concentrated state. These processes exploit the physical characteristics of particles to aid their removal. The nature and size of the particle play an important role in physical separation processes which is mostly brought about by the application of gravity or pressure. (Tchobanoglous et al., 2005) In addition to TSS and turbidity measurements, to gain a deeper understanding into the application and performance of the DAF on the laboratory scale and at the LOTUS^{HR} site, detailed particle characterization is required.

There are various properties of particles that influence how they behave in water and which have a direct correlation with the efficiency of treatment, especially for physical treatment technologies like the DAF. These encompass particle morphology, size, size distribution, shape, density, viscosity, settleability and surface charge. To understand particle removal, along with shape and densities it is important to look at the heterodispersity of the particles in water. For this, particle size distribution (PSD) measurements can give valuable information to evaluate and optimize treatment technologies. Digital image analysis combined with statistical software's like SPSS (Statistical Software for Social Science) and SAS (Statistical Analysis Systems) acts as apolitical tools that can measure and process particle size distribution data.(Lawler, 1997) Widely used methods to analyze particles include par-

ticle counter, particle size analyzer and digital image analysis. These are also employed in this thesis for deeper understanding and analysis of the DAF performance with different influents.

The performance of a DAF can be measured by the rate at which particles and liquids are separated. The performance is determined by removal efficiency, float concentration, the magnitude of subnatant suspended solids, the Particle Size Distribution (PSD), the TSS concentration and the movement of the solid liquid interface (Wang et al., 2005). Particle removal depends on particle buoyancy and the possibility of forming bubble-particle aggregates. The system should provide enough contact time to promote particle flotation. Therefore, liquid flow and hydraulic retention time are fundamental to enhance particle separation. Moreover, particle removal may be enhanced by adding certain coagulants and flocculants. According to Edzwald (Edzwald, 2010), particle surface charge is generally negative due to adsorption of natural organic matter, thus, coagulants are needed in order to destabilize particle charge. Most common used coagulants are aluminum or iron salts. However, particles in waste water may have either positive or negative charge, thus, polymers addition to DAF system should be carefully assessed according to influent qualities and particle nature. Overall, DAF systems can achieve 90 - 95% solids removal from wastewater inflow (Wang et al., 2005).

In literature, 3 liquid flow configurations for DAF operation can be found (Wang et al., 2007). Figure 2.3 shows the configuration is schematic diagrams.

1. Full flow pressure floating: In this system, all of the influent wastewater is saturated with air under pressure which is then released to the flotation basin forming bubbles (Figure 2.3 A). These systems are generally applied for influent feed with more than 800 mg/l suspended solids where large amount of air bubbles and no flocculation is required. Compared to the other 2 systems, full flow flotation is know to result in maximum air dissolution and has the most probability to lead to bubble-particle contact. However, the disadvantage of this system is it requires large saturation systems and may show coagulated floc sharing due to pressure release process. Other disadvantages include larger operation and maintenance cost due to more solids content pumping capacity. For oil, this process leads to more emulsification due to the pumping shear force which makes it more difficult to remove.

2. Partial Flow or Split Flow Pressure Floating: In this process, around 30-50% of the incoming influent feed is pressurized with air and directed to the flotation basin, without recycle. Low pressure pumps or gravitational force feeds the remaining part of the feed to the flotation tank (Figure 2.3 B). These are mostly deployed when there are low suspended solids resulting in a low air requirement. This system results in lower cost of pumping, improved system capacity to handle fluctuations in flow and less floc breaking due to shear. Similar to full flow pressure, its disadvantages include increased oil emulsification and floc shearing. The non-pressurized flow can also double as a fluctuation tank when coagulants are used. Moreover, the volume of dissolved air is lower than full flow systems. The pump operation in this system can be kept constant as flow fluctuations can remain in the non-pressurized part of the system. However, if the flow increases it might have a adverse impact on the system's

performance as a result of lower air to solids ratio. It's major disadvantage is that it dissolves low volume of gas as compared to full flow systems.

3. Recycle Flow or Re-circulation Flow Pressure systems: Here, 15 to 50 % of the treated waste water from the effluent is pressurized and re-routed to the flotation tank (Figure 2.3 C). This system is used when the influent waste water is subjected to coagulation and flocculation. This is the most popular DAF configuration for wastewater treatment. This system also helps avoid emulsification of oil and floc disruption due to shear. This however also results in increase sizing of the floating chambers.

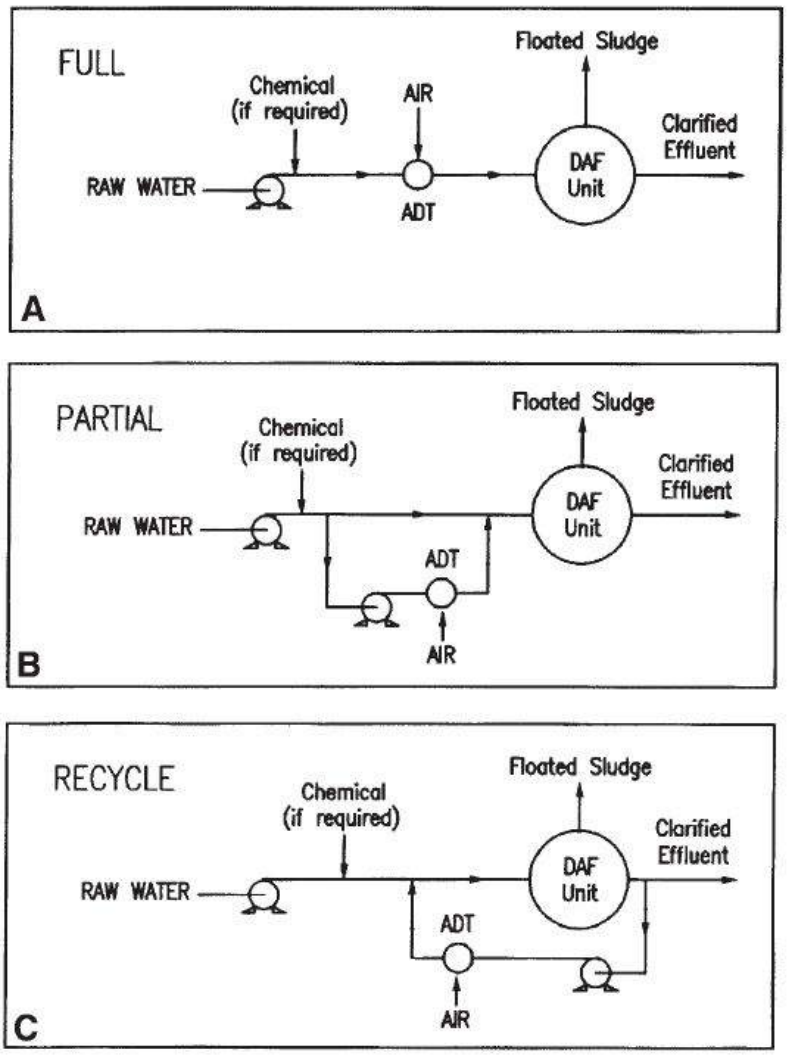

Figure 2.3: Schematic representation of the 3 different DAF liquid flow operations in a pressurized system (Wang et al., 2007).

The Column DAF designed and experimented on in this thesis was based on the Recycle Flow or Re-circulation Flow Pressure systems due to its popularity, advantages and relative ease of descaling. Chapter 3 elaborates more on the DAF experimental set up used.

DAF has been adopted to remove particles from water as an alternative to conventional sedimentation processes since the 1960's (Han et al., 2002). Sedimentation and flotation of suspended particles in water are both driven by density difference and flotation occurs when the density of a particle is lower than that of the surrounding water. When particles have a density just higher than that of the surrounding solution slow sedimentation will occur. In the DAF process, particles with a density just higher than the surrounding water, can be induced to float if one or more bubbles get attached to them. (Benjamin, 2013) According to Wang (Wang et al., 2005), DAF has been found to have many advantages over conventional sedimentation processes. These include the fact that DAF requires only around 15% of floor space and that its volume requirement is just 5% that of a settler. Moreover with the addition of the same flocculation chemicals, both processed show the same level of clarification. However, when it comes to the cost, DAFs are more expensive due to higher energy requirement for generating whitewater, but it should be noted that this can be offset by the low cost of initial installation. Furthermore, as DAF is mostly made of prefabricated stainless steel, compared to settlers, the erection cost is lower, corrosion is minimized and construction can be flexible to incorporate future modifications.

2.2.1. DAF Theory

The basic theoretical principles of the DAF can be broadly classified as - Gas solubility/-gas transfer at air - water layer interface, formation of gas bubbles (whitewater), bubble rise/transfer to achieve contact with particulate matter followed by attachment, and flotation of these bubble-particle agglomerates in flotation tank. (Vigneswaran, 2009) These are elaborated on below, followed by design consideration for the DAF.

Gas Solubility

One of the key aspects of the DAF is formation of micro-bubbles which are generated by dissolving gas (which is air in the case of DAF) under pressure and then releasing it under atmospheric conditions (depressurizing). This gas-water equilibrium and in turn the amount of gas dissolved is governed by Henry's law (Henry, 1803) (Shammas, 2010):

$$C_A = HX_AP_T \tag{2.1}$$

Here, C_A is dissolved gas A's concentration in the solution (kg/m), H is known as the Henry's law constant (kg/ml kpa), X_A is gas A's mole fraction and P_T is total pressure for all gasses together. This means that both the concentration of gas which dissolves in the liquid and the amount of gas which is eventually released upon pressure reduction are a function of initial gas pressure or in other words is proportional to the partial pressure of the gas which is known is Henry's law constant. Additionally, temperature and the concentration of dissolved solids determine the gas solubility. Table 2.1 gives the the solubility of air based on these parameters. For instance, in distilled water, air solubility can reduce up to 45% with a change in temperature from 0 to 30 °C and with an increase in salinity from 0 to 20,000 mg/l, the solubility of oxygen may decrease by 19%. In the case of oxygen, if we take air's oxygen concentration as 21% and atmospheric temperature as 20°C, the concentration of oxygen at atmospheric conditions will be;

$$C_{O2} = \frac{1(atm) * 0.21 * 1600(mg/mol) * 2mol}{769.23(Latm/mol)} = 8.73mg/L \tag{2.2}$$

Table 2.1: The calculated oxygen concentrations considering manometric pressure (0 bar is 1 atm).

Temperature (°C)	**Pressure (bar)**						
	1	2	3	4	5	6	10
25	8.1	16.1	24.2	32.3	40.3	48.4	80.6
20	8.8	17.6	26.4	35.1	43.9	52.7	87.9
15	9.6	19.2	28.8	38.4	48.0	57.6	96.0
10	10.5	21.1	31.6	42.1	52.6	63.2	105.3

Similarly, for 3 bar and 5 bar pressure, the concentration of oxygen is given in Table 2.1

It should be noted here that the values calculated by Henry's law would always show lower concentration of dissolved gas from the saturator. Therefore, efficiency factor f needs to be added. Thus, the equation becomes;

$$C_A = f H X_A P_T \tag{2.3}$$

Where, f is the ratio of gas volume form the saturator to predicted gas volume by Henry's law. f is generally taken as 0.6 - 0.7 for unpacked saturators and 0.9 for packed saturators.

Therefore, from Henry's law we can say that as the pressure on a solution is increased, the solubility of gas also increases. For the DAF process, air is dissolved at high pressure in the saturator following which the pressurized water flows through the pressure-release valve in to the flotation tank(Shammas, 2010). Here the bubbles first start to form by nucleation at low-energy sites on solid particles, in the absence of which they will homogeneously nucleate in the liquid phase (Gehr and Henry, 1983). These bubbles will keep growing till they are limited by diffusion (Massaldi et al., 1975).

Another way to describe this would be as given in equations below. These equations give the theoretical and modified calculations giving the volume of gas that will be release from the pressurized solution when the pressure will reduced to atmospheric conditions (1 atm) (Shammas, 2010).

$$S = S_g\left(\frac{P}{14.7} - 1\right) \tag{2.4}$$

Here, the amount of gas released under atmospheric pressure is given by S (mg/l), S_g gives the gas saturation value under atmospheric conditions (mg/L) and the pressurization gauge pressure is given by P (psig). Experiments have further demonstrated that in this process not all of the dissolved air will precipitate and release in the flotation chamber, which is in accordance with the diffusion theory. Thus, the dissolution mechanism is not a 100% efficient and need to be modified by a efficiency factor. For this equation it is taken as *f*, which is called as the "fractional system dissolving-efficiency factor (Bratby and Marais, 1975). The equation then becomes (Bratby and Marais, 1975);

$$S = S_g\left(\frac{fP}{14.7} - 1\right) \tag{2.5}$$

Table 2.2 and 2.3 shows the variation in volume of air dissolves at different efficiencies. From the above equations it can be observed that the f is a crucial parameter. In literature it was found that (Bratby and Marais, 1975) have come up with a useful way to estimate

AT 30 psig: Sg $\left[f\frac{P+14.7}{14.7}\right]$													
Temperature		Sg at 1 atm		$f=100\%$		$f=90\%$		$f=80\%$		$f=70\%$		$f=60\%$	
°C	°F	lb	Ft^3	lb	ft^3	lb	ft^3	lb	ft^3	lb	ft^3	lb	ft^3
0	32	0.311	3.86	0.95	11.7	0.85	10.6	0.76	9.5	0.66	8.2	0.57	7.1
10	50	0.245	3.15	0.75	9.6	0.67	8.6	0.60	7.7	0.52	6.7	0.45	5.8
20	68	0.203	2.70	0.61	8.2	0.56	7.4	0.50	6.6	0.43	5.8	0.37	4.9
30	86	0.175	2.40	0.53	7.3	0.48	6.6	0.43	5.9	0.37	5.1	0.32	4.4
40	104	0.155	2.20	0.47	6.7	0.43	6.0	0.38	5.4	0.33	4.7	0.28	4.0
50	122	0.142	2.09	0.43	6.4	0.39	5.7	0.35	5.1	0.30	4.5	0.26	3.8
60	140	0.133	2.01	0.40	6.1	0.36	6.6	0.32	4.9	0.28	4.3	0.24	3.7
70	158	0.128	2.00	0.39	6.1	0.35	5.5	0.31	4.9	0.27	4.3	0.23	3.7
80	176	0.125	2.01	0.38	6.1	0.34	5.5	0.30	4.9	0.27	4.3	0.23	3.7
90	194	0.124	2.05	0.38	6.2	0.34	5.6	0.30	5.0	0.26	4.4	0.23	3.8
100	212	0.125	2.13	0.38	6.5	0.34	5.8	0.30	5.2	0.27	4.5	0.23	3.9
$\left[f\frac{(30+14.7)}{14.7}\right]$				3.04		2.74		2.44		2.13		1.83	

Table 2.2: Volume and weight of air dissolved in water per 1,000 gal at 30 psi (Shammas, 2010).

AT 65 psig: Sg $\left[f\frac{P+14.7}{14.7}\right]$													
Temperature		Sg at 1 atm		$f=100\%$		$f=90\%$		$f=80\%$		$f=70\%$		$f=60\%$	
°C	°F	lb	ft^3	lb	ft^3	lb	ft^3	lb	ft^3	lb	ft^3	lb	ft^3
0	32	0.311	3.86	1.69	20.9	1.52	18.8	1.35	16.8	1.18	14.7	1.01	12.6
10	50	0.245	3.15	1.33	17.1	1.20	15.4	1.06	13.7	0.93	12.0	0.80	10.3
20	68	0.203	2.70	1.10	14.6	0.99	13.2	0.88	11.7	0.77	10.3	0.66	8.8
30	86	0.175	2.40	0.95	13.0	0.86	11.7	0.76	10.4	0.67	9.1	0.57	7.8
40	104	0.155	2.20	0.84	11.9	0.76	10.7	0.67	9.5	0.59	8.4	0.51	7.2
50	122	0.142	2.09	0.77	11.3	0.69	10.2	0.62	9.1	0.54	7.9	0.46	6.8
60	140	0.133	2.01	0.72	10.9	0.65	9.8	0.58	8.7	0.51	7.6	0.43	6.6
70	158	0.128	2.00	0.70	10.8	0.63	9.8	0.56	8.7	0.49	7.6	0.42	6.5
80	176	0.125	2.01	0.68	10.9	0.61	9.8	0.54	8.7	0.48	7.6	0.41	6.6
90	194	0.124	2.05	0.67	11.1	0.60	10.0	0.54	8.9	0.47	7.8	0.40	6.7
100	212	0.125	2.13	0.68	11.6	0.61	10.4	0.54	9.3	0.48	8.1	0.41	6.9
$\left[f\frac{(65+14.7)}{14.7}\right]$				5.42		4.88		4.34		3.80		3.26	

Table 2.3: Volume and weight of air dissolved in water per 1,000 gal at 65 psi (Shammas, 2010).

the dissolved air mass under pressure. They measured by volume the concentration of air being released by the pressurized liquid after being released at atmospheric pressure. Bases on this, they found important parameters by testing different components of the saturated system. According to them following are the most crucial parameters (Bratby and Marais, 1975):

1. The valve type which would release the pressurized feed, flow rate or turbulence from the valve, turbulence downstream from the valve in the flotation tank, mixing of water with the saturated feed and particulate nuclei concentration which is the ratio of the air precipitation mass to saturation feed unit volume.

2. More efficient saturation systems were the ones where water was sprayed over a packing medium (Raschig rings). These were found to be more efficient as compared to sparging air or air injection suction by centrifugal pumps.

3. Dissolution of air in the liquid was found to be more efficient at higher pressure than lower pressure due to absorptive mass transfer by reduced driving force.

These parameters have shown similar behaviour in other literature. In the case of refinery waste water treatment, 3 bar already provided more air dissolution and was more effective in removing suspended solids and oil than 2 bar air (Franzen et al., 1972). As per (Rezakazemi et al., 2018), the mixing degree at the point where pressure reduces and the extent of saturation together determine the volume of air release. In a convention pressure vessel design, saturation of air can be reached up to 50% and up to 90% for mechanical mixing.

Normally, air is used as the choice of gas for the formation of micro-bubbles in the DAF. However, it has been found that nitrogen, methane and carbon dioxide as well as their combination can be used. As these gases have higher solubility, therefore by reducing the recycle rate, thicker floats can be produced improving the existing DAF operation system. Table 2.4 and figure 2.4 gives the solubility values of these different gases.

Gas	Solubility	
	By weight (mg/L·atm)	By volume (mL/L·atm)
N_2	17.8	15.5
O_2	40.1	30.8
CO_2	1,493	831
Combusted digester gas (84% N_2, 4% O_2, 12% CO_2)	22.3	18.6
Oxygen-activated sludge off-gas (20% N_2, 50% O_2, 30% CO_2)	466	265.8

Table 2.4: Solubility of various gases in water at 24 °C (Rezakazemi et al., 2018).

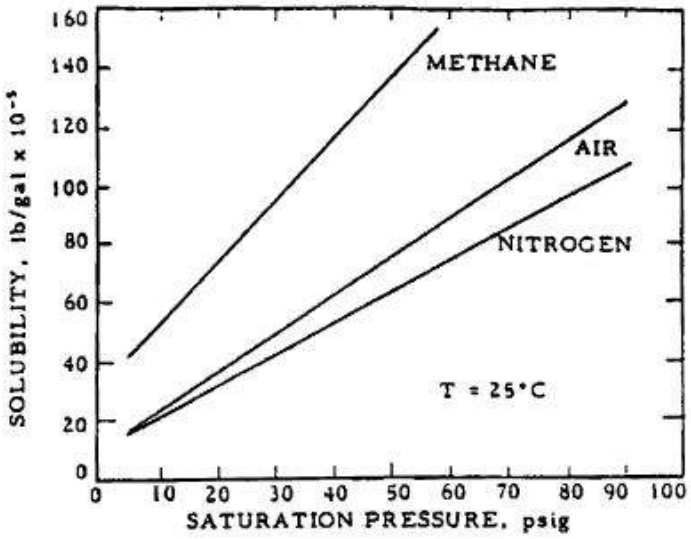

Figure 2.4: Solubility of gases in water as a function of pressure. (Rezakazemi et al., 2018).

Bases on these theories, a design equation can be drawn to calculate the gas to suspended solids ratio as follows (Shammas, 2010):

$$\frac{G}{S} = \frac{RC_s f \frac{P}{101.3}}{S_o Q - S_e R} \tag{2.6}$$

Here, G gives the concentration of gas (mg/L), S gives the suspended solids concentration (mg/L), flow rate of the pressurized liquid is given by R (L/d), C_s is the gas concentration of thw saturated gas at atmospheric pressure (mg/L), Saturation efficency is given by *f*, P gives the saturation pressure gauge (kN/m^2), S_o is waste water's suspended solids concentration (mg/L), Q is the flow of the raw water and S_e the liquid pressurized stream suspended solids (mg/L). (Shammas, 2010)

Gas Transfer Rate

Going from inter-phase of gas to dissolved gas, the rate of gas transfer is proportional to the deficit in saturation. This can be shown as (Vigneswaran, 2009);

$$[\frac{dC}{dt}]_t = K_L\alpha(C_s - C) \tag{2.7}$$

Here $[\frac{dC}{dt}]_t$ is the dissolved gas concentration rate of change (kg/m^3/s), t is time elapsed (s), $K_L\alpha$ is the coefficient of mass transfer (s$^-$1), C_s is the saturation concentration (kg/M^3), C is at given time t the aqueous phase gas concentration. This equation concludes that the saturators rate of gas transfer is proportional to the pressure of saturator and the per unit inter-facial saturator surface area. (Vigneswaran, 2009)

Bubble Formation

In the DAF process, the needle valve/nozzle injects pressurized re-circulated water in to the floating chamber thus crating micro air-bubbles (100 μm) or smaller). These bubbles are formed in 2 steps - nucleation followed by growth. (Vigneswaran, 2009) According to (Shammas, 2010), to generate micro-bubbles in for the DAF process, 2 methods are known:

1. Wastewater is pressurized from 2-6 bars to dissolve air.This pressurized water is discharged at the bottom of the flotation basin by passing thought a pressure release valve. Here, the atmospheric air pressure combined with the floating tanks hydrostatic head will equal to the total pressure. This will result in small bubbles nucleating and rising to remove suspended matter.

2. Aeration is performed on wastewater till it is at atmospheric pressure saturation. Then vacuum is applied to yield the bubbles. This process is no longer used

Bubble nuclei are spontaneously formed in the super-saturated water system due to the large pressure difference as per the free energy change minimizing principle. This formation of spontaneous bubble is also referred to as gas precipitation. These micro-bubbles formed then rise, entrap or attach to flocs and thus remove the suspended matter. (Vigneswaran, 2009)

Bubble Size

The size of the bubble in a DAF system is one of the most important dependant variable (Shammas, 2010). It is known that DAF systems keep the micro-bubble size range steady around 10 - 100 μm with an average bubble diameter recommended between 40 - 60 μm (Vigneswaran, 2009). Figure 2.5 give the data for bubble size distribution for 20 psig (1.3 bar) and 50 psig (3.4 bar) (Vrablik, 1960). Here, the bubble sizes observed at 20 and 50 psig

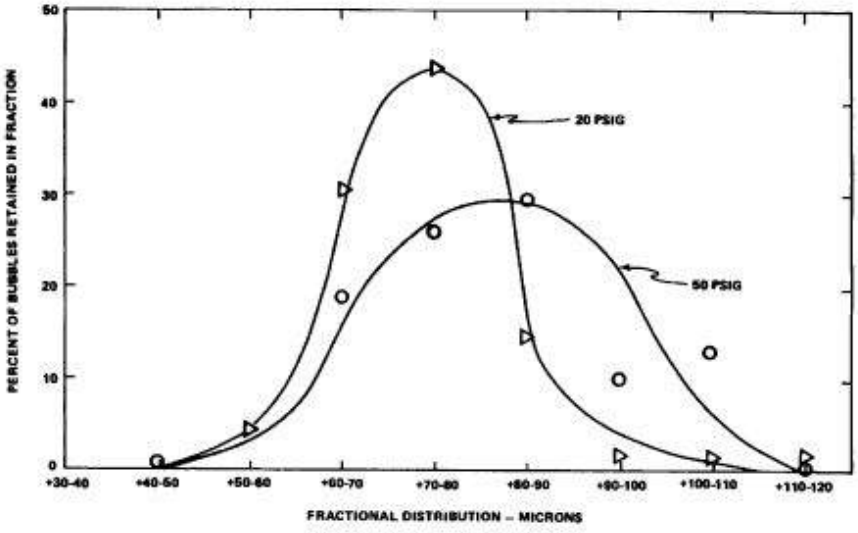

Figure 2.5: Bubble size distribution for 20 psig (1.3 bar) and 50 psig (3.4 bar) (Vrablik, 1960).

are in the range of 45 -115 µm with an average diameter of 75 - 85 µm. The largest size of bubble that can rise in laminar flow was found to be 130 mm. (Vrablik, 1960) The steady bubble size is in turn dependent on the injected flow rate and the pressure maintained in the saturator. Increasing the pressure would result in a decrease of bubble size. However, literature suggests that above 5 bar, increase in pressure no longer shows an effect on the size of the bubbles (Wang et al., 2005). In the DAF systems, smaller bubbles are preferred. This is because smaller bubbles obediently follow Stokes' law and in laminar flow tend to rise as rigid spheres whereas, large bubbles take a more ellipsoidal shape and have higher rise velocities. Small bubbles can be more effectively ensured at a 4-6 bar pressure difference. (Vigneswaran, 2009)

According to (Shammas, 2010), in a certain amount of water, the size and number of air micro-bubbles formed in the DAF are both a function of the amount of chemical in the waste water and the physical systems involved. and the amount of dissolved solids as well as the surface tension are vital parameters. Many small bubbles in large amounts can be formed when there is a decrease in surface tension (Katz et al., 1960). Furthermore, with an increase in temperature (50 -80 °C) DAF systems have shown a significant change in size of bubble recorded with a mean of 66 µm at 2 bar and 42 µm at 3 bar (Shannon and Buisson, 1980). In the DAF process, micro-bubbles stream by releasing air from the liquid solution, following Stokes' law rising velocity and with sizes ranging from 30 -120 µm. As long as the bubbles stick or entrap the particles, the floation effect will remain which indicated that the diameter of the bubbles would be less than the particle or floc diameter (Shammas, 2010).

Literature also finds variation in bubble sizes when different gases are used for micro-bubble formation. When bubble sizes were measured for both air and carbon dioxide saturated systems at 2 bar pressure, it was found that when carbon dioxide was used, the bubble sizes after 10 seconds of operation were 5 times bigger than air and thus had higher rising velocity leading to more turbulent conditions in the flotation tank. When nitrogen was used, bubble sizes were found to be 80 μm (Sato et al., 1979) and 48 μm (Shammas, 2010). Formation of bubbles is a detailed scientific topic itself. It is also interesting to note that experiments show generally gases which are super-saturated are stable in solutions and there is a need for external agitation to form bubbles. With an increase in the velocity of the solution and by lowering the viscosity, surface tension and nozzle size, the nucleus formed would increase in number. (Shammas, 2010)

Bubble-Particle interaction

To ensure particles are removed, once gas precipitation is done, gas micro-bubbles must come in contact with the particles to be separated and removed. There mechanisms are known for bubble-particle interaction - structures of large flocs being entrapped by the bubbles, formation and growth of bubble nuclei inside the floc and bubble particle collision-adhesion. (Vigneswaran, 2009) Figure 2.6 diagrammatically depicts these 3 mechanism.

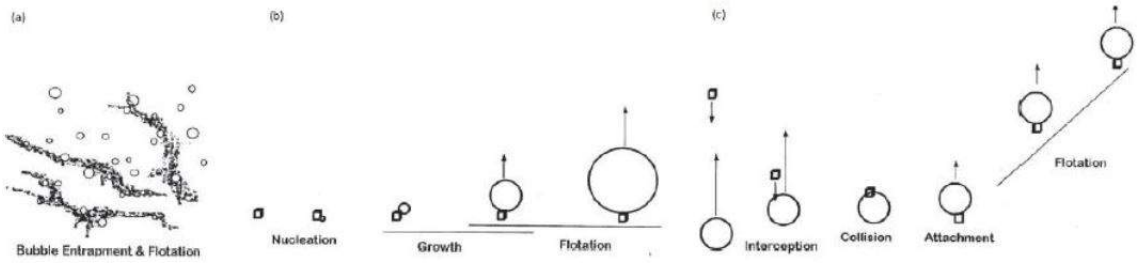

Figure 2.6: Bubble-particle agglomeration mechanism in the DAF (Wang et al., 2005).

When there are large suspended flocs which are either already present in the waste water or are generated by rapid high rate flocculation, mechanism 1 is observed. Mechanism 2 occurs most probably to a varying extent in most DAF application. For diluted waste water suspension and a given time scale to form air bubbles, mechanism 3 is applicable.

For bubble attachment to take place, the inter-facial tension due to molecular forces at equilibrium must be in balance (Wang et al., 2005). This is given by the following equation (Vigneswaran, 2009):

$$T_{AS} = T_{WS} + T_{AW} \cos\theta \tag{2.8}$$

Here, T_{AS} is the inter-facial tension at the air-solids level (N/m), T_{WS} is the inter-facial tension at the water-solids level (N/m) and θ is the contact angle (Vigneswaran, 2009). Particulate matter flotation by the micro-bubbles can be described by the contact angle created between the particle and the adsorbed bubble. Water's cohesion energy should be larger than adhesion energy of water making the contact angle big enough and finite.

Bubbles Supplied

Stokes' law describes the rise velocity of the bubble-particle agglomerate, as given in the equation below:

$$V_{\rho b} = \frac{g(\rho_w - \rho_{pb})d^2}{18\mu} \tag{2.9}$$

Where, $V_{\rho b}$ is the particle-bubble agglomerate velocity (m/s), g is gravity acceleration (m/s), ρ_w is water density (kg/m^3), ρ_{pb} is the particle-bubble agglomerate density (kg/m^3) and μ is the particles dynamic viscosity at certain temperature (Ns/m). Bubbles in the DAF, attach to particles and create a buoyant force on the formed agglomerate which increases as more bubbles attach. As this process continues, a point is reached where this buoyant force becomes equal to or exceeds the particle's weight leading to the rise of the particle, given by Stokes' law. Air supplied in a DAF system has 3 basic measures - mass concentration, the concentration of the air-bubble volume and the number of bubbles. Mass concentration of the bubbles is the concentration of air bubble mass that is produced to meet the particle concentration demand (mg gas/ ml water). The volume of air-bubbles (ϕ_b) and the number of bubbles (N_b) can be derived as follows (Vigneswaran, 2009):

$$\phi_b = \frac{C_b}{\rho_{(air,sat)}} \tag{2.10}$$

$$N_b = \frac{\phi_b}{\frac{\pi d_(b^3)}{6}} \tag{2.11}$$

Here, ρ(air,sat) is the density of the water vapour saturated air (kPa) and d is the air bubble's mean diameter (cm) (Vigneswaran, 2009).

Recycle ratio is important to design and operate the DAF system. This is because the amount of air bubbles supplied due to the injection of the recycle water under pressure are a mix of water and water undergoing treatment. Generally, the recycles ration can be used as an approximate for the air supplied from a saturator at constant pressure. Recycle ratio (R) can be given as (Vigneswaran, 2009):

$$R = \frac{Recycle flow}{Influent flow} \tag{2.12}$$

Rise Rate

DAF and other flotation systems generally treat large amounts of water, thus making the retention time in the flotation tank an important parameter. The retention time is dependent on rise rate of the air bubbles which is calculated based on Stokes' law. Figure 2.7 and Table 2.5 show the general rise rates of bubbles in tap water and the calculated bubble rise velocity as a function of time. When comparing the rate of bubble rise in flotation systems to the coagulation-sedimentation systems systems, it was found that flotation systems required smaller unit area as compared to sedimentation (Jafarinejad, 2017). It is possible that bubbles rise velocity is taken as lower than reality due to collision with each other and entrapment in the flocs (Vigneswaran, 2009). In reality the rise velocities of the bubbles might be bigger than calculated by Stokes' law especially for bubbles greater than 150 mm as they are more elliptical and thus have less resistance to the flow (Ramirez, 1979). This paper further suggests, that with higher pressure, the size of micro-bubbles increases.

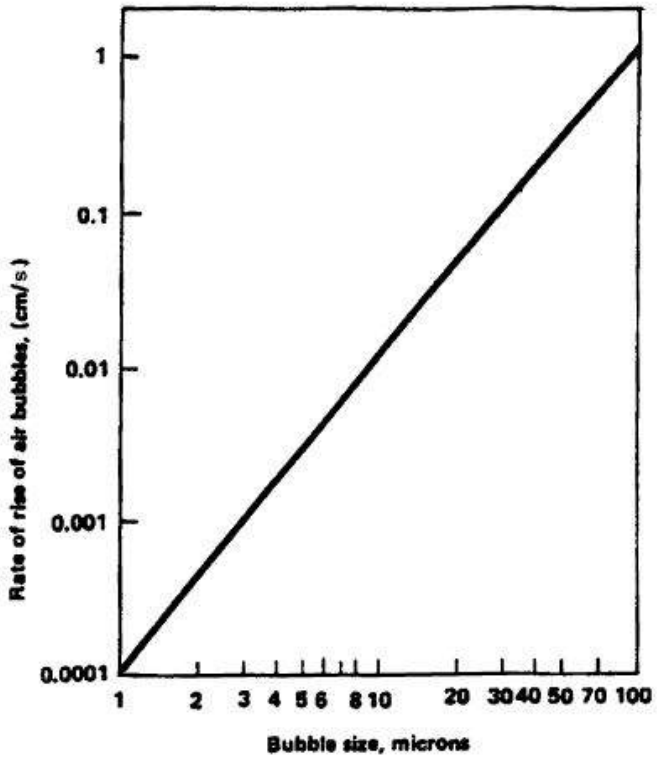

Figure 2.7: Rise rates of bubbles in water (Vigneswaran, 2009).

Bubble diameter (mm)	Upward vertical rise rate	
	(cm/s)	(ft/min)
0.2	1	2
1	15	30
10	25	50
50	55	110

Table 2.5: Bubble rise velocity as a function of time (Vigneswaran, 2009).

For activated sludge (91% solids) when exposed to air flotation, it has been found that their rate of bubble rise can range from 0.3 ft/min to 1.8 ft/min with increasing air content 3 fold (Katz and Geinopolos, 1967). Other literature has found activated sludge from wastewater showing initial up flow rise rates from 0.17 to 0.42 ft/min with dissolved air content being increased 4 fold. Furthermore, as the character of the waste water changes, the initial rise rate would also change (Eckenfelder and O'Connor, 2013). For pulp and page waste activated sludge, the initial rise rate was found to be 0.75 to 0.83 ft/min as the air-to-solids ratio was increased (Shammas, 2010). Oil and grease dominant wastewater form a poultry treatment plant have shown 2 rise rates with better solids removal that just a solids removal system and in line with small size bubble data (Woodward et al., 1977).

2.2.2. DAF Design Considerations

Literature recommends a plethora of different values for DAF design parameters. Most of them typically consider air to solids (A/S) ratio, air pressure, retention time, solids loading rate, hydraulic loading rate, suspended solids concentration and recycle ratio as important design parameters (Wang et al., 2005) (Vigneswaran, 2009). Table 2.6, 2.9, 2.8 and 2.7 give the design values found in literature.

Table 2.6: Design parameter values of the DAF (Shammas, 2010).

Parameter	**Range**	**Unit**
Air pressure in saturation tank	172-482	kPa
Air to solids ratio	0.01-0.1	kg/kg
Retention time		
Floatation tank	20-60	min
Pressurizing tank	0.5-3.0	min
Hydraulic loading	24.5-39	m^3dat/m^2
Recycle	5-120	%

Operation Parameter	Range
Solids loading, lb dry solids/hr/ft^2 of surface	
with chemicals	2–5
without chemicals	1–2
detention time (min)	3–60
Air-to-solids ratio	0.01–0.1
Blanket thickness (in.)	1–24
Retention tank pressure (psi)	25–70
Recycle ratio (% of influent flow)	5–50
Hydraulic loading rate	
gpd/ft^2	2880–7200
gpm/ft^2	2–5
Solids removal efficiency	
with flotation aid (% removal)	95
without flotation aid (% removal)	50–80
Float solids concentration (%)	2–10
Oil and grease removal efficiency	
with flotation aid (% removal)	85–99
without flotation aid (% removal)	60–80

Table 2.7: Significant design and operating parameters of the DAF (Wang et al., 2005)

Parameter	Variable
Flotation tank retention time	20–40 min
Air pressure	40–60 psi
Hydraulic loading	1–4 gal/min/ft^2 (including recycle)
Recycle ratio	10–60%

Table 2.8: Significant design and operating parameters of the DAF (Adams et al., 1981)

Here, the Air to Solid ratio (A/S), is a major design and operational parameter for dissolved air flotation, the performance of the DAF separation process increases dramatically with an increased A/S ratio (Wang et al., 2005). Another important parameter is bubble

Parameter	Variable
Air pressure	35–55 psi
Saturation retention time	2 min (based on recycle flow)
Air requirements	0.25–0.50 SCF/min/100 gal total flow
Flotation tank retention time	15–20 min (based on raw plus recycle flow)
Recycle rate	50% of raw influent feed rate
Hydraulic loading rate	3.0 gal/min/ft^2 (based on raw plus recycle flow)
Ph	7.5–8.5
Chemicals	25 mg/L alum (based on raw plus recycle flow)
Flotation tank depth	6–8 ft

SCF = standard cubic feet.

Table 2.9: Design basis for a recycle pressurization air flotation unit (Jafarinejad, 2017)

size. Bubble size, together with the concentration of supplied bubbles, in form of bubble volume concentration, and the number of bubbles per liter are fundamental parameters for the DAF process. The smaller the bubbles lower its up-flow velocity and therefore, the higher the chances to collide with particles/colloidal matter promoting their suspension. Additionally, a larger gas surface area per unit of volume is achieved when small bubbles are produced instead of bigger ones, allowing better contact possibilities between bubbles and particles. (Edzwald, 2010) Increasing the saturation pressure above 5 bars has a very little effect on bubble size and shape. Most bubbles formed in DAF have diameters below 100 m, rise as rigid spheres following Stokes' law and under laminar flow conditions (Edzwald, 1995). Bubble rising velocities can be calculated based on the Navier-Stokes equation.

However, some literature suggests that there is still a lot unknown about the DAF mechanism and it's rate controlling parameters (Adams, 1974). Based on some studies which concluded that DAF's performance can not be completely from conventional parameters like solids loading, hydraulic loading and availability of air, therefore it's recommended that the actual wastewater should be tested on a pilot scale before designing a full scale unit (Wang et al., 2005). One of the first compilation was published by (Jafarinejad, 2017) given in 2.9 where the parameters were quite specific. (Adams et al., 1981) in 1981 published similar data, however it wasn't that comprehensive. It is given in table 2.8 and gave values in the range of the publication before it. Then a comprehensive range was given by (Wang et al., 2005) as given in table 2.7.

Influent Feed Characteristics

When designing a DAF system, the first step is to evaluate feed stream characteristics. Information about the source of waste water and the range of solids concentration is required. An evaluation of the feed stream characteristics is recommended in order to estimate which aspects of the feed water could effect the solubility (eg. range to solution temperature, dissolved salts concentration etc.). (Vigneswaran, 2009) These aspects include :

1. Nature of particles: Specific gravity is an important property for the particle suspended in the waste water to be separated. This is shown by the fact that sand is difficult to be made afloat whereas activated sludge which has more volume or immiscible liquid such as oil floats more easily. (Wang et al., 2005)

2. Particle size: It is difficult to float very small particles, especially that are granular in nature and have high specific gravity. As the size of the particle increases, so does it's ability to float. Generally, addition of chemical coagulants combined with flocculation increases the size of the particle which results in improved floating. (Wang et al., 2005)

3. Influent composition: If the influent is more equalized in composition and flow, the performance of the flotation unit improves (Wang et al., 2005).

4. Dispersing agents: If the waste water contains unexpected chemical concentrations, the flotation system might be subjected to specific problems or in some cases advantages. For example, detergents or other such surfactants will alter the sludge particle's physical properties. Thus the type and quality of surfctant present in the waste water stream may positively or negatively influence the flotation results. (Shammas, 2010)

5. Influent Density: Density: Calculated as mass (kg)/ volume (l) density is one of the most important physical characteristic of any matter sample. As the numerical value of density of any pure substance would be constant at a certain temperature, it can be considered more important than other physical properties such as shape or size. Hence, it can be readily reproducible.

Air-To-Solids Ratio

As mentioned before, air to solids (A/S) ratio is one of the most important design parameters of the DAF and is needed to reach clarification to a certain degree by governing the rate of rise if particle-bubble agglomerates. It can be defined as the mass of air coming out of a pressurized system when pressure is reduced to atmospheric conditions (Shammas, 2010). Primarily, the DAF performance depends on this ratio - volume of air per mass of solids. Which means that amount of air need for flotation to take place is proportional to amounts of solids being added to the reactor. (Vigneswaran, 2009) Equation below gives the A/S ratio and the air solubility, operating pressure and solids concentration in pressurized system is given by (Vigneswaran, 2009):

$$\frac{A}{S} = \frac{1.3s(fP-1)}{S_a} \tag{2.13}$$

Where, A/S gives the air to solids ratio (ml air/ mg solids), s is the air solubility (ml/L), f is the fraction of dissolved air at a certain pressure P (generally 0.5), P is the pressure (atm), p is gauge pressure (kPa) and S_a is the suspended solids in the influent (g/m^3) Ṫable 2.11 gives the give air solubility in air based on temperature.

Table 2.10: Air solubility as a function of temperature (Vigneswaran, 2009)

Temperature (deg C)	**Volume Soluability**	**Weight Soluability**	**Density**
	ml/L	mg/L	g/L
0	28.8	37.2	1.293
10	23.5	29.3	1.249
20	20.1	24.3	1.206
30	17.9	20.9	1.166

This equation can also be written as (Shammas, 2010):

$$\frac{A}{S} = \frac{C_s}{X_f}(fP_a - 1) \tag{2.14}$$

Where, A/S gives the air to solids ratio (mg/mg), C_s is the solubility of air at a given pressure (1 atm) and temperature (mg/l), X_f is suspended solids concentration (mg/l), $P-a$ is the saturation pressure (atm) and f is the efficiency fraction of air (generally 0.8)

The efficiency of particle removal may be reduced if the optimum amount of air is not employed. On the other hand if too much air is supplied power is lost. Hence, optimization of this value is essential in DAF systems. The desired result of particle-bubble interaction in the DAF system is the reduction in net specific gravity of the agglomerate and thus increase in rise velocity. Rise velocity is described as per Stokes' law mentioned before which shows that with increase in the number of bubbles attaching to the aggregate, it's net density goes down, the rise velocity increases. (Shammas, 2010) In thickening, higher removal efficiencies are seen with higher A/S ratios (Vigneswaran, 2009). For a certain A/S ratio, the amount of air required to float solids is dependent on the operating pressure to dissolve more air increases with increasing the pressure up to a certain extent. This can also be done by increasing the pressurized liquids volume and decreasing the pressure (Vigneswaran, 2009).

For a recycle pressurized system, majority of the air is sent to the recycle stream and suspended solids are in the waste water stream. This is given by a modified equation (Shammas, 2010):

$$\frac{A}{S} = \frac{RC_s}{Q_x X_f}(fP_a - 1) \tag{2.15}$$

Where R gives the recycle flow rate (gpm) and Q is the raw water flow rate (gpm). Table gives some examples of A/S ration used.

Author	Air/solids ratio	Wastewater system	Influent suspended solids concentration (mg/L)
Beisinger et al. (53)	0.026	Poultry processing	900
	0.020	Poultry processing	1,300
	0.020	Beef packing	2,000
	0.007	Beef packing	5,000
	0.07	Soybean oil	200
	0.7	Refinery	50
Steiner (51)	0.02–0.12	Refinery	50 (oil)[a]
Reed and Woodward (54)	0.12[a]	Poultry processing	43–273
Abo-El Ela and Nawar (55)	0.008[b]	Soap factory	1,100 (oil)
Zimmerman and Jacquez (56)	0.006	Poultry processing	250 (SS) 4,000 (O & G)
McIntyre (57)	0.02	Parts manufacturing	–
Moursy and El-Ela (58)	0.001	Refinery	56
Average	0.08 (or 0.03 if one very high value is not included)		

[a]Pilot-plant scale.
[b]Optimum value.

Table 2.11: A/S ratio for different treatment plants (Shammas, 2010)

Hydraulic Loading Rate (HRL)

As mentioned before, vertical rise rate (V_T) in induced to particles due to the attachment of air bubbles. For this particle to float it needs to have enough rise velocity in order to travel the width depth of the flotation tank in a certain retention time. Therefore, this rise rate must at least be equal to the depth divided by retention time, or flow rate divided by surface area:

$$V_T = \frac{D}{Q} = \frac{Q}{A_s} \tag{2.16}$$

Here, V_T give the suspended solids rate of rise (m/s), D is the flotation tanks effective depth (m), T is the retention time (s), Q is the flow rate of the influent (m^2/s) and A_s is the flotation tanks surface area (m^2). This ratio gives hydraulic loading which is an important design parameter. In theory, any particle with the same or greater rise rate than the hydraulic loading will float and be removed in ideal floating tank conditions. (Vigneswaran, 2009)

Solids Loading Rate (SLR) and Surface area

Solids loading, expressed as kg dry ss/h/m^2, is defined as suspended solids dry weight per unit time per meter square surface area of flotation. With an increase in the solids loading rate the concentration of flotation decreases. SLR is in the allowable range when minimum solids flux is reached within the concentration range of solids. This makes flux a function of concentration of solids, desired concentration of float and the added chemicals. To calculating the effective surface area of a DAF system, the effective surface loading rate of solids and hydraulic surface loading rate should be known. Thus, the required area can be calculated from solids rise velocity, concentration of solids, targeted thickness degree and solids loading rate. (Vigneswaran, 2009)

Chemical Usage

Chemical addition has become almost synonymous with air flotation systems. From an early stage of the development of this technology, the important role of chemicals to break emulsions and form flocs was understood. Various studies were done to compare the efficiency of a DAF unit with and without chemicals (Shammas, 2010). Waste water with a recycle DAF system from a beef packing plant was sampled and tested with and without the addition of chemicals. In this study it was found that without the addition of chemicals, a particle removal efficiency of 73% was reached, whereas when 10 mg/l of alum was added the removal efficiency reached 86% (Biesinger et al., 1974). Experiments done with refinery waste water showed a similar trend. Without chemicals 65% of the particulate matter was removed and with chemicals this reached up to 79% (Pearson, 1976). Figure 2.8 give the comparison of refinery waste water subjected to air flotation with and without chemical Alum (aluminium sulphate), ferric chloride, inorganic and organic polymers are the most common chemicals added to aid air floating. These attach better to air bubbles as they demonstrate surfactant properties. The is a particular effect of polymers on the DAF removal efficiency. These Polyelectrolytes substantially increases the particles size present in the waste water thus improving flotation and separation rate. This may further lead to a decreased size of the DAF tank, reducing the recycle back to the system. (Shammas, 2010)

Calcium hydroxide is used as flocculant in water and wastewater treatment. It helps produce clearer effluents by charged solids that removes smaller particles from the water. It is known to be lower in cost and toxicity than other coagulants. Additionally, in fresh

Treatment process	Removals (%)			
	Oil	SS	COD	BOD
DAF				
Without chemicals	65	55	30	33
With 2 mg/L polyelectrolyte	79	75	42	40
IAF				
Without chemicals	93			
With chemicals	96			

Figure 2.8: Comparison of refinery waste water subjected to air floatation with and without chemicals) (Shammas, 2010).

water treatment it is used to raise the pH, avoiding corrosion of pipes when water is acidic. (Wikipedia contributors, 2019)

Retention Time

In literature, DAF loading data has been reported in hydraulic loading (gal/min/ft2) terms. It can then be related to retention time based on available data. Table 2.12 gives retention time and other design parameters for the DAF (Shammas, 2010). These values show that the retention time should be 10 - 60 minutes for a DAF flotation chamber. Therefore, considering the process water characteristics and the floating tank performance, flotation units are usually designed for a retention time of 3 - 60 min (Wang et al., 2007). When plot-

Air pressure in saturation tank (psi)		
Adams et al. (60)	40–60	
DeRenzo (82)	25–70	
Beychock (45)	35–55	
Wang et al. (2)	25–75	
Retention time (min)	Flotation tank	Pressurization tank
DeRenzo (82)	20–60	0.5–3.0
Beychock (45)	15–20	2
API (85)	10–40	1–2
Wang et al. (2)	3–5	0.17
Hydraulic loading (gal/min/ft^2)		
Adams et al. (60)		1–4
Beychock (45)		3–0
API (85)		2–2.5
Wang et al. (2)		3.5–5
Air requirement (SCF/100 gal)		
Beychock (45)		0.25–5.0
API (85)		0.5–1.0

SCF = standard cubic feet.

Table 2.12: Retention time and other design ranges for the DAF) (Shammas, 2010).

ting the degree of removal to the surface lading, we see that the curve sharply breaks in the upward direction as solids loading rate becomes more than 2.5 gal/min/ft2 (Adams et al., 1981). For batch studies, retention time is considerably important. Studies have found that for maximizing COD removal, 7 min of residence time was optimum (Moursy and El-Ela,

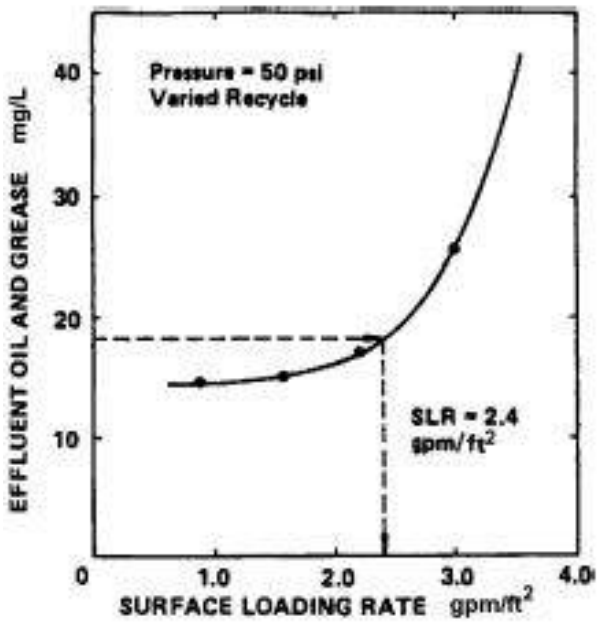

Figure 2.9: Effect of surface loading rate on effluent quality) (Shammas, 2010).

1982), for waste water electrolytic desalting and removal in a DAF batch test, 4 min was the best (Pearson, 1976), and for general DAF design 3-5 min is optimal (Wang et al., 2007).

Tank Shape and Float Removal

The shape of an air floating tank can be either circular or rectangular, with circular being more popular (Shammas, 2010). Equipment manufactures like Krofta, recommend that the circular design is more efficient because of its circular construction that saves cost, ability to maintain low velocity in the active flotation zone, less lubrication and maintenance requirement because of pivoted arm skimmer and possibility of addition of bottom scrapers at low cost. Advantages of a rectangular design include - space conservation, standardisation of size for shipping and erection and eliminating the need for bottom scraper due to a hopper bottom. (Shammas, 2010) The flotation tank can be made shallower if there is a more even distribution of the water flow and micro-bubbles, with a average depth of 4 - 9 ft (De Renzo, 1981) (Jafarinejad, 2017) (Wang et al., 2007). When designing a mechanism to remove the float in the DAF, it should be designed to the carry over of water adequately. Factors that should be considered are submergence depth, mechanism of scooping and scoop speed.

2.3. Application of DAF

In the waste water treatment system, the DAF can find application in primary treatment, secondary treatment, tertiary treatment, Industrial waste water treatment and bio-solids treatment. Table 2.13 gives the removal efficiencies of constituents from primary and secondary treatment. DAF is used in primary treatment to remove suspended solids. From the table it can be seen that primary treatment can remove up to 90% suspended solids, 30% of organic carbon, 10% of organic nitrogen, and around 15% of total phosphorus (Krofta and Wang, 1982). In secondary treatment, biological processes are used to remove organics by

Parameter	Concentration (mg/L except as noted)		Removal (%)	
	Range	Typical	Primary	Secondary
Physical				
Total Solids	350–1,250	750		
Settleable solids	50–200	100	90	
Total suspended solids	100–400	250		50–90
Volatile suspended solids	70–300	150		60–90
Total dissolved solids	250–850	500		5
Volatile dissolved solids	100–300	150		30
Chemical				
pH, unit	7–7.5	7.0		
Calcium	30–50	40		
Chlorides	30–85	50		
Sulphate	20–60	15		
Organic carbon				
BOD_5	100–400	250	10–30	>90
COD	200–1,000	500	10–30	70–80
TOD	200–1,100	500	10–30	70–80
TOC	100–400	250	10–30	60–80
Nitrogen				
Total (as N)	15–90	40		35
Organic	5–40	25	10	50–80
Ammonia	10–50	25		0–20
Nitrites			Produced	
Nitrates			Produced	
Phosphorus				
Total (as P)	5–20	12	0–15	20–40
Organic	1–5	2		
Inorganic	5–15	10		

Table 2.13: Removal domestic waste water constituents in primary and secondary treatment) (Krofta and Wang, 1982).

bio-chemical methods and oxidation. Here DAF is applied as a secondary clarification unit. As given in the table, secondry treatment can remove about 90% of suspende matter, 30% if dissolved volatile solids, more than 90% BOD, 80% COD, TOC and nitrogen. For bio-solids removal, the DAF is used for sludge thickening. (Shammas, 2010)

2.4. Design of Experiments (DOE)

A Design of Experiments (DOE) approach was used for the DAF experiments done in this thesis. DOE was first developed by Sir Ronald Fisher in the 1920s in England. He initially experimented with various fertilizers and their effect of plots of land. Through this method he showed the effect of different factors apart from fertilizer, like soil condition, moisture content etc. on the final crops condition in the land plots. This way by using DOE he showed the effect of different factors. Since then DOE has been used for a wide variety of applications. (Antony, 2014) DOE is process encompass the planning, designing and analysing experiments to draw objective and valid conclusions efficiently and effectively. It helps draw conclusion from experiments which are sadistically sound by integrating powerful and simple statistical methods within the experimental design methodology. (Del Vecchio, 1997) Figure 2.10 shows the general layout of a DOE process system Here, output represents performance characteristics which measure the performance to the product or process. X's represent control variables which are varied in the experiment and Z's are the uncontrollable variables. Unlike the one factor at a time (OFAT) methodology, a DOE design helps estimate the optimal settings of X's to reduce the effect of Z's eliminates bias and it fundamental to a robust design (Roy, 2001). In practice this methodology is implemented by first making a 'black box' model with many continuous or non-continuous factors that can be controlled (varied in the experiment) and one or more response outputs. Experimental

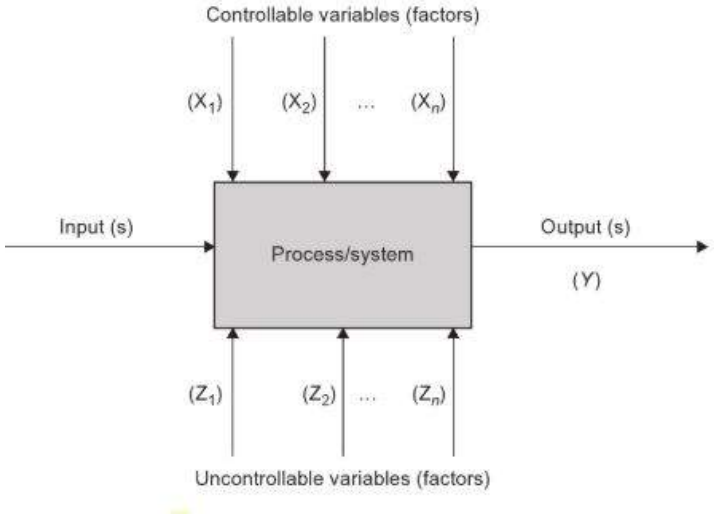

Figure 2.10: General layout of a DOE process system (Antony, 2014).

data based on this model is collected and an empirical simulation (generally first or second order) is derived linking the outputs to the inputs. (NIST, 2019)

Figure 2.11 gives an overview of the Experimental designs tools to use for experiments. This shows that DOE can be classified in 2 broad classification - Screening Design and Optimization Design (Response Surface Design (RSM)) (Sahu et al., 2018). As for the DAF

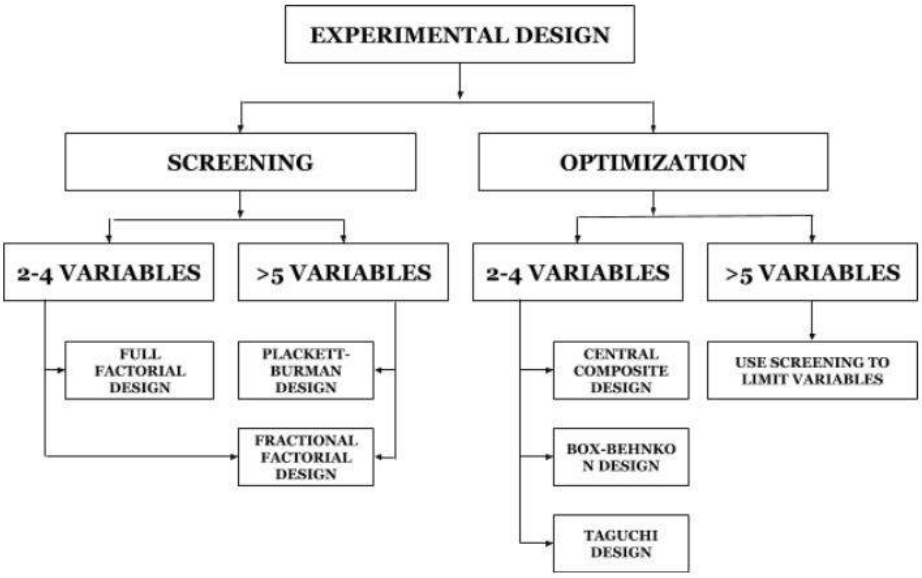

Figure 2.11: Experimental design classification (Sahu et al., 2018).

experiments there are a large number of directly or indirectly influencing factors, screening can be a powerful tool to narrow them down. This process helps highlight the most important factors and their interaction with other factors (Sahu et al., 2018). Frequently used screening designs include - Fractional Factorial Design (FrFD), Full Factorial Design (FFD) and Plackett-Burman Design (PBD). These designs allow screening of many factors

with less number of experiments. (Dejaegher and Vander, 2009) For this thesis the PBD design was chosen and investigates because of it's 2-level design and ability to identify many significant factors out of a large number of particles.

The original Plackett-Burman (1946) designs are two-level fractional factorial designs for studying factors in runs, where is a multiple of 4. If is a power of 2, these designs are identical to those of fraction factorial. However, for other cases, the Plackett-Burman designs are sometimes of interest.

2.5. Particle characterization using ImageJ - Fiji

Particle size, shape and size distribution are some important parameters that can help characterize solid, liquid and gas samples. In the fields of medicine and electronics, image analysis technologies like microscopic imaging have been used extensively. Recently, these techniques have found their way in to the civil engineering fields (Coster and Chermant, 2001). In wastewater treatment, image processing is used for monitoring activated sludge, correlating parameters like sludge volume index and mixed liquor suspended solid in filamentous bulking and many other such applications. This process comprised of acquiring the image (e.g. through a digital microscope), image processing and ext ration of quantitative and qualitative data using image analysis techniques and software (Khan et al., 2015). To determine particle sizes, there are many approaches, techniques and commercial equipment available. According to (Gregory, 2005), a 'universal' method is not known which can be applied over the whole size range of particles and the selection of methods should based on determined by the nature of suspension. Broadly there are 6 methods to determine particle sizes in water - Direct method (microscopy), Particle counting and sizing, Static light scattering, Fraunhofer diffraction, Dynamic light scattering and Sedimentation method (Gregory, 2005).

In this study, direct method using microscopic imaging was used because of its advantage of clear and apparent observation of particle shapes and morphology, and also as it was the best method available for field measurements. This method analyses particles in water taken with a high resolution microscope using a specialized image processing software (ImageJ - Fiji in this case). The software calculates statistical area and pixel values based on selections defined by the user. It has the ability to measure angles, distances, create line profile plots and density histograms. Furthermore, standard image processing functions like edge detection, sharpening, contrast manipulation, median filtering and smoothing are also supported by the software (Ferreira and Rasb, 2012). This research employed this software to understand and estimate the size and morphology of particles being removed by DAF from different influents and their relation to the operating parameters.

2.6. Particle Image Velocitimetry (PIV)

The process of flotation can be seen as made up of 2 part in 2 levels running in parallel - macroscopic level (influenced by tank geometry and flow pattern) and microscopic level (aggregate formation takes place because of bubble floc interaction) (Bondelind et al., 2013). An important process at the microscopic level is the floc-bubble aggregation and in recent literature it has been shown that in a flotation system, larger floc-bubble aggregates may be formed as a result of several bubbles attaching to flocs leading to a phenomenon

named as clustering (Leppinen and Dalziel, 2004). Even thought the formation of these aggregates in a microscopic mechanism, but they are a significant influence on the flow at the microscopic level due to their size, shape and buoyancy. Therefore, many parameters have an effect on the flotation process including influent flow, tank dimensions, rising velocity of the bubbles and aggregates, and the floc/bubbles surface properties, and these in turn effect the overall removal efficiency (Bondelind et al., 2013). It is important to understand both these levels to optimize the DAF performance thus, for inestigating the DAF performance these parameters need to be taken into account. Literature states that investigating and evaluating efficency of these DAF parameters are challenging and expensive when it comes to its construction and carrying capacity therefore non-invasive or modelling methods might be a tempting option.

Particle Image Velocitimetry (PIV) is described as an non-invasive method utilizing visualization that offers qualitative and quantitative flow visualization. Detailed information about this process can be found at (Thielicke, 2014). Furthermore, to analyse PIV measurements, a free Matlab software is available which was used to identify bubble velocity and bubble flow for the DAF experiments performed in this thesis. Video-graphic flies are first converted into a string of consecutive images on Matlab. These consecutive images are then processed in the PIV software to give determine velocity profiles. Thus, by using PIV a velocity map can be obtained by measuring the shift in particles between consecutive frames in a known time interval.

2.7. Removal of Pathogens

In developing countries, bacteria such as *E-coli*, and protozoa including *Giardia* and *Cryptosporidium* act as etiologic carriers for water-borne disease outbreaks and need to be controlled to minimize possible transmission routes. To complete their life-cycle, they need a host and even ingesting small quantities of *Cryptosporidium oocysts* or *Giardia cysts* can cause excessive diarrhea or lead to death for an immuno-compromised person. (Andreoli and Sabogal-Paz, 2019) *Giardia* and *Cryptosporidium* are parasites which have been found important in many water borne disease outbreaks in the world (Baldursson and Karanis, 2011). Recently, research has shown that the *Cryptosporidium* gene might even have the ability to reproduce in aquatic bio-films(Koh et al., 2013). Moreover, they have been found to have the ability to survive in environment for long and even known to be resistant to common disinfectants (Korich et al., 1990). In Asia, a high parasite prevalence was found with increase contact between animals and humans and in areas were there was poor sanitation (Mahmoudi et al., 2017). These organisms can be found in domestic sewage, after anaerobic treatment, food crops, ground water and even in water supply and due to lack of data about these parasites in the drainwater, accurate risk assessment models can not be developed which results in overlooking the need to control these. (Santos and Daniel, 2017b) To the authors knowledge there is no literature on the performance of DAF with drainwater, and the closest wastewater that can be considered is municipal wastewater. Although the DAF has been used for treating municipal wastewater for many years, the pathogen removal efficiency of the DAF from this wastewater has very little documentation. (Koivunen and Heinonen-Tanski, 2008).

In literature, it has been demonstrated that bacteria, along with algae and other microorganisms have shown the ability to concentrated in the froth or foam in flotation (SMITH,

1989). Many papers have report the ability of the DAF to remove micro organisms with protozoan cysts, the earliest study reported was by (Hall et al., 1995). With optimal coagulant dosage, DAF has shown removal of 85% (0.82 log) till 99.9% (3 log) depending on coagulant specifications. (Edzwald et al., 2000) in pilot studies has found DAf effective in removing *Giardia lamblia cysts* and *C. parvum oocysts* as well. DAF is also known to be more effective in removing *Cryptosporidium oocysts* and *Giardia cysts* as compared to sedimentation. For conventional DAF rates, 2-3 log removal can be achieved as compared to 1-2 log removal by sedimentation. Moreover, the DAF process acts as a filtration and polishing step as it removes most of the pathogens. These pathogens are concentrated in the floated sludge.(Edzwald, 2010) This thesis investigates the possible removal of *E-coli* and *Clostridium Perfringens* (*C.perfringens*) (as a surrogate for protozoan (oo)cysts) from DAF treatment at the lab and site scale. Figure 2.12 give the size ranges of particles and organisms captured by DAF and other treatment technologies.

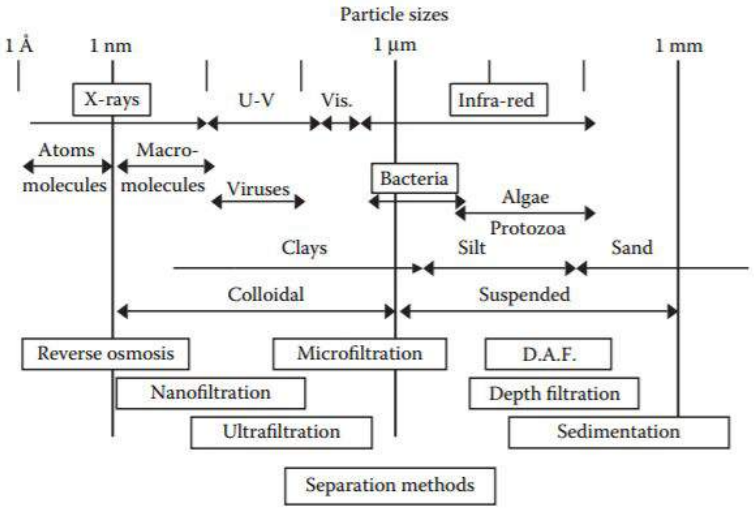

Figure 2.12: Range of particle and microorganism sizes in comparison to water treatment removal technology (Gregory, 2005).

3

Material and Methods

This section elaborates on the materials and methodology used to investigate DAF performance with the different influents. Experiments were constructed, designed and analyzed in 2 phases - the laboratory phase (at TU Delft) and the site phase (at the LOTUS^{HR} site). Furthermore, for each phase 2 different influents were tested for comparison - canal water and anaerobic sludge from Harnaschpolder waste water treatment plant in Delft, and Barapullah drain water in New Delhi and anaerobic sludge from Okhla waste water treatment plant in Delhi respectively. Samples collected from these 2 experimental setups were then analyzed for TSS removal efficiency and influent characteristics. Additionally, at the Barapullah site PIV measurements and pathogen tests for *E-coli* and *C. Prefringens* were also done. For Phase 1 the experiments and analysis were conducted at the Water Lab at TU Delft (Building 23 Stevinweg 1 2628 CN Delft, the Netherlands) and for Phase 2 the DAF experiments were done at the LOTUS^{HR} site laboratory at Barapullah, New Delhi and the analysis were done at the TERI (The Energy and Resources Institute) Laboratory in New Delhi.

3.1. Influents

For each phase 2 different influents were tested - Canal water and anaerobic sludge from Harnaschpolder waste water treatment plant in Delft, and Barapullah drain water in New Delhi and anaerobic sludge from Okhla waste water treatment plant in Delhi respectively. For the canal water and Harnaschpolder sludge, the influents were diluted to the required TSS value to simulate the condition from the Barapullah drain. Canal water was collected form the canal next to the laboratory in Delft using a scooping bucket. Sediments from the bottom of the canal were intentionally collected with the bucket to add suspended matter to the canal water samples. The collected canal water was then diluted to the TSS level obtained form the Barapullah drain data (See Appendix C). For the Harnaschpolder sludge, it was sieved with a 0.71 mm sieve, diluted to hace similar TSS conditions as the AD at the Brapullah site (10g/l) and incubated. This was done to make sure the pipes didn't clog. Both these influents were also subjected to coagulation and flocculation before starting the DAF experiments. They were placed in 6 beakers and coagulants ($CaOH_2$ and cellulose) were added in 1:1 ratio as per the experimental design. These were subjected to fast rotation (100 rpm) for 1 minute and slow rotation (40 rpm) for the remaining coagulation time designed,

to replicate industry standards. Additionally, these influents were also heated in a water bath to simulate Barapullah temperature before being pumped into the DAF.

At the site, the drain water was collected in buckets from the pipe pumping it straight from the drain. It's temperature and turbidity was recorded and it was then placed in Jerry cans and manually stirred during the experiment. Similar type of coagulation and flocculation as the laboratory setup was done before starting the DAF experiments to meet the experiment design considerations. The Sludge from Okhla was also dilute and sieved, same as the Harnaschpolder sludge to avoid sever clogging of the pipes.

3.2. DAF Experimental Design

Based on the design of experiments in chapter 2, an experiment matrix based on the Plackett Buramn Design (PBD) for the 2 phases of experiments was designed. These were based on the critical DAF parameters identified and the 2018 data available from the Barapullah drain (Appendix C). Table 3.1, 3.2 and 3.3 give the experimental design created for the 2 phases of the experiments.

Table 3.1: Experiment design for the canal water.

Run	TSS (mg/l)	Temperature (degC)	Retention time (min)	pH	Pressure (bar)	Coagulant (g/l)	Time Coagulation (min)
1	30	29	13	7.6	5	0.5	10
2	30	29	13	6.7	3	0.005	10
3	30	35	13	6.7	3	0.5	30
4	30	35	20	6.7	5	0.005	10
5	30	35	20	7.6	3	0.5	30
6	30	29	20	7.6	5	0.005	30
7	270	32	16.5	7.15	4	0.2525	20
8	270	32	16.5	7.15	4	0.2525	20
9	270	32	16.5	7.15	4	0.2525	20
10	510	35	13	7.6	3	0.005	10
11	510	35	13	7.6	5	0.005	30
12	510	29	13	6.7	5	0.5	30
13	510	29	20	7.6	3	0.5	10
14	510	35	20	6.7	5	0.5	10
15	510	29	20	6.7	3	0.005	30

For these designs, the independent variables and critical DAF parameters were TSS, temperature, pressure, coagulant, time of coagulation, pH and retention time which were studied at 2 levels and 3 center point repetitions (+1,0,-1). The ranges of these variables are given in table 3.4 which resulted in 15 experiments for each influent.

The analysis of the experimental data was performed using the Statstica 7.0 software. Test factors of X_i were coded as x_i and are given in the following equation

$$X_i = (X_i - X) = \delta X \tag{3.1}$$

Where X_i is the value of the independent variable, x_i is the coded value of the variable X_i, X_0 is the value of Xi at the center point, and δ X is the step change value. A linear model was used to optimize the media compositions using the significant coded values as shown below;

$$Y = b_0 + b_1 x1 + b_2 x2 \tag{3.2}$$

Table 3.2: Experimental design for Barapullah drain water

Run	TSS (mg/l)	Retention time (min)	Pressure (bar)	Coagulant (g/l)	Time Coagulation (min)
1	30	20	5	0.005	30
2	30	20	5	0.5	10
3	30	13	5	0.5	30
4	30	13	3	0.5	30
5	30	20	3	0.005	10
6	30	13	3	0.005	10
7	270	16.5	4	0.2525	20
8	270	16.5	4	0.2525	20
9	270	16.5	4	0.2525	20
10	510	13	5	0.005	10
11	510	20	3	0.5	10
12	510	13	5	0.5	10
13	510	20	3	0.5	30
14	510	20	5	0.005	30
15	510	13	3	0.005	30

Table 3.3: Experimental design for anaerobic sludge for both phases.

Run	TSS (g/L)	Temperature (C)	Retention time (min)	pH	Pressure (bar)	Coagulant (g/L)	Time of coagulation (min)
1	5	25	20	7	3	0.005	30
2	5	35	13	8.5	3	0.005	10
3	0.5	35	20	7	5	0.005	10
4	5	25	20	8.5	3	0.5	10
5	5	35	13	8.5	5	0.005	30
6	5	35	20	7	5	0.5	10
7	0.5	35	20	8.5	3	0.5	30
8	0.5	25	20	8.5	5	0.005	30
9	0.5	25	13	8.5	5	0.5	10
10	5	25	13	7	5	0.5	30
11	0.5	35	13	7	3	0.5	30
12	0.5	25	13	7	3	0.005	10
13	2.75	30	16.5	7.75	4	0.2525	20
14	2.75	30	16.5	7.75	4	0.2525	20
15	2.75	30	16.5	7.75	4	0.2525	20

Table 3.4: Ranges of the operating parameters used to design the DAF experiments.

Canal and Drain Water			**Anaeroic Sludge for Both Phases**		
Parameters	**Ranges**	**Source**	**Parameters**	**Ranges**	**Source**
TSS	30 - 510 (mg/l)	Barapullah Drain data (2018)	TSS	5 - 25 (g/l)	
Recycle Flow	5-50 (%) 6-12 (%)	Wang (2005) Edward (2010)	Recycle Flow	5-50 (%) 6-12 (%)	Wang (2005) Edward (2010)
Temperature	29 - 35 deg C	Barapullah Drain data (2018)	Temperature	25 - 35 deg C	Barapullah Drain data (2018)
A/S ratio	0.002 - 0.05 gAir/gTSS	Wang (2005)	A/S ratio	0.002 - 0.05 gAir/gTSS	Wang (2005)
pH	6.7 - 7.6	Barapullah Drain data (2018)	pH	7 - 8.5	
Pressure	2 - 6 bar 4-6 bar	Wang (2005) Edward (2010)	Pressure	2 - 6 bar 4-6 bar	Wang (2005) Edward (2010)
Coagulant amount	0.5 - 2g/l	Haydar (2009)	Coagulant amount	0.5 - 2g/l	Haydar (2009)
Coagulant time	10 - 30 min	Wang (2005)	Coagulant time	10 - 30 min	Wang (2005)
Retention Time	13 - 20 min		Retention Time	13 - 20 min	
Solids Loading (without chemicals)	0.0027- 0.0067 kg/sm2	Wang (2005)	Solids Loading (without chemicals)	0.0027- 0.0067 kg/sm2	Wang (2005)
Hydraulic Loading	6 - 18 m/h	Edward (2010)	Hydraulic Loading	6 - 18 m/h	Edward (2010)

Where Y is the predicted response; b_0 is a constant, x_1, x_2 and so on are the dependent variables, b_1 and b_2 are the linear coefficients for the dependent variables. The rows in the tables above represent the 15 different experiments and each column represents a different variable. For each independent variable, a high (+) or low (-) level was examined. Table 3.5 gives the design for showing the code for each factor on the perimeters.

Table 3.5: Plackett–Burman design for effect of factors in canal water, drain water and anaerobic sludge experiments experiments.

Run	**TSS (mg/l)**	**Temperature (degC)**	**Retention time (min)**	**pH**	**Pressure (bar)**	**Coagulant (g/l)**	**Time Coagulation (min)**
1	1	-1	1	-1	-1	-1	1
2	1	1	-1	1	-1	-1	-1
3	-1	1	1	-1	1	-1	-1
4	1	-1	1	1	-1	1	-1
5	1	1	-1	1	1	-1	1
6	1	1	1	-1	1	1	-1
7	-1	1	1	1	-1	1	1
8	-1	-1	1	1	1	-1	1
9	-1	-1	-1	1	1	1	-1
10	1	-1	-1	-1	1	1	1
11	-1	1	-1	-1	-1	1	1
12	-1	-1	-1	-1	-1	-1	-1
13	0	0	0	0	0	0	0
14	0	0	0	0	0	0	0
15	0	0	0	0	0	0	0

After running the experiments in each design the effect of variables was calculated and then according to the sign and magnitude of the effect, the next level was chosen. When the sign of an effect is positive that means that on increasing the level of the concerned variable the response would also be positive. The magnitude of the effect also shows the size of change to be considered in the next design. For the negative sign then the same is true but with the opposite meaning. The values of optimum were chosen from the design where the effect was calculated to be a minimum.

3.3. DAF Experimental setup

As mentioned, the DAF experiments for this thesis were conducted in 2 phases - the laboratory and the site phase. The underlying setup for DAF experiments in both the phase was the same as for the phase 2, parts of the same setup were shipped and reassembled at the site in New Delhi, with the only difference being the air compressor. For the laboratory set up the sir compressor was single line of 7 bar compressed air, whereas at the site Hitachi EC68 electric air compressor of 1.5 HP and a capacity of 24 l was used. Figure 3.1 depicts the schematic diagram for both the setups.

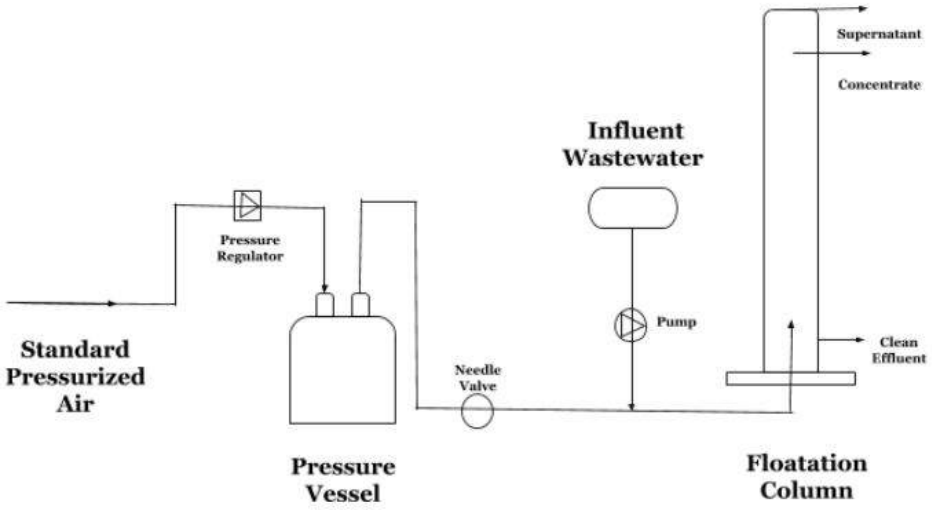

Figure 3.1: Schematic representation of the DAF set up used in both phases.

For operating the DAF, the air compressing switch/unit is first switched on. This gives a constant supply of 7 or 8 bar pressure which is connected to a pressure regulator (FESTO Pressure regulator LR/LRS) which is then connected via a valve (Festo HE Series Pneumatic Manual Control Valve, PBT) to the inlet of the pressure vessel containing 5 liters of tap water. At this point the outlet of the pressure vessel is closed using a valve. Then, by adjusting the pressure regulator to the desired pressure (3,4 or 5 bar), the amount of air introduced in to the pressure vessel is regulated. The pressure vessel is a sealed container with provision for inflow and out flow connections (Thielmann stainless steel pressure containers).

As pressure starts accumulating in the pressure vessel, it is is then mixed vigorously by hand for 5 minutes to make sure the water present in it is pressurized equally and the gas concentration in the water reachs equilibrium state. Once this is prepared, the waste water/sludge to be tested in the DAF column is put in a 5L Jerry can ready to be pumped (Watson Marlow 520s) into the system. The outlet form the pressure vessel then flows to a needle valve which regulates the pressurized white water flow into the column. A pipe from the needle valve then connects with the outlet pipe from the pump pumping the waster water/ sludge to the 20 L column. These 2 outlet pipes connect to a T-valve after which a single pipe from the the T-valve is connected to the bottom right inlet of the flotation tank. This is the inlet connection to the flotation column from where the pressurized whitewater

and the waste water will enter. For each run the column is filled with 20 L of tap water which acts a medium for the bubble rise and particle-bubble agglomerated to take place, and the needle valve and pump are calibrated to maintain the designed flow rates/recycle ratio for all the runs. The flow rate values and the retention times for the runs are is given in table 3.6 and 3.7.

Table 3.6: Flow rate values for the pump delivering the waste water and for the pump delivering the wastewater.

Needle Valve flow rates (white water)			**Sludge pump flow rate**			
Time (s)	Volume(ml)	Fow rate (ml/s)	Time (s)	Volume(ml)		Fow rate (ml/s)
20	89.00	4.45	20	85.30	89.00	4.45
40	182.40	4.67	40	173.50	88.20	4.41
50	275.40	4.65	50	261.10	87.60	4.38
Average		4.59	Average			4.41

Table 3.7: The 3 different retention time values for all the DAF experiments

Retention Time (min)	
20 minute runs	
Start	0.00
Open Clean effluent	5.00
Close Clean effluent	10.10
Stop experiement (pump and valve from pressure vessel)	13.30
open concentrate valves	15.00
Expected experiment end time	20.00
13 minute runs	
Start	0.00
Open Clean effluent	3.30
Close Clean effluent	7.30
Stop experiement (pump and valve from pressure vessel)	9.30
open concentrate valves	10.30
Expected experiment end time	13.00
16.5 minute runs	
Start	0.00
Open Clean effluent	4.15
Close Clean effluent	9.00
Stop experiement (pump and valve from pressure vessel)	11.15
open concentrate valves	12.45
Expected experiment end time	16.30

To start each batch run, the valve at the outlet of the pressure vessel and the pump to pump the waste water are opened/started simultaneously. At this time the stop watch is also started to record and maintain the designed retention time. When the experiment is completed as per the experimental design, the influent, clean effluent and concentrate samples are stored for further analysis. Next, the reactor is emptied, washed with tap water and the process is repeated for remaining experimental design runs. Figures 3.2 and 3.3 show pictures of the set ups at the lab and site.

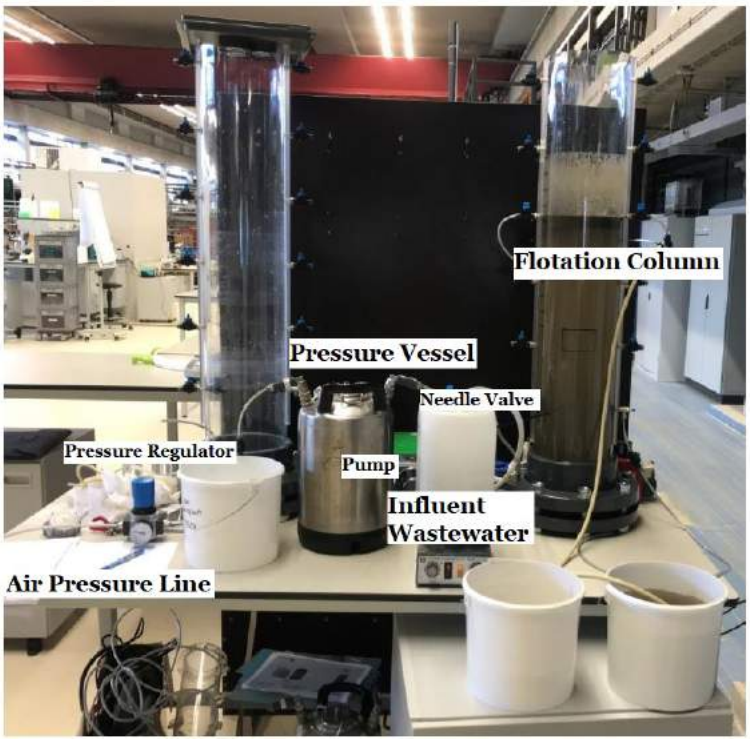

Figure 3.2: Laboratory DAF set up.

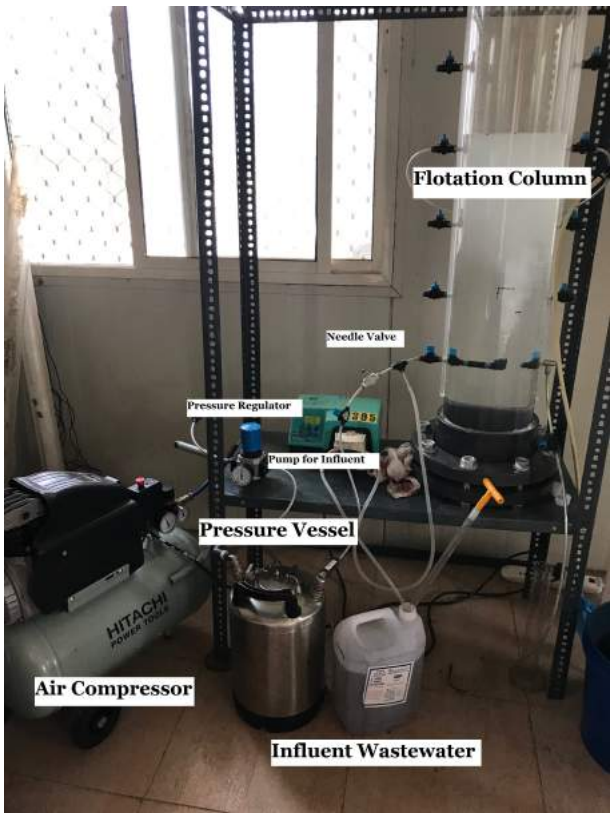

Figure 3.3: DAF set up at the LOTUS^{HR} site in New Delhi

(a) Filters showing the TSS retained after oven drying (105 °C) for the Barapullah drain water.

(b) Filters showing the TSS retained after oven drying (105 °C) for the canal water.

Figure 3.4: Filters showing the dried solids in done for TSS measurement.

3.4. Analytical Measurements

3.4.1. TSS measurements

TSS was measured at the laboratory and at the site based on the APHA method (APhA, 1998). Figure 3.4a and 3.4b give the images for the TSS measurements done at the lab and at the site. Other analytical analysis done including density which can be found in Appendix D.

3.5. Particle Characterization using ImageJ - Fiji

As mentioned in Chapter 2, microscopic image analysis is a very useful tool to understand the particle characterization and morphology of wastewater samples in more detail. In this thesis, microscopic images of canal water, drain water and anaerobic sludge from Okhla wwtp in Delhi were analysed to gather data regarding their size distribution and morphology. This information can help us further understand the affect of different influent particle characterization and morphology on the operation of the DAF. For canal water high-definition images (up to 3200x2400 pixels) were taken with a digital microscope (VHX-5000 Series by KEYENCE, illustrated in figure 3.5a). Drainwater and sludge images (up to 4x resolution) were captured with a digital microscope (NIKON ECLIPSE E600, illustrated 3.5b) as per its availability during the measurements in Delhi. Specifications and more information about these microscopes can be found in their respective user manuals.

These images were then processed using ImageJ - Fiji software and data with morphological parameters for all the particles in each image was computed and processed in excel and python. This data was then further analysed to obtain average size distributions and morphology for similar runs with different influents as well as for particle images before and after the DAF experiment. These results can help us understand the effect of the in-

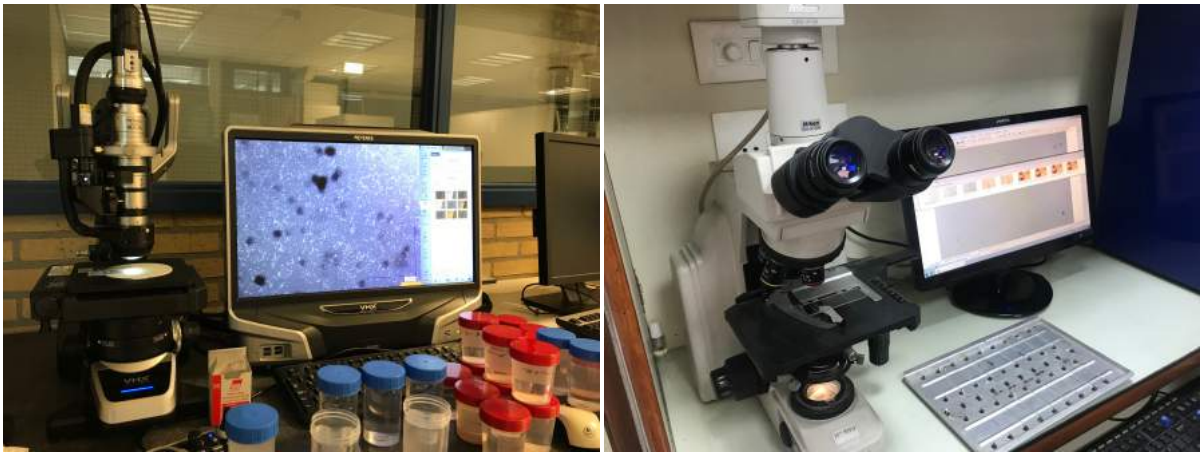

(a) Microscope VHX-5000 Series. (b) Microscope NIKON ECLIPSE E600

Figure 3.5: Digital microscopes used for analysis of canal water, drainwater and sludge from Okhla wwtp in Delhi.

fluent and operating parameters on the DAF solids removal performance. Figure 3.6 shows the sequence of steps taken to analyze the images on the software. The general process

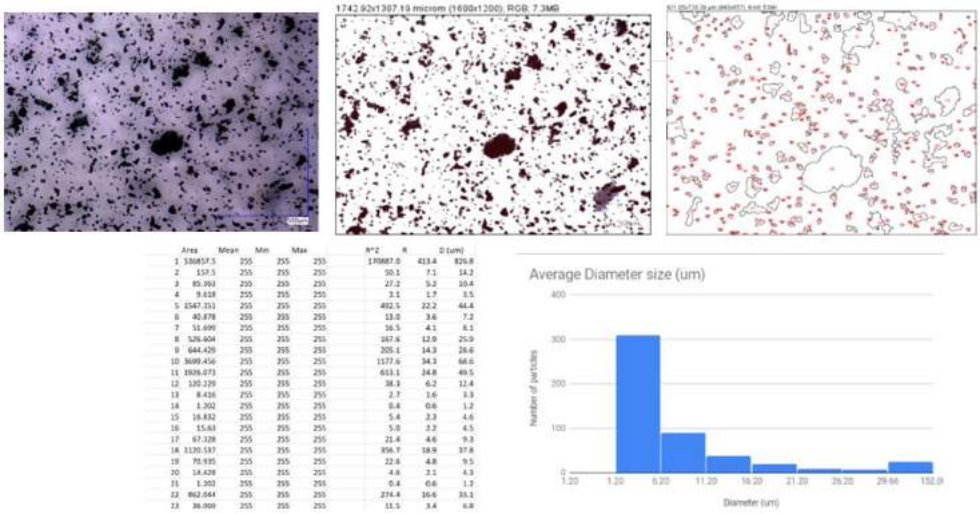

Figure 3.6: Image analysis steps for image processing and analysis by Fiji. The top 3 images show the series of steps followed to process the image in the software. The bottom left image shows how data in excel is generated from the processed image, and the bottom right image shows a size distribution histogram plotted form the excel data.

workflow followed for particle characterization is as follows :

1. Select RGB (Red Green and Blue) stack for the images. This gave a good threshold for accurate identification of most of the particles in the image.
2. The RGB stack was made binary to assign each pixel a value of 0 (white) or 255 (black).
3. The desired morphological outputs form each image were selected at from the set measurements option. The parameters selected for this study are given in Appendix E.

4. For the images the scale to measure the particles was set by using the set scale option. Based on a known distance the pixel size was calibrated. It was 0.918 pixel/µm for the canal water images and 0.854 pixel/µm for the drainwater and sludge images. All the units were in µm.

5. The threshold is checked for final adjustments.

6. The analyse particles option is selected and the following parameters are chosen - Size of particle: 0 to infinity (this will include even very fine particles including some noise which will manually be removed in the next steps), circularity: 0 to 1 , Include holes: No (This might alter the shape of the particles) and select summary

7. Save the image and parameter data.

8. Based on the instruction in the ImageJ user manual, a macros file can also be created to process many images in a short amount of time.

It is important to not here that this process was a result trial and error with many workflows. This was selected based on a balance between reliable results and time constraints. This process can be further modified for a more in depth analysis in future research.

3.6. Particle Image Velocitimetry (PIV)

To understand the bubble rise in the DAF column for the Barapullah drain water, PIV technology was deployed. PIV experiments were done using tap water (negative control), water with 10g cellulose (positive control), drain water and sludge as influnet at 3 bar and 5 bar pressure. For all these experiments, LED lights were first mounted at the top and at the back of the DAF column in a square formation. Figure 3.7 shows the location and formation of the LED lights on the DAF column. Then the DAF column with the LED lights was covered with a black garbage bag to create opaque surroundings. A slit was created in the black garbage bag at the front side of the DAF big enough for a phone camera lens to record the the bubble rise from the DAF without letting in light. An Apple iPhone 7 camera was used to record the bubble rise videos (resolution - 1334 × 750 pixels, camera - 12MP rear with OIS, 7MP front, video - 4K at 60 fps, 1080p at 240 fps)

The DAF column was then made operational with tap water, drain water and sludge as influnet at 3 bar and 5 bar pressure and each video was taken with both cameras. For each video the needle valve and the influent pump were opened for 15 secs and 2 minutes. After which the valve and the pump were stopped but the video was kept rolling for an extra 30 seconds each time to record the bubble rise right after operating the DAF. These videos were then transferred to a laptop where they were converted to frames using Matlab. There video frames were then analyzed using the PIV software for information on bubble size, bubble rise velocity magnitude and agglomerate density was gathered from the tap water samples and agglomerate information from canal water experiments. These were then calculated using the Stokes' law equation given in Chapter 2.

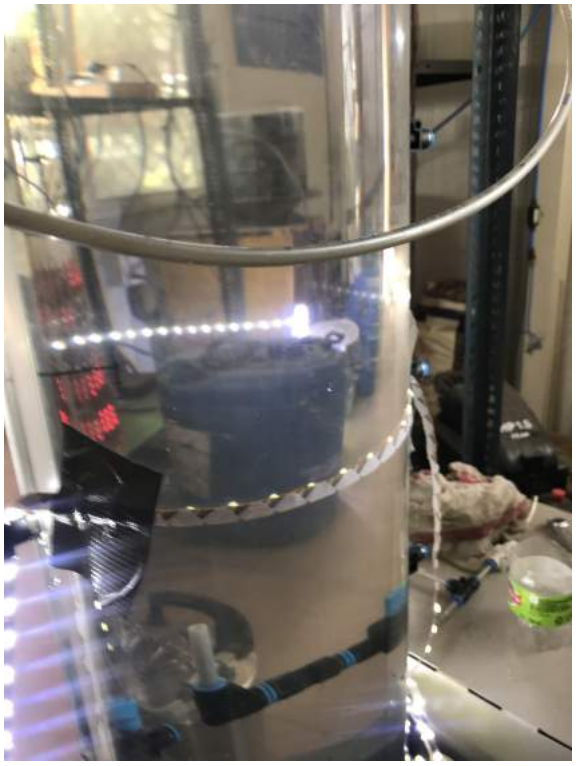

Figure 3.7: LED lights attachment on the DAF column for PIV analysis.

Figure 3.8: DAF column set up for PIV analysis.

3.6.1. Pathogen Removal

From chapter 2 it can be seen that there is an immense amount of literature to suggest that the DAF is an effective technology to remove some pathogens. To gain more insight into

the pathogen removal performance of DAF in the context of the LOTUS^{HR} project and also for the ease of testing in the field , samples taken before and after the DAF runs for Barapullah drain water were assessed for *E-coli* and *C.Prefringens* removal. *E-coli* was chosen as it is a strong indicator of bacterial presence and also for its relative ease of handling for site conditions. Measuring *C.Prefringens* removal efficiency was selected as a surrogate for *Cryptosporidium oocysts*

E-coli removal

To measure the *E-coli* removal, samples taken from the influent (Barapullah drain water) and clean effluent were analyzed using Chromocult Coliform Agar which simultaneously detects coliform bacteria and E-coli by utilizing a combination of 2 chromogenic substrates. Its mode of action is where interaction of identified pyruvate, peptones, sorbitol and phosphate buffer leads to rapid growth of colonies, even in the case of coliform bacteria which are sub-lethally injured. Tergitol which is present in the medium inhibits growth of gram positive bacteria and some gram negative bacteria, which has no effect on the growth of coliform bacteria leading to its detection. E-coli is characterized when -D-glucuronidase activity is detected by the X-glucuronide substrate. X-glucuronide and Salmon-GAL are both cleaved leading to positive colonies turning dark blue or violet color. Other colifom colonies turn pink to red, which can then be easily distinguished from E-coli. (EMD Millipore Corporation, 2019)

Before preparing the media and for plating the samples, the work bench was cleaned with ethanol to make sure all surrounding bacterial contamination was eliminated. Chromocult Coliform Agar media plates were first prepared at the TERI laboratory for sample inoculation. These were prepared based on the instructions in the technical sheet of Chromocult Coliform Agar from EMD Millipore Corporation (EMD Millipore Corporation, 2019). Once the media was prepared it was refrigerated for further use. Next for the *E-coli* removal analysis, the Barapullah water influent was first filtered to remove big suspended solids by 2m filter. Both the raw and filtered samples were then plated to see if there was any effect of filtration.

As it was expected that the Barapullah drain water would be highly contaminated, the influent samples were subjected to serial dilutions using PBS (phosphate buffer saline) solution made from mixing PBS tablets in 200ml distilled water. The serial dilutions made with the fist few samples were up to 10^{-5} to gauge the strength of the waste water. Then for each dilution, 0.1 ml was collected using a pipette and spread over the agar plates with a t-shaped spreader to ensure even distribution of the sample. To make sure there was no contamination from the surrounding air, a laminar hood was used to conduct these experiments. Next the clean water effluent samples were filtered using 0.45m membrane filters to concentrate the samples for an enhanced colony count. Using forceps these filters were then placed on the plates. Finally, both the plates prepared for the influent drain water and clean effluent were incubated at 35-37 °C overnight for 24 hours to aid bacterial growth. After incubation, the visible bacterial colonies were counted as colony forming unit (CFU/l). These indicate the colonies that would remain and rapidly grow and form colonies The equation below gives the formula for calculating CFU/l

$$\frac{colonyformingunit(CFU)}{ml} = \frac{numberofcolonies * dilutionfactor}{volumeplated(inml)} \tag{3.3}$$

After the fist few experiments it was found that only serial dilutions up to 10-2 were required. Furthermore, it was estimated that undiluted and filtered samples need to also be measured for the samples showing low colony counts with dilutions. Figure 3.9, 3.10 and 3.11 shows the plates obtained from the diluted, undiluted and filtered samples.

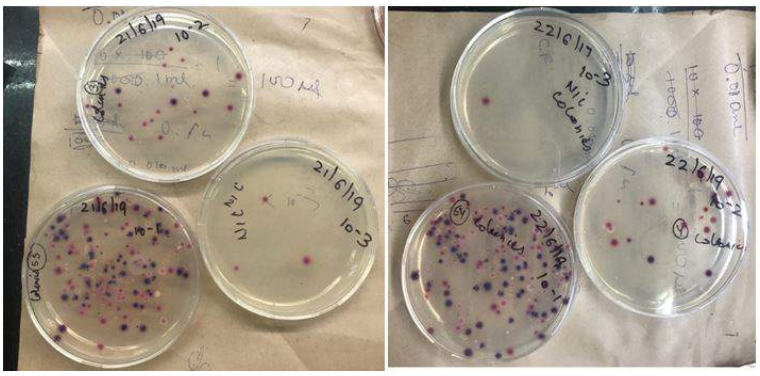

Figure 3.9: Plates for E-coli removal showing serial dilution from the DAF.

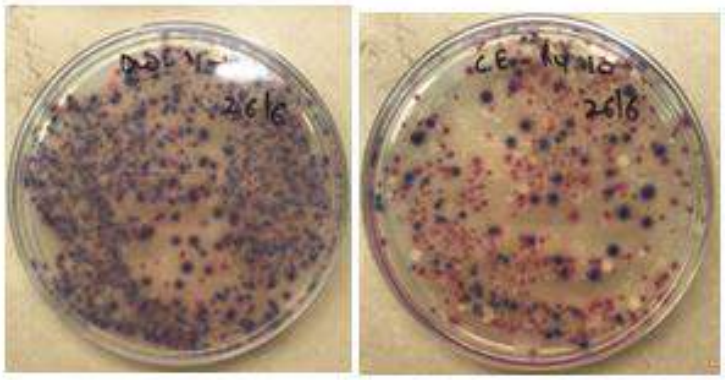

Figure 3.10: Plates for E-coli removal with neat samples from the drain water.

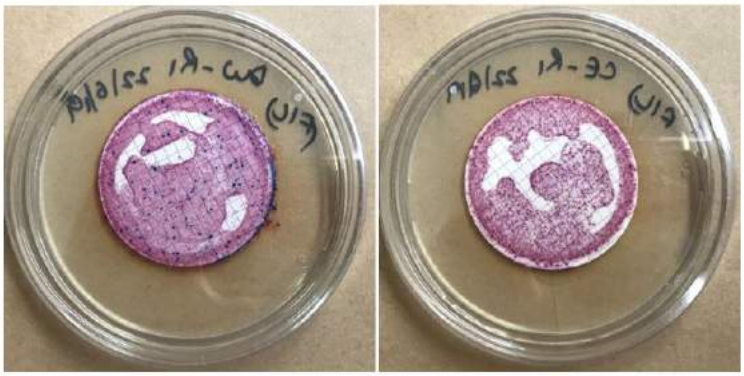

Figure 3.11: Plates for E-coli removal with membrane filtration from the drain water.

Once the number of bacterial colony count is determined, removal efficiency (in %) was estimated for the influent Barapullah drain water and compared with the clean effluent.

Equation 3.4 below gives the formula for removal efficiency.

$$Removalpercentage(\%) = \frac{C_{in} - C_{out}}{C_{in}} x100 \tag{3.4}$$

In water treatment, removal efficiencies are determined by log removal Here, Log_{10} was determined to calculate the removal in terms of relative microbes from the DAF. Log_{10} means a 10 times reduction in the microbial population calculated. Equation xx gives its formula

$$Logreduction = Log\frac{C_{in}}{C_{out}} \tag{3.5}$$

Here, C_{in} refers to the CFU/l for the influent sample and C_{out} is the CFU/l for the clean effluent samples. This analysis was repeated for all the 15 experimental design runs for the Barapullah drain water to gain a holistic understanding about the DAF capabilities to remove bacterial pathogens.

Clostridium Prefringes removal

As the DAF is known to be highly effective for *Cryptosporidium oocysts* and *Giardia cysts* removal, *Clostridium Prefringes* was identified as a surrogate for *Cryptosporidium oocysts* to measure its removal. Similar to the *E-coli* analysis, the influent Barapullah drain water samples and the clean effluent samples were filtered, stored and pasteurized at 20 °C for 15 minutes to kill other organisms apart from *Clostridium Prefringes* spores and used for plating CHROMagar C.perfringens base from CHROMagar was used as media. The preparation of this media is given in the technical data sheet of CHROMagar C.perfringens (CHROMagar, 2009). Once the media was prepared and stored, the influent and effluent samples were filtered using a cellulose nitrate membrane using a syringe vacuum mechanism due to the lack of a mechanical vacuum. The filtered membrane was then placed on the agar plant using forceps. These plates were then place in an air tight box with an oxygen depleting pack and oxygen indicator to create and identify anaerobic conditions. Figures 3.12a and 3.12b show the preparation and plating for this analysis.

This anaerobic box was then incubated at 35-37 °C for 24 hours. The anaerobic conditions are crucial for *C.perfringens* spores to grow. After incubation, the visible C.perfringens colonies were counted as colony forming unit (CFU/l) and their removal deficiencies were determined as per removal equations given before.

(a) Clostridium Prefringes procedure.

(b) Clostridium Prefringes procedure..

Figure 3.12: Images of Clostridium Prefringes experimental procedure.

4

Results and Discussion

This chapter discusses the results obtained from DAF experiments and analysis done thereafter. First, the TSS removal data obtained from the DAF experiments done with different influents - canal water, anaerobic sludge from Harnaschpolder wwtp in Delft, Barapullah drain water in New Delhi and anaerobic sludge from Okhla wwtp plant in Delhi is analyzed and compared. This is followed by a deeper look into the physical characteristics and morphology of these influents, and the velocity profiles of the bubbles and bubble-particle agglomerates. Finally, pathogen removal potential of the DAF at the Barapullah drain is reported and discussed.

4.1. DAF Critical Parameters

This section summarizes the results obtained from the DAF experiments done with different influents. Based on these results, the identified significant parameters for each influent are highlighted followed by a discussion about the effect of the chosen operating parameters on the DAF performance. These results were statistically analysed using the software Statistica 7.0 as per the Plackett Burman Design described in Chapter 3.

4.1.1. Canal water

Table 4.1 summarizes the operating parameters applied and TSS removal efficiency (in %) obtained for the 15 experiments performed using canal water as influent for the DAF. An example of the detailed calculation done for each experimental run is given in Appendix G.

For DAF experiments with canal water as influent, the lowest TSS removal was recorded as 45% (run 2) and the highest was found to be 96% (run 6). Table 4.2 and Figure 4.1 give the Analysis of Variance (ANOVA) calculation and Pareto chart based on this data. Based on these, it is noted that coagulation contact time, DAF retention time and influent TSS concentration have a significant effect (with p values below 0.05) on TSS removal efficiency. This means that in order to improve the solid-liquid separation performance of the DAF with canal water as influent, these parameters are important and further optimization can yield high DAF TSS removal efficiencies. Furthermore, experiments based on a central composite rotatable experimental design (CCRD) are recommended for the 3 significant parameters obtained for this case to optimize the operating values. Appendix H gives the response condition boundaries of the 3 significant parameters for further optimization.

Table 4.1: TSS removal efficiency (in %) recorded for DAF experiments with canal water as influent considering operating parameters - influent TSS concentration (mg/l), pressure (bar), temperature(°C),coagulant concentration (g/l), coagulation contact time (min), pH and DAF retention time (min)

Run	TSS (mg/l)	Temperature (degC)	Retention time (min)	pH	Pressure (bar)	Coagulant (g/l)	Time Coagulation (min)	TSS Removal Efficency (%)
1	30	29	13	7.6	5	0.5	10	47%
2	30	29	13	6.7	3	0.005	10	45%
3	30	35	13	6.7	3	0.5	30	72%
4	30	35	20	6.7	5	0.005	10	66%
5	30	35	20	7.6	3	0.5	30	81%
6	30	29	20	7.6	5	0.005	30	96%
7	270	32	16.5	7.15	4	0.2525	20	49%
8	270	32	16.5	7.15	4	0.2525	20	56%
9	270	32	16.5	7.15	4	0.2525	20	49%
10	510	35	13	7.6	3	0.005	10	60%
11	510	35	13	7.6	5	0.005	30	85%
12	510	29	13	6.7	5	0.5	30	88%
13	510	29	20	7.6	3	0.5	10	81%
14	510	35	20	6.7	5	0.5	10	78%
15	510	29	20	6.7	3	0.005	30	88%

Table 4.2: ANOVA statistical results showing the effect of influent TSS concentration (mg/l), pressure (bar), temperature(°C),coagulant concentration (g/l), coagulation contact time (min), pH and DAF retention time (min) for TSS removal efficiencies from canal water.

Name	Effect	Standard Error	Calculated t	p-value
Mean	69.4	1.04	66.5	0.0002
TSS(X1)	12.16	2.33	5.21	0.0348
Temperature(X2)	-0.5	2.33	-0.21	0.8501
Retention time(X3)	15.5	2.33	6.64	0.0219
pH(X4)	2.16	2.33	0.92	0.4511
Pressure(X5)	5.5	2.33	2.35	0.1424
Coagulant(X6)	1.16	2.33	0.5	0.6667
Time coagulation(X7)	22.16	2.33	9.5	0.0109

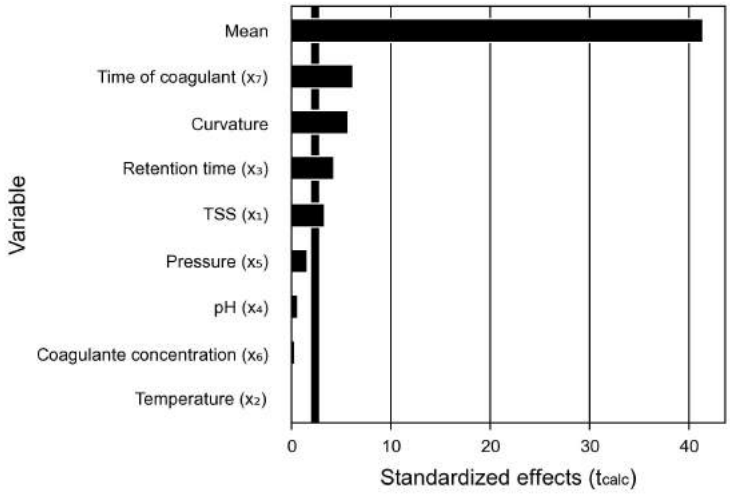

Figure 4.1: Pareto chart showing the significant effect of influent TSS concentration (mg/l), DAF retention time (min) and coagulation contact time (min) for DAF experiments with canal water (p-value at the 0,05% level).

Here, it should also be noted that the term 'curvature' shows significance. It calculates the difference of center point values from the non-center point values of the design, suggesting that there might be some factors that do not show a linear relation with the dependent variable.

Coagulation contact time shows the highest significance out of all of the parameters tested for canal water. This means that to remove more solid particles from canal water, the longer they are kept in contact with the coagulant, higher the chances are that they form flocs. As these flocs would be bigger than the particles, they would then have higher probability to collide with or entrap the micro-bubbles and thus have a greater chance of being removed. According to Stumm and O'Melia (Stumm and O'Melia, 1968), it is known that the coagulant dosage needed to destabilize the colloids dispersed in the liquid is directly related to the amount of colloid particles in the solution stoichometrically. In diluted systems however, the coagulation rate can be very slow due to a low number of colloids in the water suspension which leads to limited contact with particles. Furthermore, Shammas (Shammas, 2005) finds that increasing particle matter concentration by addition of coagulant/recycled effluent or more contact time would improve coagulation. Thus, more coagulant dosage or increase contact time would lead to more chances of colloids re-stabilization.

Taking run 12 as an example, (high removal (88%) particles from canal water with high influent TSS concentration (510 mg/l) and a high coagulation time (30 min)), figure 4.2a and 4.2b show the microscopic images of canal water particles and the floc particles formed after 30 minutes of coagulation. It can be clearly seen from these images that the coagulation process increases the size of particles from canal water (20 - 70 µm) to flocs (100-250 µm), thus increasing the removal efficiency. Moreover, on comparing run 12 to run 14, it can be observed that when coagulation time is reduced to 10 minutes and the other operating parameters are similar, run 14 showed a lower TSS removal (78%).

Hydrophilic (water loving) compounds are generally difficult to remove by coagulation as it is difficult for chemicals to compete with the sorbed molecule of water. Thus, to re-

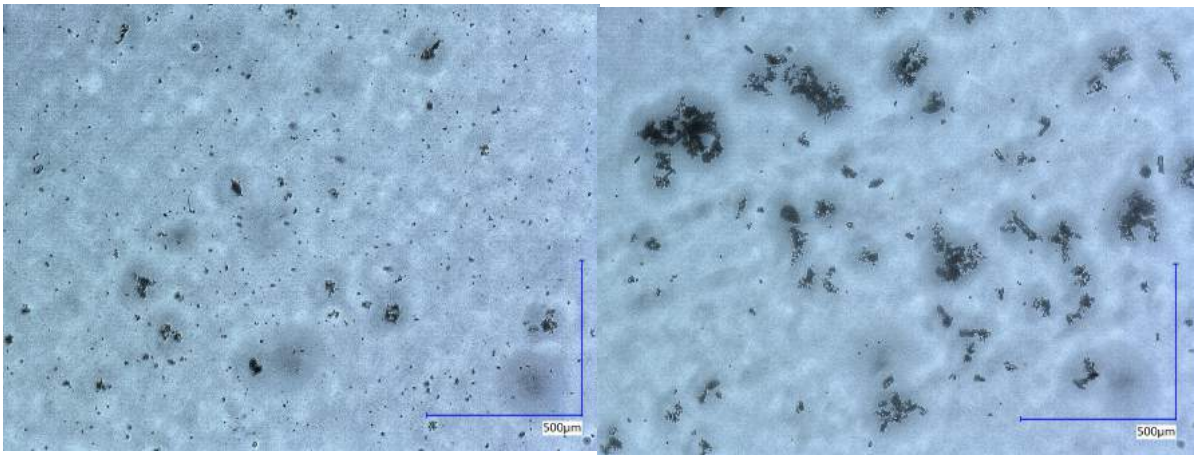

(a) Microscopic images of canal water particles.

(b) Microscopic images of flocs formed after coagulation of canal water particles with $Ca(OH)_2$ and cellulose for 30 minutes.

Figure 4.2: Microscopic images of canal water and flocs formed after coagulation.

move the suspended particles 10-20 times the amount of coagulant will be needed to destabilize than hydrophobic particles (Hammer, 1986). Generally, majority of colloid particles in wastewater show a mix of hydrophilic-hydrophobic properties leading to a suspension with an intermediate degree of coagulation. In this case, the particles are expected to be sediments found in canal water. These are mainly found to be clay, peat and fine loamy sand (Huisman et al., 1998) which are expected to be hydrophilic in nature (Chesworth, 2007). This suggests that in order to optimize the coagulant amount to remove TSS from canal water, stronger coagulants or a higher dosage is required. It should be noted here that the current coagulants used ($CaOH_2$ and Cellulose) are mild divalent coagulants and improved coagulation would be expected with stronger coagulants like alum or ferric chloride. Nevertheless, it can be observed from the microscopic images that they are in effect. Further studies are recommended with different coagulants and coagulation conditions to optimize this parameter. Significance of influent TSS concentration shows that for higher removal of particles from canal water, it is an important parameter. For diluted influents, it is is important to have good contact between bubbles and particles for removal and once this is achieved the removal is not that difficult (Benjamin, 2013).

Pressure in this case shows low significance suggesting that it doesn't have high importance for TSS removal from canal water. This trend can be observed on comparing run 13 and run 14. Both runs have similar operating conditions apart from pressure. It can be seen from these run that when 3 bar pressure is applied (run 13), TSS removal observed is 81% and for 5 bar pressure (run 14). its 78%. Both values are found in the same range. In literature, De Rijk (De Rijk et al., 1994) reports that the average bubble size decreases (from 70 to 40 µm) with increasing pressure (3.5 - 6.2 bar) indicating that with higher pressure of 5 bar there are smaller sized bubbles in the system as compared to 3 bar. However, other studies find different results. According to Rodrigues and Rubio (Rodrigues and Rubio, 2003), the average bubble diameter was found to be independent of saturation pressure ranging between 33 and 38 µm and all bubbles being less than 70 µm in size. They further suggest that by an increase in pressure the amount of air being dissolved in the satura-

tor increases resulting in a higher number of bubbles, but as the flow constrictor (needle valve) is the same, the size of the bubbles remain the same. Other studies suggest that the easiest method of bubble-particle aggregation is entrapment leading to buoyancy, which will occur when the bubbles are smaller in size than the aggregates (Rodrigues and Rubio, 2007). This also emphasises on the importance of bubble-floc collision and entrapment as compared to pressure induced effect of size or amount of bubbles for canal water.

For the case of canal water, as the influent suspension is quite diluted (as compared to sludge) the size of the bubbles or the amount doesn't show a lot of significance, rather the collision and entrapment of bubbles with the flocs are more important. This helps explain the the significance of coagulation time, retention time and influent TSS concentration as compared to pressure. To further understand the effect of pressure induced change on bubble size/amount of bubbles, and in turn the effect these variation have on the TSS removal, methods such as image analysis, laser diffraction, particle counters are recommended. A detailed list of these methods can be found in Appendix I. This discussion indicates that for canal water, lower pressures of 3 bar with optimized coagulation conditions are adequate for high removal of TSS, thus saving energy and cost. This can be observed from runs 3 (72%), 5 (81%), 13 (81%) and 15 (88%). However, it should be noted here that this is subject to the nozzle design and recycle ratio. Thus, further experimentation with the significant parameters, nozzle design and recycle ratios are suggested to optimize the overall DAF process. Also, from the Pareto chart it was observed that temperature was not a significant parameter as per the given range. This was also observed by Vlyssides (Vlyssides et al., 2004), who found that the effect of temperature from 10 °C < T < 40 °C had no statistical significance on the bubble size distribution and in turn the removal efficiency.

4.1.2. Barapullah Drainwater

Table 4.3 summarizes the operating parameter values and TSS removal efficiency (in %) obtained for the 15 experiments performed using Barapullah drain water as influent for the DAF. An example of the detailed calculation for each experimental run can be found in Appendix G. The lowest removal is observed as 69% (run 2) and the highest as 94% (run 11). Table 4.4 and 4.5 give the Analysis of Variance (ANOVA) calculation and Pareto chart based on this data. It can be seen from this that influent TSS concentration has a significant effect on the drain water TSS removal efficiency (with p values below 0.05). Similar to canal water, this can be attributed to the fact that the drain water is a diluted suspension and with more particles the chances of colliding with or entrapping bubbles and forming bubble-particle agglomerate increases. The other parameters did not show a statically significant effect.

Comparing these results to canal water it can be observed that with similar operating parameters (for individual runs) the removal efficiencies and significant parameters are different. The operating parameters are kept the same so it is hypothesized that the variation is due to difference in the characteristics and properties of the influents. This is suggested in literature as well. Shammas and his colleagues (Shammas et al., 2010) in their studies observed that complication in flotation for wastewater arose from the changing composition of the solid and liquid phases and that there were deviation in the results found in practice as compared to laboratory experiments. Figure 4.3 and 4.4 show images of samples from canal water and drain water, and images during the DAF flotation process.

Table 4.3: TSS removal efficiency (in %) recorded for DAF experiments with Barapullah Drainwater as influent considering operating parameters - influent TSS concentration (mg/l), pressure (bar),coagulant concentration (g/l), coagulation contact time (min), and DAF retention time (min)

Run	TSS (mg/l)	Retention time (min)	Pressure (bar)	Coagulant (g/l)	Time Coagulation (min)	TSS Removal Efficency
1	30	20	5	0.005	30	83%
2	30	20	5	0.5	10	69%
3	30	13	5	0.5	30	81%
4	30	13	3	0.5	30	89%
5	30	20	3	0.005	10	85%
6	30	13	3	0.005	10	70%
7	270	16.5	4	0.2525	20	92%
8	270	16.5	4	0.2525	20	85%
9	270	16.5	4	0.2525	20	87%
10	510	13	5	0.005	10	72%
11	510	20	3	0.5	10	94%
12	510	13	5	0.5	10	83%
13	510	20	3	0.5	30	90%
14	510	20	5	0.005	30	83%
15	510	13	3	0.005	30	88%

Table 4.4: Effect of TSS, temperature, DAF HRT, pressure, pH, coagulant concentration and coagulation contact time on TSS removal efficiency.

Name	Effect	Standard Error	Calculated t	p-value
Mean	0.83	0.02	40.65	0.0000
Curvature	0.09	0.09	0.99	0.3504
TSS(X1)	-0.09	0.04	-2.22	0.0574
Retention time(X3)	-0.01	0.04	-0.22	0.7510
Pressure(X5)	0.02	0.04	0.41	0.6921
Coagulant(X6)	0.04	0.04	0.99	0.3532
Time coagulation(X7)	-0.05	0.04	-1.23	0.2529

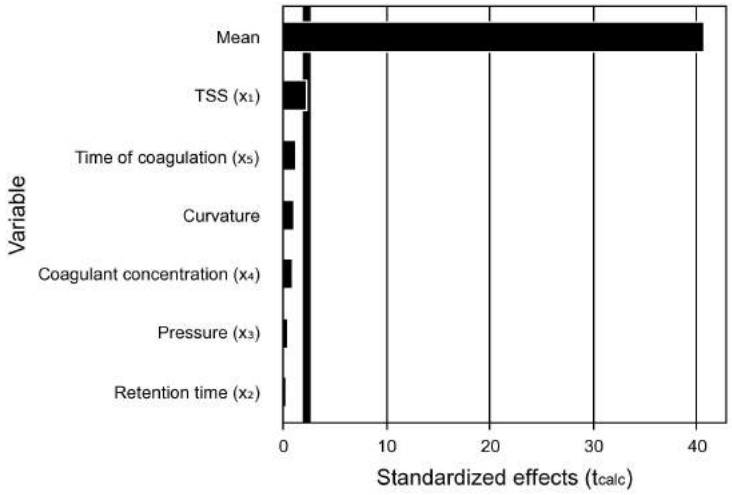

Table 4.5: Pareto chard showing the significant effect of TSS (p-value at the 0,05% level).

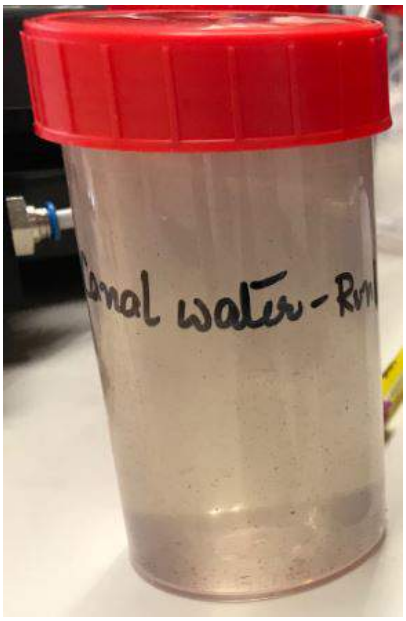

(a) Picture of canal water sample.

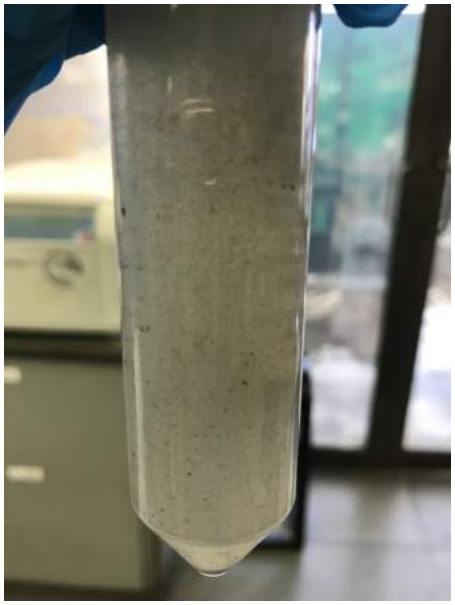

(b) Picture of Barapullah drain water sample.

Figure 4.3: Images of canal water and drain water samples

From these images it can be observed that drain water is more turbid than canal water and interestingly, during the drain water DAF experiments, significant foaming was observed at the surface of the flotation column. This means there is presence of large quantities of surfactant like chemicals in the drain. It could be that due the presence of these substances, drain water tends to be more hydrophobic in nature and this could help explains higher average TSS removal rates. Bubbles might adhere better to drain water particles and thus, low significance of parameters like time of coagulation and retention time, which were found to be important for canal water is observed in this case. A direct comparison between canal water and drain water runs is by comparing runs 7, 8 and 9 for both influents, as all operating parameters are kept the same. Average TSS removal efficiencies with canal water are 51 (+/- 4) % and for drain water are 88 (+/- 4) %. This indicates that

(a) Picture of foaming in a drain water DAF run.

(b) Picture of canal water during the DAF process

Figure 4.4: Images of Canal water and Drainwater during the DAF process.

drain water possesses certain characteristics which aid the flotation process. Further research is needed to validate this and methods such as Atomic Force Microscopy (AFM) as well as simple qualitative methods like extraction of particles from a liquid medium into an oil medium (Mellgren and Shergold, 1966) for hydrophobicity measurements can be done. Figure 4.6 shows good solid-liquid separation of drain water by the DAF for influents with high removal (run 11).

Table 4.6: Image showing good solid-liquid separation by the DAF with drain water.

In literature, Koivunen and Tanski (Koivunen and Heinonen-Tanski, 2008) reported sim-

ilar results with primary treated wastewater with an average reduction of 77% suspended solids. Other authors have also reported comparable effluent quality at pilot scale and full scale (Ødegaard, 2001) and with low quality effluents with a laboratory scale DAF (Pinto Filho and Brandão, 2001). other studies indicate that the DAF is a promising technology for treating primary wastewater and can also be considered as an efficient purification system by by-passing wastewater during overloading as well (Koivunen and Heinonen-Tanski, 2008).

4.1.3. Anaerobic sludge

Figure 4.7 summarizes the TSS removal efficiencies (in %) obtained for the 15 experiments performed using anaerobic sludge from Harnaschpolder wwtp in Delft as influent for the DAF. An example of a detailed calculation for each experimental run can be found in Appendix G. The lowest removal is observed as 66% (run 2 - this is different from canal and drain water as those had run 2 with 5 bar and sludge has run 2 with 3 bar) and the highest as 92% (run 3). Table 4.7 and figure 4.10 give the Analysis of Variance (ANOVA) calculation and Pareto chart based of this data. It can be seen from these tables that pressure has a significant effect on TSS removal efficiency (with p values below 0.05). This means that to optimize solids removal for sludge, pressure is an important parameter to be optimized. It should be noted here that the sludge was subject to dilution and sieving due to experimental limitations, therefore experiments with original sludge might yield different results. It is recommended that DAF TSS removal performance with anaerobic sludge as influent be validated at the pilot scale.

Table 4.7: TSS removal efficiency (in %) recorded for DAF experiments with anaerobic sludge from wwtp in Delft as influent considering operating parameters - influent TSS concentration (mg/l), pressure (bar), temperature(°C),coagulant concentration (g/l), coagulation contact time (min), pH and DAF retention time (min)

Run	TSS (g/L)	Temperature (C)	Retention time (min)	pH	Pressure (bar)	Coagulant (g/L)	Time of coagulation (min)	TSS RE in Effluent(%)
1	5	25	20	7	3	0.005	30	68.37
2	5	35	13	8.5	3	0.005	10	66.43
3	0.5	35	20	7	5	0.005	10	91.7
4	5	25	20	8.5	3	0.5	10	87.7
5	5	35	13	8.5	5	0.005	30	83.5
6	5	35	20	7	5	0.5	10	86.9
7	0.5	35	20	8.5	3	0.5	30	78.6
8	0.5	25	20	8.5	5	0.005	30	90.9
9	0.5	25	13	8.5	5	0.5	10	83.6
10	5	25	13	7	5	0.5	30	87
11	0.5	35	13	7	3	0.5	30	72.2
12	0.5	25	13	7	3	0.005	10	87.1
13	2.75	30	16.5	7.75	4	0.2525	20	88
14	2.75	30	16.5	7.75	4	0.2525	20	86.7
15	2.75	30	16.5	7.75	4	0.2525	20	90

These results suggest that pressure is quite significant to have higher TSS removal from sludge. As mentioned in the discussion for canal water, literature is conflicted in showing that the size of bubbles decrease with increasing pressure, however majority finds that the amount of bubbles does increase with pressure. Benjamin (Benjamin, 2013) states that for concentrated influents like sludge, contact between bubbles and particles in unavoidable, the important aspect is to have enough volume of bubbles to make the particles float and remove the sludge layer. Thus for runs (3, 6, 8 and 10) with higher pressure higher concentration of air is available and more amount of bubbles are present to collide with particles.

Table 4.8: ANOVA analysis for TSS removal results obtained for sludge.

Name	Effect	Standard Error	Calculated t	p-value
Mean	82	2.02	40.65	0.0000
Curvature	12.47	9.02	1.38	0.2163
TSS(X1)	-4.03	4.03	-1	0.3560
Temperature(X2)	-4.22	4.03	-1.05	0.3355
Retention time(X3)	4.06	4.03	1.01	0.3535
pH(X4)	-0.42	4.03	-0.1	0.9199
Pressure(X5)	10.53	4.03	2.61	0.0401
Coagulant(X6)	1.33	4.03	0.33	0.7523
Time coagulation(X7)	-3.81	4.03	-0.94	0.3814

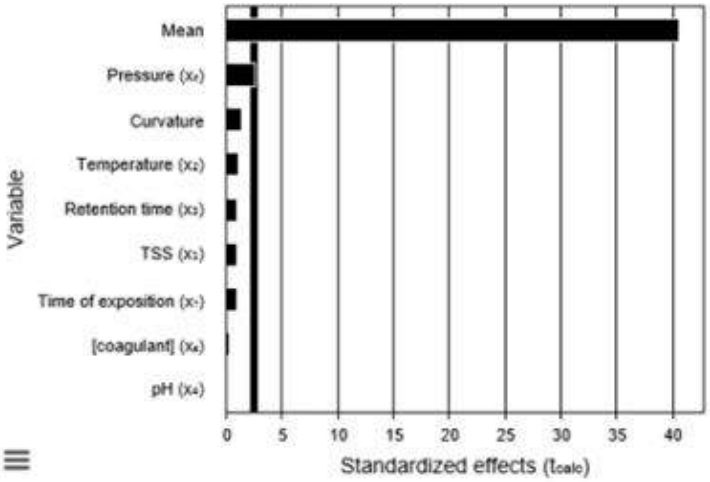

Table 4.9: Pareto chard showing the significant effect of TSS (p-value at the 0,05% level).

Comparing the results obtained from anaerobic sludge experiments with the canal water experiments, it can be seen that as in the case of canal water, time of coagulation is not a significant parameters for sludge. This can be attributed to the fact that divalent coagulants ($CaOH_2$ and cellulose) were used for this study and do not show a significant effect. However, experiments with stronger coagulants like alum and ferric chloride should give improved coagulation, as is found in literature.

Table 4.10 shows the TSS removal efficiency (in %)of anaerobic sludge from from Okhla wwtp in Delhi. Removal of solids can be seen as high as 96.6% for run 15. An example of detailed calculation for these results is given in Appendix G. Although all 15 experiments were not conducted due to time constraints, it can be observed from these results that a similar trend (with pressure as a significant parameter) is observed as for the anaerobic sludge from Delft. Moreover, the solids removal from the Okhla wwtp is higher.

Run	TSS (g/L)	Temperature ©	Retention time (min)	pH	Pressure (bar)	Coagulant (g/L)	Time of coagulation (min)	TSS RE in Effluent (%)
4	5	25	20	8.5	3	0.5	10	95.93
6	5	35	20	7	5	0.5	10	92.95
15	2.75	30	16.5	7.75	4	0.2525	20	96.64

Table 4.10: TSS removal efficiency (in %) recorded for DAF experiments with sludge from wwtp in Delhi as influent considering operating parameters - influent TSS concentration (mg/l), pressure (bar), temperature(°C),coagulant concentration (g/l), coagulation contact time (min), pH and DAF retention time (min)

High TSS removal efficiencies were achieved with DAF for the 3 different effluents. Nevertheless, their critical parameters have an important variation: coagulation time, retention time and TSS concentration for canal water; TSS concentration for drain water and Pressure for Sludge. Even when canal and drain water had similar operating parameters, very different removal efficiencies were found for the same runs (for instance in run 4 has a 66% removal for canal water and 89% for drain water). One possible explanation for this might be linked with the different characteristics of solids in both influents. Thus, further particle analysis is performed below.

4.2. Particle Characterization by Image analysis

The characteristics of influents selected for this research show variation in TSS removal in the DAF experiments. This indicates that the influents need to be investigated further to understand the effect of particles on the TSS removal performance of the DAF. This subsection reports and discusses the particle size distribution and morphology of the different influnets. The images were taken with digital microscopes and analysed using the software ImageJ-Fiji as described in Chapter 3. Appendix J presents the particle size distributions and particle circularity values for the 15 drain water, canal water runs and the 2 runs with anaerobic sludge from the Delhi wwtp. Figures 4.5 (run 2) and 4.6 (run 15) show general examples the particle size distribution and circularity for canal water and drain water.

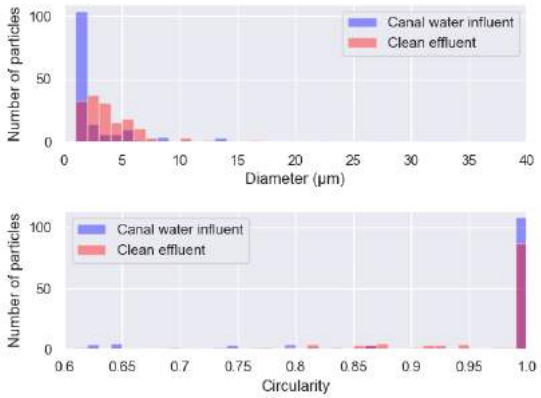

(a) Particle size distribution and circularity of Run 2 with canal water (TSS = 30 mg/l, Temperature = 29 °C, Retention Time = 13, pH = 6.7, Pressure = 3bar, Coagulant = 0.005 g/l and Time of Coagulation = 10 min)

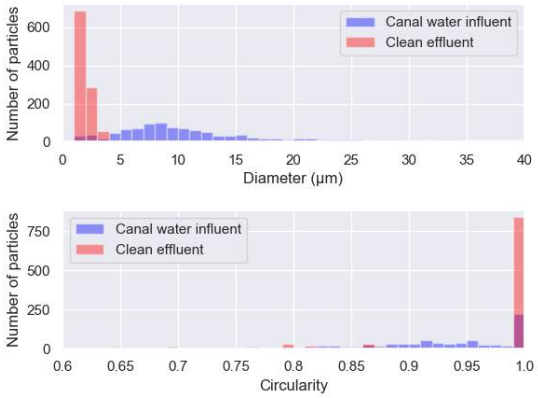

(b) Particle size distribution and circularity of Run 15 with canal water (TSS = 510 mg/l, Temperature = 29 °C, Retention Time = 20, pH = 6.7, Pressure = 3bar, Coagulant = 0.005 g/l and Time of Coagulation = 30 min)

Figure 4.5: Particle size distribution and circularity of Run 2 and Run 15 with canal water

As for both canal water and drain water influents, the influent TSS concentration was a significant parameter, this analysis gives us more information about the relationship between the influent particles and the performance of the DAF. It can be observed from these graphs that canal water with higher influent TSS concentration (run 15) showed average influent diameters of 12-14 µm, where as drain water showed average influent diameters (run 10) be lower at around 3-5 µm. For both canal water and drain water influents, av-

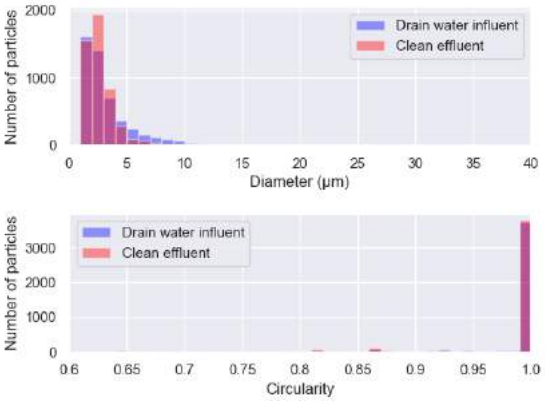

(a) Particle size distribution and circularity of Run 2 with drain water (TSS = 30 mg/l, Retention Time = 20, Pressure = 5 bar, Coagulant = 0.005 g/l and Time of Coagulation = 30 min)

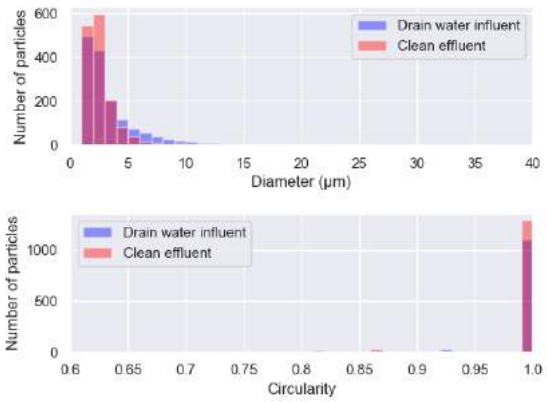

(b) Particle size distribution and circularity of Run 10 with drain water (TSS = 510 mg/l, Retention Time = 13, Pressure = 3 bar, Coagulant = 0.005 g/l and Time of Coagulation = 30 min)

Figure 4.6: Particle size distribution and circularity of Run 2 and Run 10 with drain water

erage clean effluent particle diameters were observed to be around 2 - 3 µm. In terms of shape, influent canal water was seen to be more irregular with an average circularity of 0.83, whereas majority of influent drain water particles were observed to have more circular shape with an average circularity value of 0.92. The clean effluents for both cases was found to be quite high in circularity with an average value of 0.95.

Looking into these graphs a bit deeper, Table 4.11 summarized the average, standard deviation, minimum, maximum, and percentiles (5,25,75,95 and 99) for the diameters and circularity of the drain water (run 2 and run 10) and canal water (run 2 and run 15) runs.

These give us an indication about the fate of majority of the particles within the size distribution. As these runs are extreme cases for canal water and drain water (which show low and high TSS removal), these values help us relate the operation of the DAF with the particle characteristics. It is observed from this table that canal water with higher influent TSS (run 15) has larger average particle diameter (12 µm) than drain water (2 µm) with higher influent TSS (run 10). For both cases the runs (run 2) with low TSS have smaller average diameters (3 - 4 µm). The maximum particle diameters and circularity for canal water are recorded up to 78 µm and 1 respectively, and for drain water they are noted up to 86 µm (particle diameters can reach up to 541.37 µm as well, see Appendix K) and 1 respectively. The minimum particle diameters was found to be between 1-2 µm for all cases.

Interestingly, the biggest variation can be seen in the 95 percentile value between the influent canal water and drain water. Canal water is observed to have a more spread out size distribution with 95% of the particles falling in the range of 0-42 µm, whereas for drain water 95% of the particles fall in the range of 0 - 17 µm. This means that the canal water has bigger average diameters and drain water has majority of particles which are of a smaller size range and more circular (with a really small percentage of huge irregular particles). This also indicates that the density of canal water particles would be higher due to

Table 4.11: Comparison values of Particle sizes and circularity for canal water(run 2 and 15) and drain water (run 2 and run 10)

Influent	Run	Influent water								
		Diameter(um)								
		Average	Std	max	min	Percentile (5)	Percentile (25)	Percentile (75)	Percentile (95)	Percentile (99)
Canal Water	Run 2	4.07	4.92	25.90	1.23	1.23	1.23	5.01	14.63	24.26
	Run 15	12.00	8.55	78.17	1.23	2.45	6.81	14.70	28.51	42.24
Drain Water	Run 2	3.84	3.90	65.77	1.32	1.32	1.87	4.38	9.34	15.91
	Run 10	3.72	3.74	86.36	1.32	1.32	1.87	4.18	9.98	17.23

Influent	Run	Clean Effluent								
		Diameter(um)								
		Average	Std	max	min	Percentile (5)	Percentile (25)	Percentile (75)	Percentile (95)	Percentile (99)
Canal Water	Run 2	3.76	2.57	16.96	1.23	1.23	1.73	5.05	7.64	14.51
	Run 15	1.77	0.59	4.41	1.23	1.23	1.23	2.12	3.00	3.24
Drain Water	Run 2	3.53	3.35	42.51	1.13	1.13	1.95	4.07	9.13	15.23
	Run 10	2.84	1.97	25.99	1.32	1.32	1.87	3.24	5.45	11.42

Influent	Run	Influent water								
		Circularity								
		Average	Std	max	min	Percentile (5)	Percentile (25)	Percentile (75)	Percentile (95)	Percentile (99)
Canal Water	Run 2	0.86	0.19	1	0.38	0.44	0.73	1	1	1
	Run 15	0.83	0.19	1	0.11	0.40	0.75	0.97	1	1
Drain Water	Run 2	0.92	0.15	1	0.06	0.57	0.90	1	1	1
	Run 10	0.92	0.17	1	0.13	0.52	0.92	1	1	1

Influent	Run	Clean Effluent								
		Circularity								
		Average	Std	max	min	Percentile (5)	Percentile (25)	Percentile (75)	Percentile (95)	Percentile (99)
Canal Water	Run 2	0.88	0.19	1	0.13	0.48	0.81	1	1	1
	Run 15	0.95	0.11	1	0.33	0.69	1	1	1	1
Drain Water	Run 2	0.91	0.17	1	0.13	0.55	1.95	1	1	1
	Run 10	0.96	0.10	1	0.25	0.73	1	1	1	1

higher average particle sizes as well as due to larger densities of sediments as compared to colloidal particles in drain water. This reason coupled with the hydrophilicity of the canal water particles could help explain lower average removal TSS removal efficiencies as compared to drain water.

Looking at the clean effluent values, a relation can be made between the particle characteristics and the operating conditions. For canal water, when low TSS removal is observed (run 2), 95% of the particles found in the clean effluent have particle diameters around 8 µm where as when there is high TSS removal (run 15) 95% of the particle diameters are observed to be about 3 µm. This shows that with optimized operating conditions (run 15 for instance), particle diameters of 28 µm can be removed by the micro-bubbles, leaving only up to 3 µm diameters in the clean effluents. Similarly for drain water, with optimized operating condition (run 10 for instance), influent particle diameters of 10 - 15 µm can be removed by micro-bubbles leaving only about 5 µm sized particles in the clean effluent.

Microscopic images of anaerobic sludge from Delhi (influent and clean effluent) were also taken for image analysis. Figure 4.7 shows the pictures of the samples with sludge, clean effluent and supernatant of run 4. The data generated from the image analysis for these images was not very reliable as the flocs of the sludge could not be identified by the software and read these big flocs as small particles. Nevertheless, it can be observed from these images that the anaerobic sludge has a spread-out structure with particle diameters as big as 100-200 µm. Post the DAF process, clean effluent shows smaller diameters between 10 - 80 µm and the supernatant image shows a heavy concentration of flocs indicating that the sludge gets well concentrated at the DAF surface.

4.3. Agglomerate analysis using Particle Image Velocitimetry (PIV)

As discussed it Chapter 2, in order to separate the solid phase from the liquid phase in the DAF process, the solids from the wastewater influent are coagulated to form flocs. These flocs then form agglomerates when they collide and attach to the bubbles in the floating tank and rise to the top to be removed. Many bubbles characteristically attach to individual flocs but Leppinen and Dalziel (Leppinen and Dalziel, 2004) suggests that even larger bubble-floc agglomerates are formed when several bubbles attach to flocs; this is known as clustering. Therefore, it is important to understand the surface properties of the bubbles and flocs, and the influence of aggregates and rising bubbles to further understand the removal efficiency of the DAF.

Videos of bubbles rising in the DAF process with just tap water as influent were first analysed by obtaining their bubble velocity profiles and scatter plots for 3 stages of the DAF process - 10 seconds at the start of the flow, 10 seconds in between and 10 seconds in the end (after the flow had been stopped for 10 seconds). Figure 4.8a, 4.8b and 4.9 give the bubble rise vector velocities for the 3 stages. Figure 4.10a and 4.10b show the scatter plot for velocities for the start and middle flows and figure 4.11a and 4.11b show the scatter plot for velocities at the end of the DAF flow.

Here, it can be observed that at the start and middle of the DAF run the velocities are quite erratic and spread out. At the end of the run, the bubble rise velocities are found to

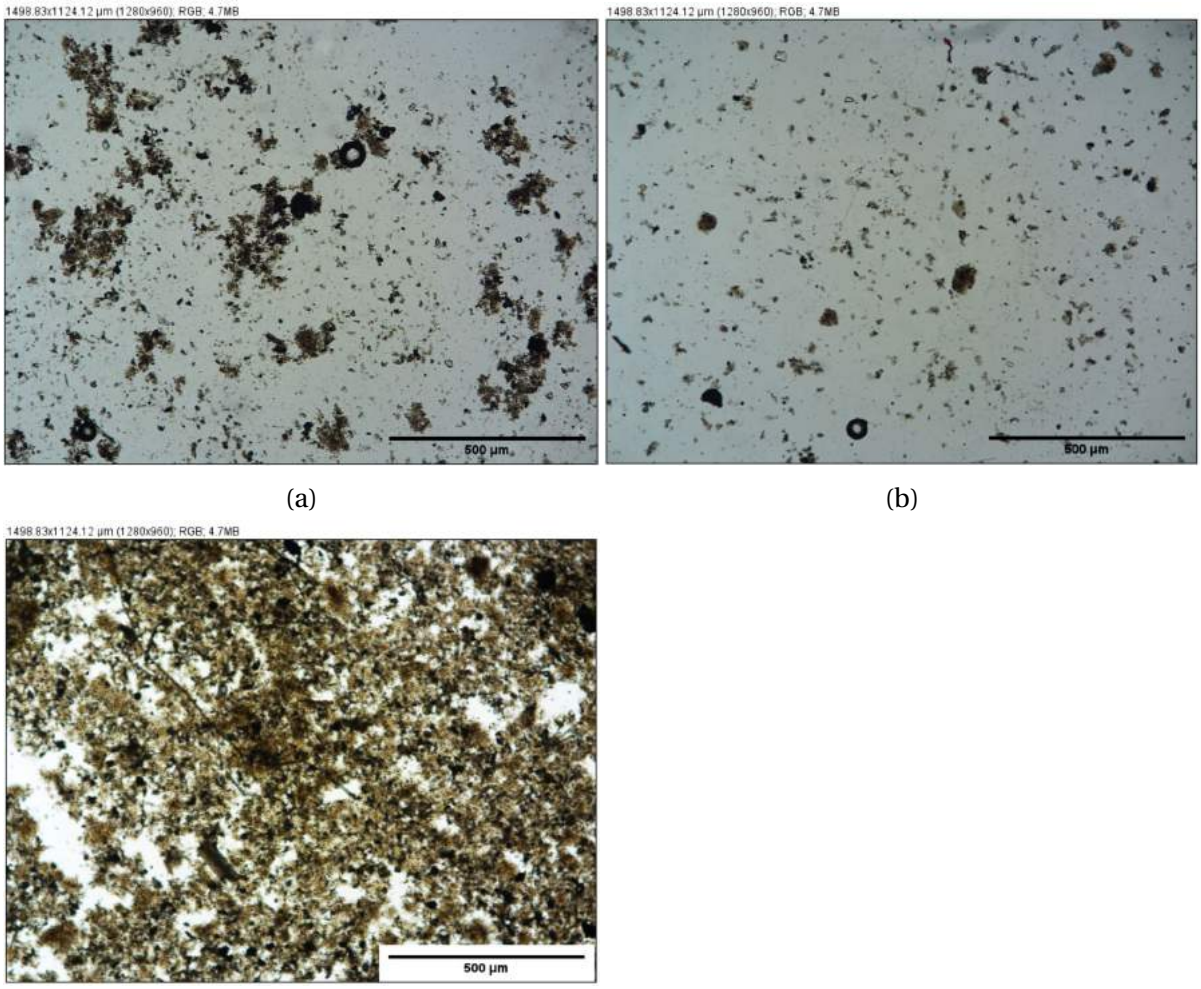

(a) (b)

(c)

Figure 4.7: Microscopic images of sludge influent, clean effluent and supernatant of DAF experiments (run 4) with sludge done in Delhi

be more stable and reliable. Therefore, for the next PIV analysis of the influents, velocity profiles were analysed at the end of the DAF run, 10 seconds after closing the inlet valve. Figure 4.11a and 4.11b show the scatter plot for tap water velocities at 5 bar with the DAF and 4.12a and 4.12b show the scatter plot for drain water (run 10 - TSS = 510 mg/l, Retention Time = 13, Pressure = 3 bar, Coagulant = 0.005 g/l and Time of Coagulation = 30 min) with the DAF.

The mean velocities calculated from these graphs were u = 1.55E-04 m/s, v = -2.22E-03 m/s for tap water and u = 6.34E-04 m/s, v = -1.42E-03 m/s for drain water. It should be noted here that u represents horizontal velocities with negative sign indicating the flow is towards the left and v represents vertical velocities with negative sign meaning the flow is upwards. Comparing the tap water bubble velocities with the drain water particle-bubble agglomerate velocities, it can be observed that the drain water agglomerate velocities are more scattered as compared to the tap water velocities which are more stable. Furthermore, it can be seen that the average velocity of the drain water agglomerates are lower than for the tap water bubbles, indicating lower velocities when the drain water particles

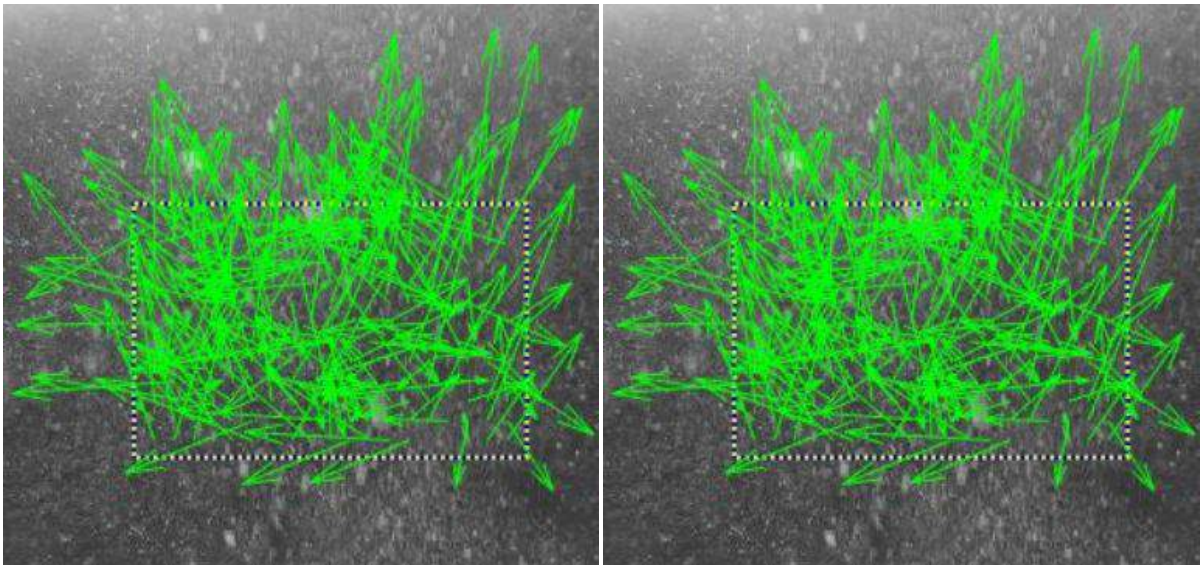

(a) Vector profile for bubble rise velocities at the start of the DAF flow..

(b) Scatter plot for bubble velocities at the middle of the flow.

Figure 4.8: Vector profile for bubble rise velocities at the end of the DAF flow.

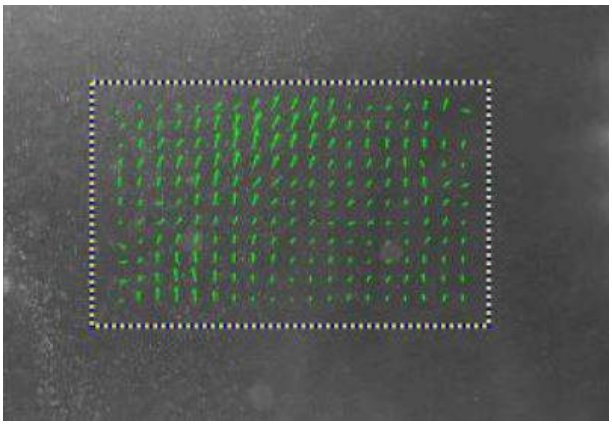

Figure 4.9: Vector profile for bubble rise velocities at the end of the DAF flow.

are attached to the bubbles. This shows that videos captured by an iPhone coupled with analysis by the PIVlab software does show the ability to estimate approximate velocities for the batch scale DAF system. However, these results might not be very robust and do not include the effect of macroscopic factors. These can be further validated bt modelling.

Based on this analysis and from the particle size information gathered for drain water in the previous section, a theoretical estimate of the rise rate of bubble-particle agglomerates can be made. Based on the velocities computed from the tap water videos, an estimate of the bubble diameter is made. It is calculated from Stokes' law given by equation 2.9 and is calculated as follows (at a temperature of 30 °C):

$$D_b = \sqrt{\frac{(0.002219(m/s)x10^8 x0.007978(g/cm.s)x18x100}{(0.996(g/cm^3) - 0.00117(g/cm^3))x981(cm/s^2)}} = 57.14\mu m \tag{4.1}$$

Where Db is the diameter of the bubbles (µm), Vb is the rise velocity of the bubbles (de-

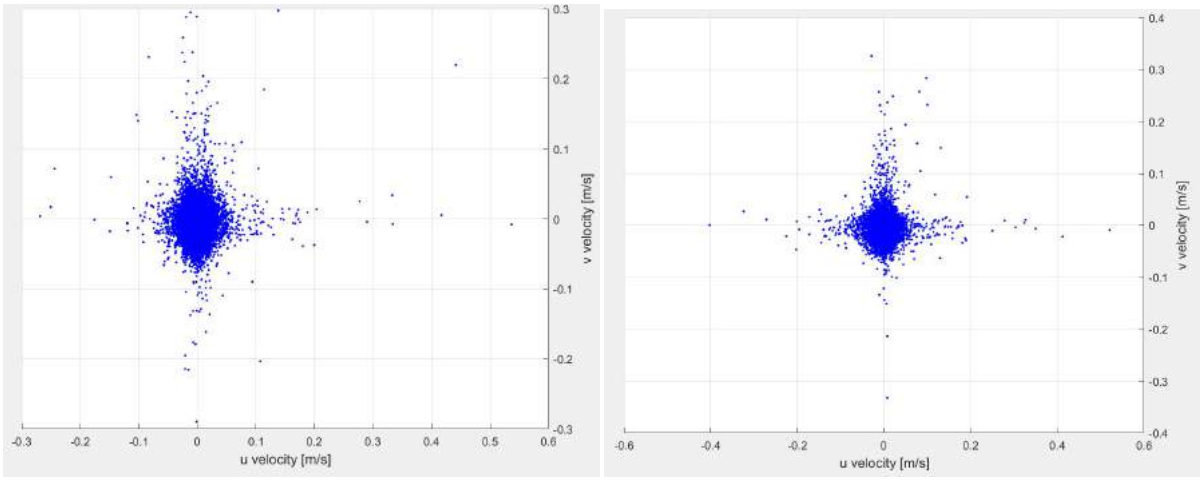

(a) Scatter plot for bubble velocities at the start of the flow.

(b) Scatter plot for bubble velocities at the middle of the flow.

Figure 4.10: Scatter plot for bubble velocities at the start and middle of the flow.

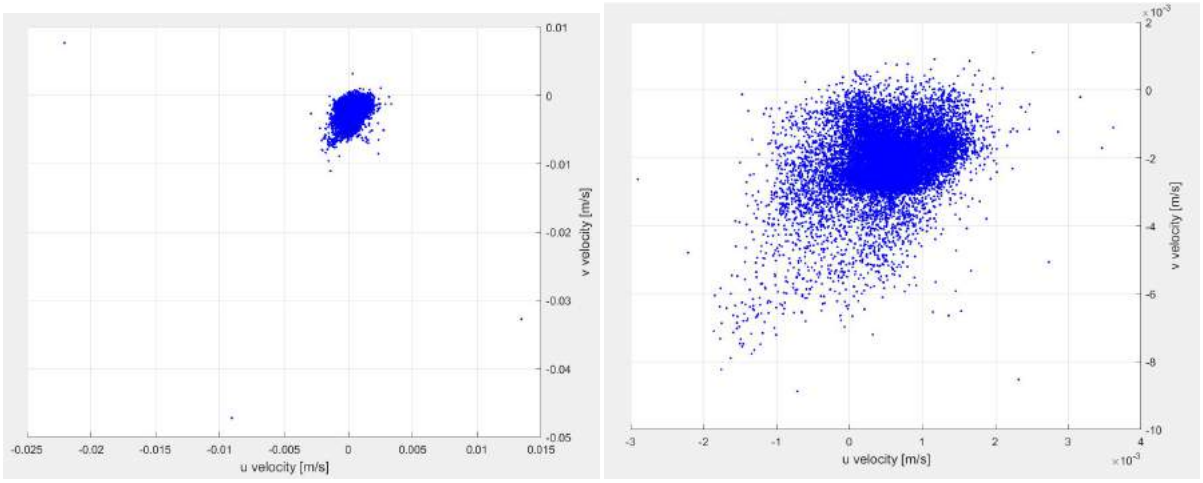

(a) Scatter plot for bubble velocities at the end of the flow.

(b) Zoomed in scatter plot for bubble velocities at the end of the flow.

Figure 4.11: Scatter plot for bubble velocities at the end of the flow.

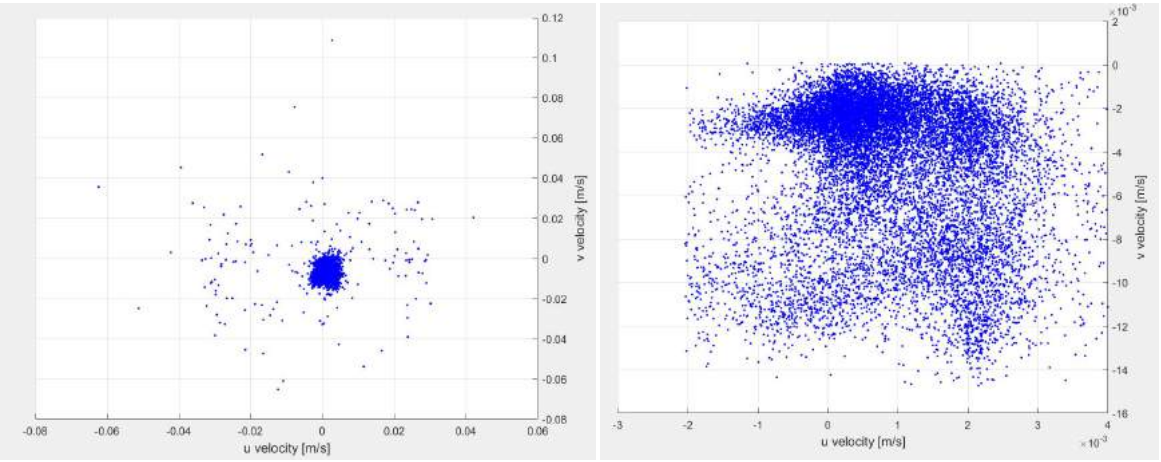

(a) Scatter plot of velocities of drain water particles and bubble agglomerate.

(b) Zoomed in scatter plot of velocities of drain water particles and bubble agglomerate.

Figure 4.12: Scatter plot of velocities of drain water particles and bubble agglomerate.

termined by the PIV analysis) = 2.22E-03 (m/s), g is the gravity acceleration = 981 (cm/s^2), ρ_w is the density of water = 0.996 (g/cm3) , ρ_f is the air density = 0.00117 (g/cm3), μ is the dynamic viscosity at 30 °C = 0.007978 (g/cm.s). This calculates the value of Db as 57.14 µm. Thus the averages size of bubbles formed are found to be between 50 - 60 µm at 30 °C for the DAF experiments. Now, taking the density of drain water = 1.002 g/cm^3 (based on the values calculated by Pycnometer analysis, see Appendix D) and assuming a particle diameter of drain water between 5 - 10 µm (based on the particle characteristic image analysis found in the previous section), the settling velocity of the of the particles (run 10 with drain water) can be found based on stokes' law (equation 2.9) as follows:

$$V_p = \frac{((5x10^{-4})^2(\mu m)x(1.002(g/cm^3) - 0.996(g/cm^3))x981(cm/s^2)}{18x0.007978((g/cm.s)x100)}] = 1.02469E^{-7}m/s \tag{4.2}$$

This is the theoretical settling velocity of drain water particles which comes out to be around 1.02469E-7 m/s. Now, assuming that one bubble attaches to one particle, its total volume is conserved and this gives us the total volume of the particle bubble floc as follows (Benjamin, 2013):

$$V_{pbb} = V_p + V_{bb} = \frac{\pi}{6}(D_p^3 + D_{bb}^3) = \frac{\pi}{6}(5^3 + 60^3) = 113163\mu m^3 \tag{4.3}$$

This comes out to be around 113163 m^3 . Based on this the spherical particle-bubble floc diameter can be calculated as follows (Benjamin, 2013):

$$D_{pbb} = (\frac{6V_{pbb}}{\pi})^{1/3} = (\frac{6113163}{\pi})^{1/3} = 60.01\mu m \tag{4.4}$$

Now the density of the particle-bubble floc is given as follows (Benjamin, 2013):

$$\rho_{pbb} = \frac{\rho_p V_p + \rho_{bb} V_{bb}}{V_{pbb}} = \frac{(1.002(\pi/6)(5\mu m)^3) + 0.00117(\pi/6)60(\mu m)^3}{113163\mu m^3)} = 0.0017g/cm^3 \tag{4.5}$$

This is the theoretical density of the particle-bubble floc. As the floc density is less than that of water, it should rise upwards. Assuming the floc is a spherical particle the rise velocity of the particle-bubble floc can be calculated by stokes' law (equation 2.9) as follows:

$$V_{rise} = -\frac{(0.996-0.0017)(g/cm^3)x981x(cm/s^2)x(60.1x10^{-4}cm)^2}{18x0.007978(g/cms)x100} = -2.45E-03m/s \quad (4.6)$$

Based on these calculations it was estimated that the rise velocity of a single bubble attaching to a drain water particle is around 1.70E-03 - 2.45E-03 m/s, which is similar but slightly higher to the rise velocity found by the PIV analysis (drain water v = -1.42E-03 m/s). However, the theoretical values are calculated assuming one bubble attaches to one particle but in real applications more bubbles will attach to particles possibly clustering resulting in slightly different rise velocity values. This is further recommended to be examined by additional PIV analysis of individual runs or modelling approaches.

Similarly, calculating the rise velocities of particle-bubble agglomerate in the case of sludge (run 4, see appendix L for detailed calculation) settling velocity of particles are found to be 5.9E10-5 m/s bubble-particle agglomerate density is 0.7177 g/cm3 and bubble particle rise velocity is 1.53E-03 m/s. This is observed to be lesser than the drain water particle-bubble rise velocity.

Apart from bubble-particle rise velocities it is important to know the concentration of bubbles in the DAF system to estimate the amount of bubbles available to to float the influent particles. As an example, run 10 for drain water is taken. Mass of air in the DAF tank is given as follows:

$$C_b = \frac{e(C_r - C_{s,air})R - k_a}{1+R} = \frac{0.9x(130-23.7)(mg/l)x(0.5-0)}{1+0.5} = 34.6mg/l \quad (4.7)$$

Now the bubble concentration can be calculated as given bt equation 2.10:

$$\phi_b = \frac{C_b}{\rho_{air}} = \frac{34.6(mg/l)}{0.00117(g/cm^3)} = 29564ppm \quad (4.8)$$

From this the bubble number density can be estimated as per equation 2.11:

$$n_b = \frac{6x\phi_b}{\pi(d_b)^3} = 2.61x10^{11}bubbles \quad (4.9)$$

Finally, we can find the ratio of the concentrations of bubbles/particle as follows(assuming there are 7.62E+06 particles (based on average size of 5 µm and 1.002 g/cm3 density) of drain water per ml in the DAF system):

$$\frac{\phi_b}{\phi_p} = 34bubbles/particle \quad (4.10)$$

From this calculation it can be estimated that for run 10 with drain water, the number of bubbles per particle are theoretically around 34. Following a similar calculation for sludge (run 4), theoretically there would be around 14000 (50 times more - with 80 µm average particle diameters and density 1.02 g/cm3) bubbles per anaerobic sludge particle. However,

for both these cases it should be noted that the recycle ratio is taken as 0.5. In practice for a recycle flow system, recycle ratios are around 0.1. In that case the theoretical number of bubbles per particle for drain water will be 4 and for anaerobic sludge about 3000.

From these results it was found that using PIV software methodology coupled with an iPhone camera worked in a field set up, but it had it's operating and analytical limitations. Furthermore, for a reliable conclusions the PIV analysis should be done for each run for a robust analysis. This is extremely challenging, time consuming and expensive. Other authors, even with more equipment heavy experiments have found difficulties in reporting agglomerate properties due to concentration of dense air bubbles in the flotation tank. Lundh (Lundh, 2002) reports that when deploying Acoustic Doppler Velocimetry (ADV) air bubbles were interfere with the equipment and reduce the magnitude of water of velocity measured. For non-intrusive measurements like the PIV, Laser Doppler Velocimetry (LDV) (Hague et al., 2001) and image processing (Honkanen et al., 2010) had problems with dense bubble concentrations. Thus, modelling can be a good alternative. It is evident from literature that there is very less information about the measurement of aggregate sizes, which are considered difficult to measure because of their delicate structure (Bondelind et al., 2013). Attempts to record the behaviour of aggregates in the flotation tank by image processing were found to have difficulties (Honkanen et al., 2010). Fukushi (Fukushi et al., 1998) however, in spite of the difficulties experimentally was able to count the number of bubbles attached to a floc and the mean bubble size was found to be 63 µm. Kwak (Kwak et al., 2009) looked into the maximum amount of bubbles that could attach to a floc by using the rise velocities and measured floc sizes. (Ljunggren et al., 2004) recorded the size of the rising aggregate to be 300 µm. None of these studies could measure the real size of the aggregate.

4.4. Pathogen Removal Efficiency

For the drain water, removal efficiencies for *E-coli* and *C. Perfringens* (as an indicator for *Cryptosporidium* oocysts) were analysed for the 15 DAF experimental runs. Figure 4.13 and Table 4.12 give the log reductions for *E-coli* and table 4.13 shows the correlation between *E-coli* log reduction and the DAF operation parameters tested in this study. Appendix (F) gives the detailed calculation for these analysis.

Run	TSS (mg/l)	tention time (m	Pressure (bar)	Coagulant (g/l)	Time Coagulation (min)	ainwater (CFU/n	DAF Clean Effluent (CFU/ml)	Log Reduction
1	30	20	5	0.005	30	8.5E+03	2.0E+03	0.63
2	30	20	5	0.5	10	4.8E+04	2.1E+04	0.35
3	30	13	5	0.5	30	6.5E+00	1.5E+00	0.64
4	30	13	3	0.5	30	8.5E+00	1.5E+00	0.75
5	30	20	3	0.005	10	1.1E+01	1.0E+00	1.02
6	30	13	3	0.005	10	9.8E+01	2.7E+01	0.56
7	270	16.5	4	0.2525	20	6.0E+00	1.5E+00	0.60
8	270	16.5	4	0.2525	20	5.0E+00	1.5E+00	0.52
9	270	16.5	4	0.2525	20	3.0E+00	1.0E+00	0.48
10	510	13	5	0.005	10	1.8E+04	1.2E+03	1.18
11	510	20	3	0.5	10	6.6E+01	4.9E+01	0.13
12	510	13	5	0.5	10	2.0E+03	1.8E+03	0.05
13	510	20	3	0.5	30	1.6E+03	5.5E+02	0.46
14	510	20	5	0.005	30	3.5E+04	8.0E+02	1.64
15	510	13	3	0.005	30	2.9E+04	6.5E+02	1.65

Table 4.12: E-coli Log-reduction for 15 experiments with drain water.

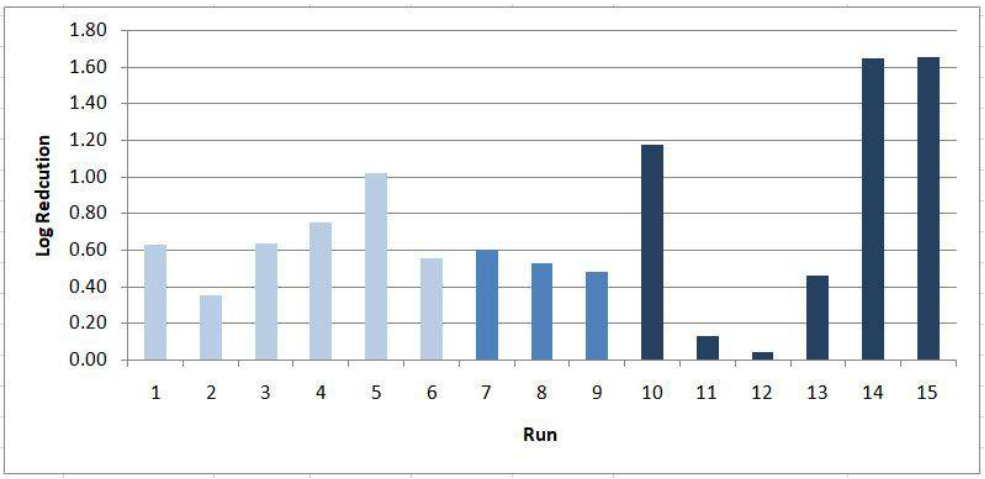

Figure 4.13: Graphical representation of E-coli Log-reduction for 15 experiments with drainwater. The light blue bars represent the suns with low TSS values (30 mg/l), medium blue bars represent the mid range TSS values (270 mg/l) and bard blue bars represent the high range TSS values (510 mg/l) for the 15 drainwater runs.

DAF Parameter	Spearman's Correlation
TSS (mg/l)	-0.05
Retention time (min)	-0.22
Pressure (bar)	-0.02
Coagulant (g/l)	-0.67
Time Coagulation (min)	0.43

Table 4.13: Spearman's correlation estimation for DAF parameters studied and the E-coli removal.

E-coli removal range was found to be from 0.05 - 1.65 log with the highest removal being 1.65 log for run 15, showing that the DAF can remove more than 90% *E-coli* from the drain water which will help reduce the pathogen load and energy consumption for the next treatment steps. On comparison with the removal percentages of TSS removal, no correlation and a negative trend was observed with a corelation value of -0.055 (Pearson's co-relation) and -0.093 (Spearman's co-relation) for the DAF with Barapullah drain water as influent. Based on this it is inferred that most of the E-coli organisms do not get captured on the flocs/particles and they do not adhere to the bubbles as well. Furthermore, it is interesting to note from these analysis that the time of coagulation shows the highest correlation (0.43) and coagulant concentration shows a high negative correlation (-0.67).

Santos and Daniel (Santos and Daniel, 2017a) observed that indicator organisms like *E-coli* and total coliforms show high concentrations after flotation and are not easily removed. This indicates that these organisms may not have characteristics to adhere to flocs or bubbles maybe because of biological characteristics on the surface of the organisms. They found that *E-coli* and total coliform mean removal to be less than 1 log for different flocculating conditions (13 - 20 minutes retention time) while treating anaerobically treated sludge. Other authors like De Nardi (De Nardi et al., 2011) in contrast found 3-4 log removal for *E-coli* and total coliform removal by the DAF to treat wastewater from a poul-

try slaughterhouse with ferric chloride as coagulant. For municipal wastewater Koivunen and Tanski (Koivunen and Heinonen-Tanski, 2008) reported 90–99.8% (1-3 log) reduction of enteric microbes like enterococci, total coliforms and F-RNA coliphages by DAF treatment with different floculating conditions (4-8 minutes retention time) for primary wastewater effluent. They compared these results with the DAF removal efficiency as tertiary treatment and found that DAF has higher efficiency as primary treatment due to the presence of more microorganisms in the influent suggesting that DAF is an effective primary wastewater treatment option. These differences in effect of operating condition in literature can be attributed to the influent wastewater and the different DAF operating conditions such as type of coagulant, conditions of coagulation and flocculation, and recycle ratios).

E-coli removal results by the DAF obtained in this study does show a good relation to the municipal wastewater *E-coli* removal results obtained in literature. Furthermore, the coagulation mechanism and *E-coli* organism physical properties including the size and surface attraction) are identified as parameters impacting *E-coli* removal efficiency of the DAF. With an increase in coagulation time it might have been that the floc size could have increased and resulted in better removal, however a low correlation is observed. The mechanisms behind these parameters need to be studied further to in order to optimize E-coli removal by the DAF. More experiments should be conducted to understand the influence of coagulation type and conditions, floc size and microorganism surface properties on the removal of these organisms by the DAF.

As discussed in Chapter 2, the DAF is known to be extremely effective in removing *Giardia* and *Cryptosporidium* with many studies in drinking water. However, not many studies are recorded with sewage (Santos and Daniel, 2017a). In this study, experiments were done to the *C. Perfringens* (as an indicator for *Cryptosporidium*) removal from the drain water for 3 out of the 15 runs for drain water - run 6 (TSS = 30 mg/l), run 7 (TSS = 270 mg/l) and run 14 (TSS = 510 mg/l). Table 4.14 gives the log reduction value for these analysis. Only with run 14 recorded a removal efficiency (0.58 log reduction). Due to no vacuum setup being present at the site and in turn using a 50 ml syringe to create a vacuum, the filtration mechanism for plating *C. Perfringens* samples was ineffective an no result can be inferred from these experiments. This analysis was unsuccessful and for future analysis accessibility of a vacuum at the site/lab for filtration is recommended.

Run	TSS Removal Efficency	Drainwater Colonies		Average	Volume for plating (ml)	Dilution factor	CFU/ml	Clean Eff. Colonies		Average	Volume for plating (ml)	Dilution factor	CFU/ml	Cin/Cout	log reduction	Perc red
6	70%	19	20	19.5	1	1	1.95E+01	0	0	0	1	1	0.00E+00	x	x	x
7	92%	10	12	11	1	1	1.10E+01	0	0	0	1	1	0.00E+00	x	x	x
14	83%	12	7	9.5	1	1	9.50E+00	2	3	2.5	1	1	2.50E+00	3.80E+00	0.58	73.68

Table 4.14: E-coli Log-reduction for 15 experiments with drain water.

In literature, Andreoli and Sabogal-Paz (Andreoli and Sabogal-Paz, 2019) have reported a removal of 1.31 log to 1.79 log for *Giardia* cycts and between 1.08 log to 1.42 log for *Cryptosporidium* oocysts from a water supply system by DAF with coagulation and flocculation. Furthermore, they recorded that by adding filtration with these processes, removal of cysts and oocysts improved by 2.2 log. Plummer (Plummer et al., 1995) recorded 2-3 log removal of *Cryptosporidium* at bench scale and Hall (Hall et al., 1995) showed a removal of 3-4 log with a combination of DAF and filtration. Edward (Edzwald et al., 2000) found

a 5 log removal for *Cryptosporidium* and *Giardia* when the DAF followed by filtration was studied for water with low turbidity, with cationic polymer and aluminum sulphate coagulants and detection by centrifugation followed by epifluorescence microscope. Even with a filtration step, coagulation and DAF treatment failed to remove protozoa completely from the wastewater which indicates the disinfection is important to reduce microbial risk from wastewater to bring it to drinking water standards (Andreoli and Sabogal-Paz, 2019). For sewage, DAF process has been found to be a more effective barrier against cysts from anaerobic effluents. For anaerobically treated sewage, Santos and Daniel (Santos and Daniel, 2017a) reported protozoa removal by the DAF from 1.8 to 3.3 log with an average value of 2.37 - 2.52 log as per the flocculation conditions, and suggests that optimum conditions for coagulation, bubble characteristics and re-circulation ratios are needed for good removal of cysts with the DAF. Moreover to remove cysts, particle interaction forces, interaction between air and the cyst, particle and cyst and the cysts surface properties should be known.

Edward (Edzwald et al., 2000) suggests that the inter-particle attraction forces and the hydro-dynamic interactions such as the van der waals, electrostatic and hydrophobic forces lead to the particle-bubble interactions in the DAF. The surface hydrophobic surface properties of cysts govern their mechanism of adhesion with particles (Dai et al., 2004). Therefore, in the case of interactions between the cyst and bubble, hydrophobic forces may be more dominant which might explain the ability of cysts to adhere to the suspended particles resulting in the cyst sticking to the floc and being removed (Medema et al., 1998). DAF experiments with effluent from different flocculating conditions and anaerobic effluent showed that cysts found after DAF treatment were influenced by the cyst concentration present in the influent (Santos and Daniel, 2017a).

Other authors have also found similar results for *Giardia* cyst of 2.4 log removal. In these studies different flocculating conditions didn't show a statistical significant relation to the cysts concentration and its removal. (Edzwald et al., 2000) Edward (Edzwald et al., 2000) suggests that the floc size is an important parameter to remove these pathogens efficiently by the DAF by entrapping the protozoa in flocs of 30 µm size with large enough rise rates to be removed by flotation. This author recommends a floc size of 30 µm for efficiently removing (oo)cysts by the DAF. The size range of *Cryptosporidium* particles is from 8-15 µm and for *Giardia* its from 4-6 µm with both particles having a density of about 1,100 kg/m^3. This results in low settling velocities (0.02 m/h) having more time entrap even within small flocs. He further demonstrated that even when the organisms are not entrapped in the floc, it tends to attache to the bubbles forming an (oo)cysts - bubble aggregate which is low in density resulting in higher rise rate leading to increased removal of these pathogens. He further states that the rise velocities of the particles attaching and to the bubbles and floc particle entrapment explains how the DAF is effective in removing low density particles such as *Cryptosporidium* and *Giardia*. Moreover, it was found that DAF has higher removal efficiencies of these cysts in warmer water. This was attributed to the fact that cold water results in high viscosity decreasing the rising velocity. Factors like pH, temperature and ionic strength may also influence the detection of (oo)cyst in sludge samples (Bonatti and Franco, 2016) . For municipal wastewater treatment Santos and Daniel (Santos and Daniel, 2017a) found an average removal of cysts as 0.47 log (66.5%) and an average removal of 1.57 log (97.3%) with biological treatment by a UASB reactor, showing that anaerobic biological treatment might be more efficient in removing these parasites.

Thus to estimate reliable parasitological quality of the drain water for *Giardia* and *Cryptosporidium* more experiments are required, and most of the indicator organism might not be a reliable tool. Literature suggests that cycts removal by the DAF is significant and higher than *E-coli* and other indicators. Only *C.perfringens* removal was found to be the relatively closest to removal of cysts thus, indicating that for removal of pathogens from the DAF *C.perfringens* indicates good removal of cysts. Studies by Santos and Daniel (Santos and Daniel, 2017a) have shown by Sperman's correlation that there wasn't a common relation between microbial indicators and Giardia cysts. Studies by Briancesco and Bonadonna (Briancesco and Bonadonna, 2005) also did not show a correlation between microbial indicators (enterococci, E. coli, coliphages, total coliforms, Clostridium spores, fecal streptococci) and protozoa. They state that this difference should be due to the difference in the organisms behaviours and properties. Thus, as per other studies it is indicated that the occurrence of cysts can not be determined by microbial parameters consistently and that directly analysing the presence of cysts is recommended. Finally, it is suggested that the DAF achieves low removal of *E-coli* but can achieve high removal of *Giardia* and *Cryptosporidium*. Thus, the DAF can help reduce the bacteria load from the drain water by 1.65 logs and possible high amounts of protozoa as well, acting as effective barriers and saving energy for the next treatment steps. This means that the chunk of these pathogens will be concentrated in the DAF froth removed and care must be taken when handling and treating the removed particles.

5

Conclusions

This study investigated and compared the effect of operating parameters on the TSS removal performance of a bench scale DAF column set up with different influents - Canal Water, Barapullah Drain Water from Delhi, Anaerobic Sludge from a wwtp in Delft and Anaerobic Sludge from a wwtp in Delhi. Furthermore, particle characteristics and morphology of the influent and clean effluent suspended matter were studied to understand their relation to the TSS removal performance of the DAF. The rise velocities of particle-bubble agglomerates for experimental runs with higher TSS removal were also estimated. This gives us more insight into the correlation between better performing operating parameter ranges and then bubble-particle interaction. Additionally, pathogen removal potential of the DAF with Barapullah drain water as influent was studied. The results presented in the study give us further insight into the effectiveness of the DAF and its ability to be optimized for treating different types of wastewater. This chapter summarizes the results for the research questions given in Chapter 1 as follows:

1. **DAF critical parameters:** Variations were observed in the critical parameters for the different influents. Optimum TSS removal and DAF critical parameters investigations with the different influents showed that for canal water time of coagulation, retention time and influent TSS concentration had a statistically significant effect, whereas for drain water, the influent TSS concentration was the most significant. Coagulation is a an extremely effective pre-treatment to improve the DAFs performance (Tsai et al., 2007). As canal water is a diluted suspension, it was found that it relied on coagulation contact time for formation of bigger flocs for particles to eventually be removed. However, the same was not observed for drain water with the only significant operating parameter being influent TSS concentration. It is hypothesized that reason for this could be due to the presence of more hydrobhobic particles in the drain. Excessive foaming was observed during the DAF experiments with drain water which might have had an effect on the coagulation mechanism for drain water. Moreover, higher removal efficiencies were observed with drain water as influent for similar experimental runs as compared to canal water. This indicates that the density of drain water particles is lower than particles in canal water. The influent TSS concentration showed statistical significance for both canal water and drain water and generally very different removal efficiencies for same runs (run 4 has a 66% removal for canal

water and 89% for drain water) was observed, indicating that difference in the particle characteristics of the different influents has an impact on the eventual removal performance.

With anaerobic sludge from Delft as influent, pressure showed the most significance and similar (but higher) TSS removal trends were observed for anaerobic sludge from Delhi. As with concentrated suspensions like sludge, it is important to have sufficient volume of bubbles for higher removal efficiencies (Benjamin, 2013). Thus, higher pressure (5 bar) showed increased removal efficiencies due to the presence of more bubble volume as compared to lower pressure. Unlike canal water, anaerobic sludge did not show a significant effect on coagulation. It is concluded from this result that the coagulants and coagulation condition considered for the DAF anaerobic sludge experiments are not optimum and need to be investigated further.

2. **Particle characteristics and morphology:** The size, size distribution and shape of particles in canal water and drain water were found to be different. Canal water with higher influent TSS concentration showed average influent particle diameters of 12-14 µm, whereas average drain water influent particle diameters were observed to be lower at around 3-5 µm. For both canal water and drain water influents, clean effluent particle diameters were observed to be around 2 - 3 µm. Thus, this shows that DAF poorly removes particles below 3 - 5 µm with small variations in sizes observed depending on the operating conditions. Densities found for drain water was 1.002 g/cm^3 and for anaerobic sludge from Delhi was 1.02 g/cm^3. In terms of shape, influent canal water particles were seen to be more irregular with an average circularity of 0.83 and majority of influent drain water particles were observed to have a more circular shape with a average circularity value of 0.92. The clean effluents for both these cases were found to quite high in circularity with an average value of 0.95. It is concluded from these results that for both canal water and drain water, the operating parameters selected for all cases did mange to remove average particles above 3-5 µm, with more dramatic reductions observed with higher TSS influent concentrations. Microscopic images of anaerobic sludge particles from Delhi, indicated a reduction of average particle diameter from 150 µm to 80 µm.

3. **Particle-bubble rise velocities:** Based on the velocity profile of tap water and drain water estimated, it was observed that the velocity of drain water (v = -1.42E-03 m/s) was lower than tap water (v = -2.22E-03 m/s) indicating higher densities of drain water particle-bubble agglomerates. This velocity value was found to be in the range of theoretical calculations of particle-bubble agglomerate rise velocities for drain water (v = 1.69E-03 m/s). Therefore, we are able to gather significant information with everyday use technology (like phones), making data acquisition easier under difficult environmental circumstances. Furthermore, the bubble concentration and bubble-particle ratio was estimated for drain water and anaerobic sludge from Delhi. It was found that for higher TSS removal runs, drain water DAF experiments had 34 bubbles/particle and sludge would have around 50 times more.

4. **Pathogen removal:** Maximum removal of *E-coli* from the DAF was observed to be 1.65 log indicating that it is possible to remove more than 90% of the bacterial load

which could increase the efficiency and save energy for the next treatment step. Furthermore, coagulation concentration showed the most significance for E-coli removal. Based on literature and these results, it is recommended that *E-coli* removal is not a reliable estimate for predicting the removal of *Giardia* and *Cryptosporidium*. Moreover, *Giardia* and *Cryptosporidium* would be removed in higher concentrations from this system. Finally, no significant correlation was found between the TSS removal efficiencies and *E-coli* removal efficiencies of the DAF for treating Barapullah drain water.

6

Recommendations

These results demonstrated that the DAF can be optimized for high removal efficiencies for different influents. Insights on the effect of influent characteristics, particle-bubble agglomerate, and their relation to operating parameters of the DAF were found. Further research to fill the gaps between operating parameters and optimum DAF removal efficiencies found in this research is recommended as follows:

1. Since these experiments were conducted during the summer months in Delhi, it is recommended that data regarding DAF TSS removal is collected and analysed throughout the year for a more accurate estimation about its performance and effect of operating parameters.

2. For future studies it is recommended that a CCRD experimental design is conducted for the significant parameters with canal water. This will give a modelled second degree response surface with optimum values for these parameters.

3. Also, based on the analysis and literature more coagulation experiments are recommended to optimize this parameter further. Other coagulants such as alum or ferric chloride are recommended for canal water and drain water experiments.

4. Further research is needed to validate the effect of hydrophobicity on the significance of operating parameters for drain water. Methods such as Atomic Force Microscopy (AFM) as well as simple qualitative methods like extraction of particles from a liquid medium into an oil medium can be done.

5. To validate and improve the results obtained from the PIV experiments, analysis by CFD modelling can be explored.

6. The results obtained from this study, help us estimate the TSS removal that can be achieved and to zoom in on the critical operating parameter for the different influents tested. For a holistic understanding of the the relation between the parameters and TSS removal obtained, further research is recommended with individual significant operating parameters, the influent characteristics and bubble-particle interaction based on the results obtained.

7. Other morphological parameters such as Ferret diameter and Aspect ratio of the particles from the different influents is recommended to be studied for a deeper understanding of the effect of particle shape on the TSS removal.

8. DAF experiments with raw wastewater influent from wwtps are recommended. This can be an intermediate between the drain water and anaerobic sludge to further understand the DAF oper.

9. And finally, for concrete estimation of cysts removal and its correlation to the operating parameters of the DAF, experiments with *C.Prefringens* to find *Giardia* and *Cryptosporidium* removal should be done with adequate equipment at the site.

Appendix A

Figure A.1 illustrates the water stress levels globally ranging from low to extremely high. Here, it can be seen that India falls under an extremely high level of water stress. Figure A.2 and A.3 give an indication of the economical and physical water stress of the world, and the levels of water stress in highly populated cities of the world respectively. This helps us identify cities with the most water stress and co-relate the data to economical and physical water scarcity indicators. Figure A.3 zeros in on water stressed cities in India where it can be seen that Delhi is quite high up. Finally, figure J.13 and A.6 give data and trends for the reasons for India's water stress in depth.

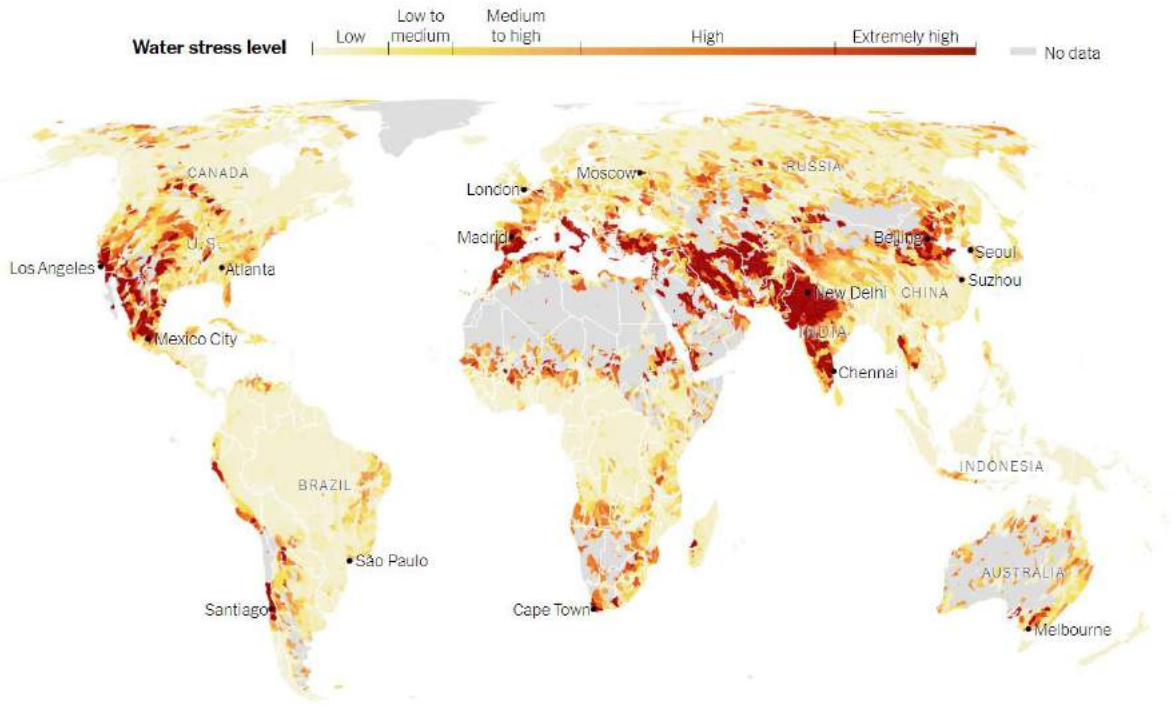

Figure A.1: Water stressed regions of the world (New York Times, 2019).

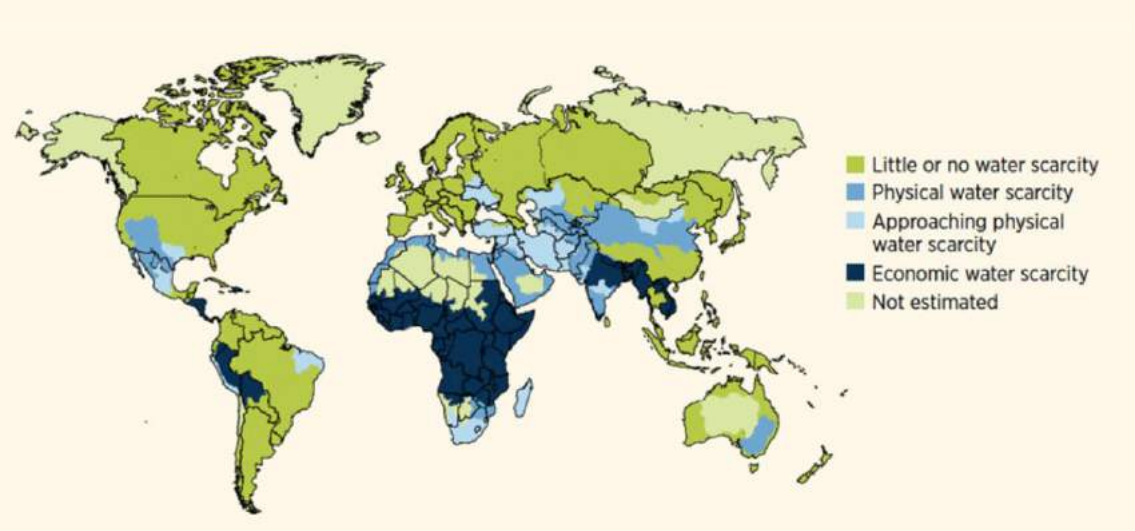

Figure A.2: Economical and physical water scarcity globally (WWAP, 2012).

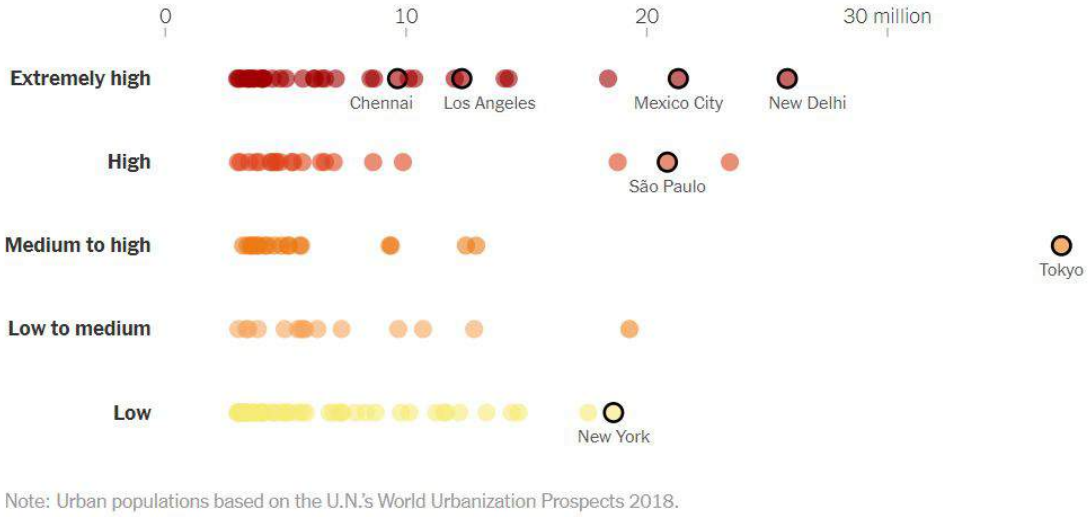

Figure A.3: Levels of water stress in urban areas (population 3 million or more) (New York Times, 2019).

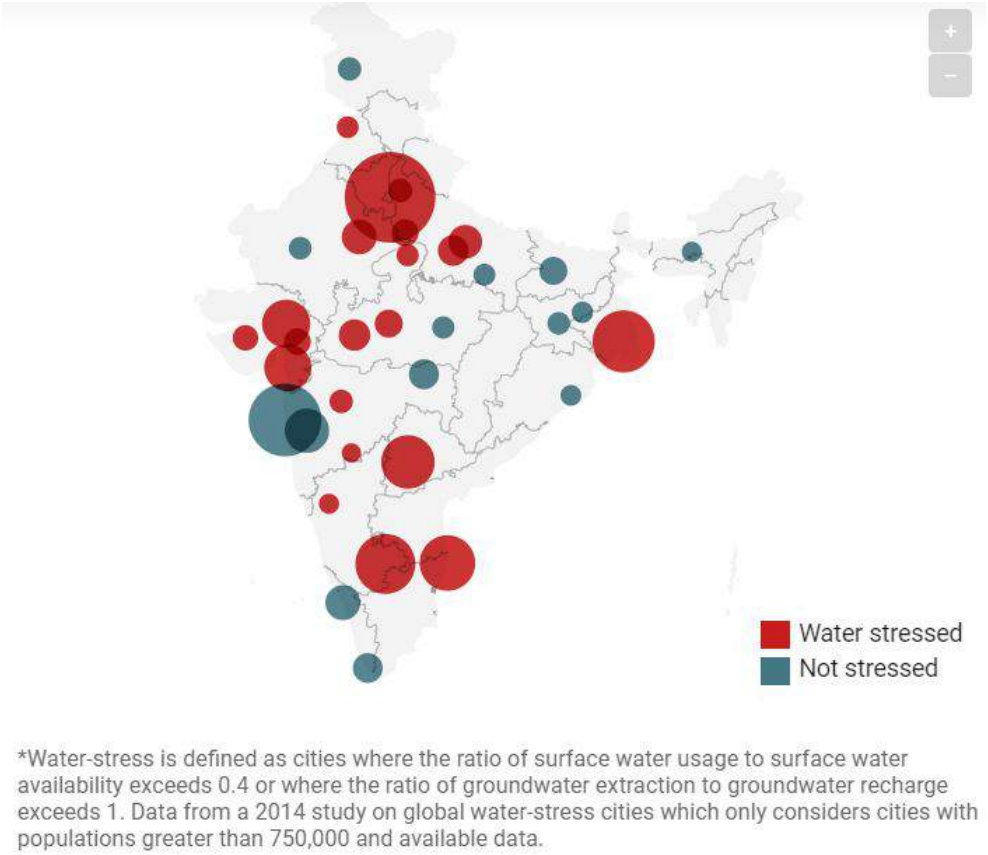

Figure A.4: Indian cities under water-stress by 2030 (McDonald et al., 2014).

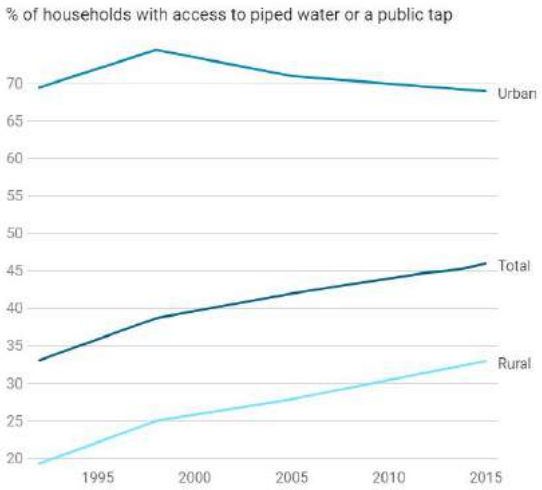

(a) Percentage of Indian households with access to piped water supply or pipe tap based on National Family Health Surveys I, II, III and IV (livemint, 2019).

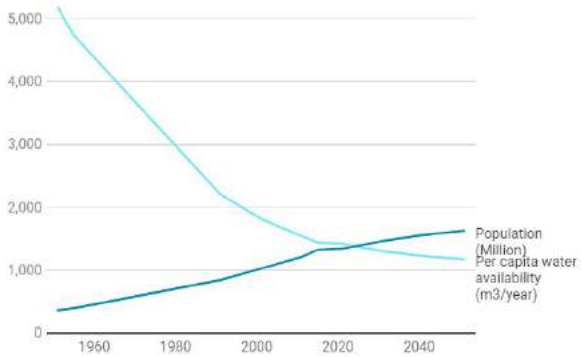

(b) Trends for India's per-capita water supply and population growth based on Envirstats 2018 - MOSPI (livemint, 2019).

Figure A.5: Tends showing India's access to piped water and water supply compared to population growth.

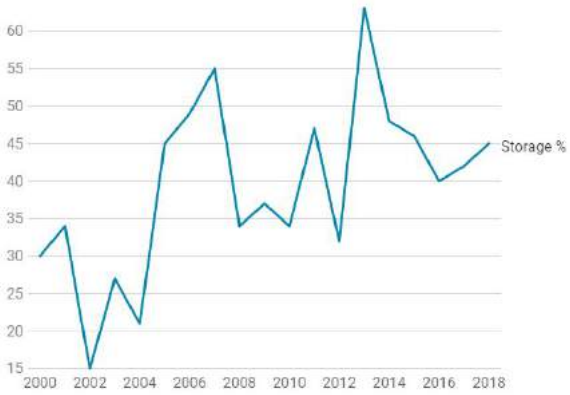

(a) Percentage of filled capacity in India's 92 reservoirs based on data by Central Water Commission (livemint, 2019).

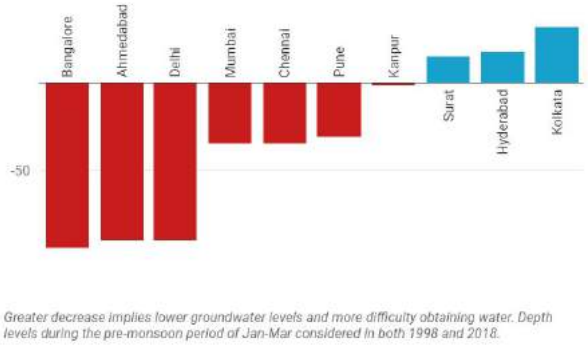

(b) Decline in India's percentage change in ground level from 1998 to 2018 in it's 10 most populated cities (livemint, 2019).

Figure A.6: Trends showing decline in India's reservoir capacity and decrease in ground water levels.

B

Appendix B

B.1. The Barapullah Nallah

Delhi and it's surrounding regions referred to as National Capital Region (NCR) are historically made up of 5 major drainage systems - Mehrauli basin, Shahdara basin, Alipur basin, Najafgarh basin and the Kushak-Barapullah basin. Figure B.1 gives graphical depiction of these streams, their catchment area and location (Cherian, 2004).

The Barapullah drain covers a catchment area of around 137 sq. km. and makes up the regions of south and central Delhi. This being one of the largest streams circuits around 10 kms and can reach up to widths of 100 m and eventually joins the Yamuna river, making it a vital part of the entire drainage system of Delhi.(Cherian, 2004) The nallah gets a majority of its water from the highly dense residential colonies not connected to the sewage grid including slums and unauthorized neighbourhoods from Mehrauli all the way to Sarai Kale Khan (Amita Bhaduri, 2016). Referred to as Nizammuddin darya (creek) by locals, it was named Barapullah based on the pul (bridge) which was built over it by Mihir Banu Agha, who was the chief eunuch of emperor Jahangir. The bridge comprised of 10 piers and exactly Bara (12) pallahs (columns), hence the name. In the 1800's, the drain has been known to be perennial, however due to deforestation around the southern ridge as a result of rapid growth, the stream's flow has become seasonal, following the monsoon pattern. Over the years, as the city has expanded, sewers have been buried, diversions and embankments have altered runoff flows, the city's hydraulic structures like nahrs (canals), baolis (step wells), hauz (lakes) etc. that allowed groundwater recharge have also been damaged, resulting in overpowering the profile and capacity of the streams. (Amita Bhaduri, 2016) Furthermore, apart from being overburdened by the city's sewage, the natural flow of the nallah has also been affected by natural changes in the terrain and soil (Cherian, 2004). In 2014, to ease the congestion in Delhi, the elevated fly-over was constructed along the lower stretch of the Barapullah. This led to the further dumping of constructing waste in the drain and increased encroachment into the drain's flood plain directly threating the drainage system. Moreover, Architects have referred to this as stripping Delhi of its urban charm. (Amita Bhaduri, 2016) Figure B.3 gives the current location of the LOTUS^{HR} project site which is at the confluence of the Barapullah Nallah and the Yamuna River.

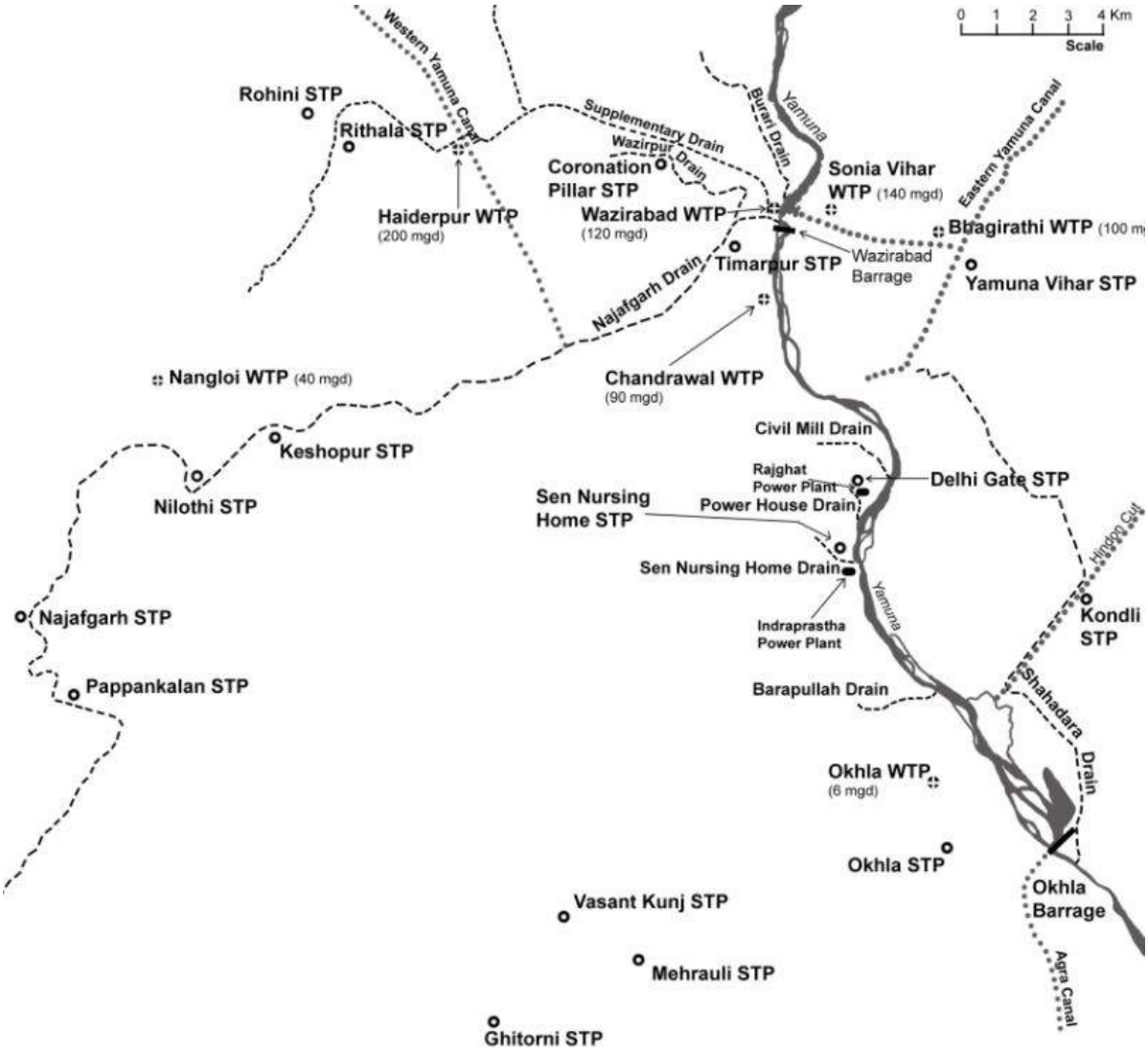

Figure B.1: Image of a drains and catchment area leading to the Yamuna (Cherian, 2004).

Figure B.2: Image of a section of the Barapullah nallah (source:cityblob.com)

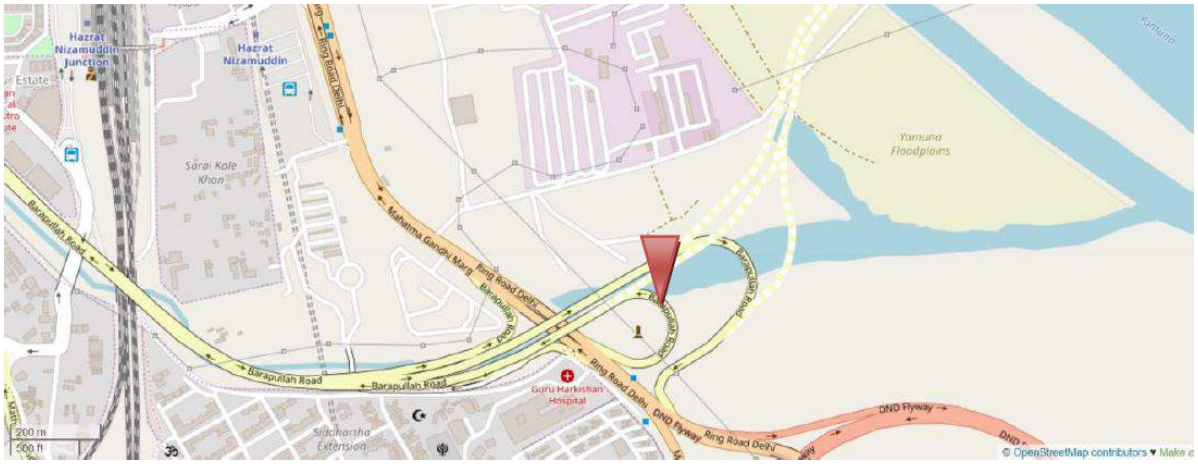

Figure B.3: Map showing the location of the project site in New Delhi.

C

Appendix C

Please see next page for Table C.1 - Barapullah drain data from 2018.

Table C.1: Barapullah Drain Data 2018

DATE	pH	Temperature(°C)	DO(ppm)	Conductivity(µS)	BOD(mg/L)	COD(mg/L)	TS(mg/L)	TVS(mg/L)	TDS(mg/L)	TVDS(mg/L)	TSS(mg/L)	TVSS(mg/L)	TC [log (CFU/ml)]	FC [log (CFU/ml)]
16-10-2017	7.05	26.70		1448.00	150.00	208.33	885.00		680.00		205.00		5.08	4.64
30-10-2017	7.21	24.30	0.45	573.00	80.00	291.67	450.00		300.00		150.00		4.92	4.57
14-11-2017	7.35	22.30	0.43	320.00	420.00	841.65	725.00		685.00		40.00		6.07	4.81
27-11-2017	7.16	19.40	0.37	1179.00	165.00	250.00	980.00		860.00		120.00		5.92	4.83
11-12-2017	7.08	18.70	1.83	1480.00	450.00	768.75	740.00	130.00	630.00		110.00		5.76	4.70
26-12-2017	7.41	18.10	0.89	1125.00	500.00	662.50	710.00	180.00	640.00	50.00	70.00	130.00	5.95	4.63
08-01-2018	7.67	21.00		1168.00	250.00	783.33	760.00	280.00	690.00	160.00	70.00	110.00	5.92	3.62
25-01-2018	7.45	12.30	0.78	1072.00	300.00	1191.67	620.00	470.00	550.00	20.00	70.00	450.00	5.93	3.61
08-02-2018	6.88	18.70	0.79	1118.00	500.00	760.00	1150.00	300.00	1010.00	150.00	140.00	150.00	5.98	4.71
20-02-2018	7.07	11.30		1237.00	150.00	890.00	950.00	260.00	890.00	140.00	60.00	120.00	4.92	4.16
09-03-2018	7.18	24.60	0.79	1103.00	200.00	375.00	940.00	650.00	910.00	500.00	30.00	150.00	5.75	4.69
20-03-2018	7.17	24.70	0.44	1135.00	345.00	475.00	670.00	70.00	630.00	30.00	40.00	40.00	5.21	3.84
09-04-2018	7.32	24.50	0.70	1098.00	230.00	1087.50	810.00	45.00	590.00	44.00	220.00	1.00	5.57	4.77
24-04-2018	7.06	28.30	0.27	1280.00	438.75	687.50	910.00	780.00	650.00	460.00	260.00	320.00	5.08	3.97
05-11-2018	7.14	29.70	0.27	1240.00	312.00	1312.50	620.00	80.00	580.00	70.00	40.00	10.00	5.63	4.76
25-05-2018	6.98	31.70	0.25	1030.00	190.00	387.50	730.00	330.00	700.00	300.00	30.00	30.00	4.99	4.12
06-12-2018	7.00	33.10	0.22	1000.00	310.00	287.50	860.00	750.00	760.00	640.00	100.00	110.00	4.98	4.82
24-06-2018	7.43	34.90	0.38	1093.00	140.00	220.00	580.00	375.00	460.00	280.00	120.00	95.00	5.61	4.86
16-07-2018	7.38	31.30	0.94	1100.00	180.00	331.25	1130.00	680.00	1060.00	300.00	70.00	380.00	5.08	4.07
31-07-2018	7.17	30.40	0.62	878.00	165.00	387.50	920.00	260.00	710.00	80.00	210.00	180.00	5.31	4.22
13-08-2018	7.00			690.00	270.00	356.40	470.00	290.00	420.00	280.00	50.00	10.00	5.91	4.92
28-08-2018	7.61	29.10	0.89	344.00	100.00	114.30	770.00	320.00	260.00	170.00	510.00	150.00	6.02	5.78
09-12-2018	7.66	30.50	0.60	920.00	135.00	437.50	680.00	280.00	240.00	160.00	440.00	120.00	5.23	4.36

Appendix D

D.0.1. Density

Pyconmeter test was done to measure the density of the drain water and site sludge. It is a glassware as a precision piece that has two parts - a stopper and a bottle. The stopper comprises of a capillary tune with a frosted bottom which fits in the frosted neck of the bottle quite snugly. The bottom glass part in small in size to accurately determine volume from the mass of water it can contain at a particular temperature. For the experiment, first the clean dry pycnometer bottle is dried and weighed to the nearest 0.001g. Then 15 ml of the unknown sample was poured into the bottle till its almost full followed by inserting the stopper keeping the frosted end in the bottle. Excess liquid from the outside of the bottle is dried and the bottle with the stopper is weighed. Clean and dry the bottle and stopper and repeat the same procedure with distilled water at the room temperature. The volume of pycnometer is calculated by the literature value of density of water at certain temperature. These values are then further used to determine the specific gravity and temperature of the unknown liquid samples. Figure D.1 shows an image of the pyconometer analysis done for Barapullah drain water and Table D.1 give the density values calculated.

Figure D.1: Image of Pycnometer experiments with drain water.

Table D.1: Tabulated values of densities by Pycnometer experiments with drain water and sludge.

Run (at T = 23C)	Empty weight of Pycnometer (g)	Weight of Pycnometer and tap water (g)	Mass of water (g)	Volume of water (L)	Weight of Pycnometer and sample (g)	Mass of sample (g)	Density of sample (g/l)
Formulas	A	B	C = B-A	C/0.99754 (Density of water at 23 C)	D	E = D-A	E/C
Date: 01-07-2019							
Sludge 2	74.75	128.15	53.40	53.53	128.79	54.04	1.01
Sludge2.1	74.74	128.13	53.38	53.51	128.79	54.04	1.01
Date: 06-07-2019							
Drainwater							
Drainwater 3	74.48	128.03	53.55	53.68	128.29	53.81	1.002
Drainwater 4	74.87	128.04	53.17	53.30	128.31	53.44	1.002

Appendix E

Table E.1: Morphological parameters extracted for each image with ImageJ

Parameter	**Unit**	**Description**
Area	µm²	Area of selected region (caliberated by user)
Mean		Mean gray value (grey values of all pixes/no. of pixels)
StdDev		Mean gray value (grey values of all pixes/no. of pixels)
Mode		Most Frequently occuring grey value
Min		Minimum gray value
Max		Maximum grey value
X		Center of x coordinate
Y		Center of y coordinate
Perimeter	µm	Length of boundary of selected region
BX		X coordinate of upper left corner of rectangle
BY		Y coordinate of upper left corner of rectangle
Width	µm	Rectangle width
Height	µm	Rectangle height
Major	µm	Major axis of ellipse
Minor	µm	Minor axis of ellipse
Angle	Degree	Angle between primary axis and a line parallel
Circularity		4² area/perimeter²
Feret	µm	Longest diatance between any 2 points along the selected boundry
FeretX		Starting X coordiante of Feret's diameter
FeretY		Starting Y coordiante of Feret's diameter
Feret Angle	Degree	Angle between Feret diameter and a line parallel
MinFeret	µm	Minimum Feret Diameter
AR		Aspect ratio = major axis/minor axis
Round		Roundness = 4 area/² majoraxis² = inverse of AS
Solidity		area/convex area
IntDen		Integrated Density= Area*mean gray value
Median		The median value of the pixels in the image or
Skewness		The third order moment about the mean
Kurt		Kurtuosis- The fourth order moment about the mean
%Area	%	The percentage of pixels in the image or selection that havebeen highlighted in red
RawIntDen		Sum of the values of the pixels in the image selected
RawIntden		IntDen if image is uncalibrated
Slice		Current position in the stack

Table E.2: Example (run 2 canal water) of image data extracted from ImageJ-Fiji

	Area	Mean	StdDev	Min	Max	X	Y	XM	YM	Perim.	BX	BY	Width	Height	Major	Minor	Angle	Circ.	Feret	IntDen	Median	Skew	Kurt	%Area	RawIntDen	Slice	FeretX	FeretY	FeretAngle	MinFeret	AR	Round	Solidity
1	25.88	255	0	255	255	634.9	11.73	634.9	11.73	28.62	631.21	7.59	7.59	7.59	7.27	4.54	160.97	0.4	10	6598.8	255	NaN	NaN	100	5610	1	582	7	139.4	6.79	1.6	0.62	0.61
2	1.18	255	0	255	255	20.06	34.16	20.06	34.16	3.07	19.52	33.62	1.08	1.08	1.22	1.22	0	1	1.53	299.94	255	NaN	NaN	100	255	1	18	31	135	1.08	1	1	1
3	1.18	255	0	255	255	187.08	38.5	187.08	38.5	3.07	186.54	37.96	1.08	1.08	1.22	1.22	0	1	1.53	299.94	255	NaN	NaN	100	255	1	172	35	135	1.08	1	1	1
4	1.18	255	0	255	255	42.84	43.92	42.84	43.92	3.07	42.3	43.38	1.08	1.08	1.22	1.22	0	1	1.53	299.94	255	NaN	NaN	100	255	1	39	40	135	1.08	1	1	1
5	1.18	255	0	255	255	16.81	61.28	16.81	61.28	3.07	16.27	60.73	1.08	1.08	1.22	1.22	0	1	1.53	299.94	255	NaN	NaN	100	255	1	15	56	135	1.08	1	1	1
6	18.82	255	0	255	255	1429.6	89.88	1429.6	89.88	16.61	1426.2	87.85	6.51	4.34	5.78	4.15	167.55	0.86	6.6	4799.1	255	NaN	NaN	100	4080	1	1315	83	170.54	4.34	1.39	0.72	0.8
7	58.81	255	0	255	255	555.94	128.02	555.94	128.02	34.75	550.95	123.64	9.76	8.68	8.95	8.37	155.81	0.61	11.53	14997	255	NaN	NaN	100	12750	1	509	122	41.19	8.68	1.07	0.94	0.79
8	2.35	255	0	255	255	116.05	148.04	116.05	148.04	4.6	114.96	147.5	2.17	1.08	2.45	1.22	0	1	2.43	599.89	255	NaN	NaN	100	510	1	106	136	153.43	1.08	2	0.5	1
9	2.35	255	0	255	255	740.75	260.83	740.75	260.83	4.6	739.66	260.29	2.17	1.08	2.45	1.22	0	1	2.43	599.89	255	NaN	NaN	100	510	1	682	240	153.43	1.08	2	0.5	1
10	20	255	0	255	255	739.12	268.23	739.12	268.23	17.24	736.41	264.63	4.34	6.51	6.86	3.71	77.66	0.85	7.28	5099	255	NaN	NaN	100	4335	1	680	250	63.43	4.34	1.85	0.54	0.87
11	22.35	255	0	255	255	429.51	272.94	429.51	272.94	25.55	426.23	270.05	8.68	5.42	7.4	3.85	8.62	0.43	9.27	5698.9	255	NaN	NaN	100	4845	1	393	250	159.44	4.89	1.92	0.52	0.59
12	3.53	255	0	255	255	553.66	293.37	553.66	293.37	6.77	552.04	292.83	3.25	1.08	3.67	1.22	0	0.97	3.43	899.83	255	NaN	NaN	100	765	1	509	270	161.57	1.08	3	0.33	1
13	1.18	255	0	255	255	554.75	295.54	554.75	295.54	3.07	554.2	295	1.08	1.08	1.22	1.22	0	1	1.53	299.94	255	NaN	NaN	100	255	1	511	272	135	1.08	1	1	1
14	18.82	255	0	255	255	787.86	306.11	787.86	306.11	18.14	784.13	303.67	7.59	4.34	7.74	3.09	13.05	0.72	8.26	4799.1	255	NaN	NaN	100	4080	1	723	284	23.2	4.21	2.5	0.4	0.74
15	142.33	255	0	255	255	483.88	328.89	483.88	328.89	52.63	473.95	322.11	18.44	14.1	20.92	8.66	32.58	0.65	21.06	36293	255	NaN	NaN	100	30855	1	438	309	34.51	10.49	2.42	0.41	0.81
16	2.35	255	0	255	255	117.13	362.78	117.13	362.78	4.6	116.05	362.24	2.17	1.08	2.45	1.22	0	1	2.43	599.89	255	NaN	NaN	100	510	1	107	334	153.43	1.08	2	0.5	1
17	1.18	255	0	255	255	8.13	395.32	8.13	395.32	3.07	7.59	394.78	1.08	1.08	1.22	1.22	0	1	1.53	299.94	255	NaN	NaN	100	255	1	7	364	135	1.08	1	1	1
18	20	255	0	255	255	1377.6	400.42	1377.6	400.42	20.31	1373	398.03	8.68	4.34	7.98	3.19	12.32	0.61	8.94	5099	255	NaN	NaN	100	4335	1	1266	370	14.04	3.95	2.5	0.4	0.74
19	1.18	255	0	255	255	34.16	399.66	34.16	399.66	3.07	33.62	399.11	1.08	1.08	1.22	1.22	0	1	1.53	299.94	255	NaN	NaN	100	255	1	31	368	135	1.08	1	1	1
20	1.18	255	0	255	255	1383.3	399.66	1383.3	399.66	3.07	1382.8	399.11	1.08	1.08	1.22	1.22	0	1	1.53	299.94	255	NaN	NaN	100	255	1	1275	368	135	1.08	1	1	1
21	1.18	255	0	255	255	110.08	424.6	110.08	424.6	3.07	109.54	424.06	1.08	1.08	1.22	1.22	0	1	1.53	299.94	255	NaN	NaN	100	255	1	101	391	135	1.08	1	1	1
22	4.7	255	0	255	255	111.17	429.48	111.17	429.48	9.57	110.62	427.31	1.08	4.34	4.9	1.22	90	0.64	4.47	1199.8	255	NaN	NaN	100	1020	1	102	394	104.04	1.08	4	0.25	1
23	9.41	255	0	255	255	1142	449.68	1142	449.68	13.54	1139.9	447.92	5.42	3.25	5.03	2.38	7.55	0.64	5.84	2399.5	255	NaN	NaN	100	2040	1	1051	416	21.8	3.25	2.11	0.47	0.7
24	1.18	255	0	255	255	1146.9	448.46	1146.9	448.46	3.07	1146.4	447.92	1.08	1.08	1.22	1.22	0	1	1.53	299.94	255	NaN	NaN	100	255	1	1057	413	135	1.08	1	1	1
25	7.06	255	0	255	255	403.99	478.29	403.99	478.29	8.3	402.37	477.2	3.25	2.17	3.67	2.45	0	1	3.91	1799.7	255	NaN	NaN	100	1530	1	371	440	146.31	2.17	1.5	0.67	1
26	27.05	255	0	255	255	1682.8	495.43	1682.8	495.43	23.38	1678.9	491.3	7.59	7.59	7.83	4.4	143.81	0.62	9.33	6898.7	255	NaN	NaN	100	5865	1	1548	455	144.46	6.02	1.78	0.56	0.71
27	1.18	255	0	255	255	102.49	498.35	102.49	498.35	3.07	101.95	497.81	1.08	1.08	1.22	1.22	0	1	1.53	299.94	255	NaN	NaN	100	255	1	94	459	135	1.08	1	1	1
28	2.35	255	0	255	255	1141	534.14	1141	534.14	4.6	1139.9	533.6	2.17	1.08	2.45	1.22	0	1	2.43	599.89	255	NaN	NaN	100	510	1	1051	492	153.43	1.08	2	0.5	1
29	16.47	255	0	255	255	1146.5	536.54	1146.5	536.54	21.85	1143.1	533.6	6.51	7.59	7.9	2.65	127.87	0.43	9.33	4199.2	255	NaN	NaN	100	3570	1	1054	492	125.54	4.07	2.98	0.34	0.55
30	169.38	253.23	21.25	0	255	1143.6	545.97	1143.6	545.96	69.87	1134.4	536.85	20.61	19.52	25.3	8.52	140.31	0.44	26.94	42892	255	-11.87	139.01	99.31	36465	1	1046	496	139.9	11.66	2.97	0.34	0.73
31	5.88	255	0	255	255	1553.2	540.86	1553.2	540.86	9.84	1550.9	540.11	4.34	2.17	4.05	1.85	174.85	0.76	4.47	1499.7	255	NaN	NaN	100	1275	1	1430	498	165.96	2.17	2.19	0.46	0.77
32	2.35	255	0	255	255	208.78	543.36	208.78	543.36	5.24	208.23	542.27	1.08	2.17	2.45	1.22	90	1	2.43	599.89	255	NaN	NaN	100	510	1	192	500	116.57	1.08	2	0.5	1
33	4.7	255	0	255	255	342.45	546.88	342.45	546.88	8.3	340.55	545.53	3.25	2.17	3.46	1.73	18.43	0.86	3.91	1199.8	255	NaN	NaN	100	1020	1	314	505	33.69	2.17	2	0.5	0.8
34	41.17	255	0	255	255	1019	591.22	1019	591.22	24.91	1015.1	586.74	7.59	7.59	8.21	6.38	141.41	0.83	9.33	10498	255	NaN	NaN	100	8925	1	938	541	125.54	7.52	1.29	0.78	0.86
35	8.23	255	0	255	255	1339.8	621.21	1339.8	621.21	12.91	1337.3	619.28	4.34	4.34	4.43	2.37	133.09	0.62	5.42	2099.6	255	NaN	NaN	100	1785	1	1233	571	126.87	3.61	1.87	0.53	0.61
36	31.76	255	0	255	255	1331.5	623.88	1331.5	623.88	23.38	1326.4	621.45	9.76	5.42	9.65	4.19	166.69	0.73	10	8098.5	255	NaN	NaN	100	6885	1	1223	575	167.47	4.8	2.3	0.43	0.79
37	16.47	255	0	255	255	1632.8	669.71	1632.8	669.71	15.07	1630.1	668.08	5.42	4.34	5.27	3.98	0	0.91	5.84	4199.2	255	NaN	NaN	100	3570	1	1503	616	158.2	4.34	1.33	0.75	0.88
38	16.47	255	0	255	255	692.56	604.17	692.56	604.17	18.14	690.84	689.77	6.51	5.42	5.41	3.88	159.93	0.63	7.28	4199.2	255	NaN	NaN	100	3570	1	554	638	153.43	4.73	1.4	0.72	0.67
39	2.35	255	0	255	255	1395.8	744	1395.8	744	6.14	1394.7	742.92	2.17	2.17	2.82	1.06	135	0.79	3.07	599.89	255	NaN	NaN	100	510	1	1286	685	135	1.53	2.65	0.38	0.67
40	134.09	255	0	255	255	1263.2	781.22	1263.2	781.22	51.36	1254.8	774.37	16.27	15.18	17.77	9.61	140.82	0.64	20	34194	255	NaN	NaN	100	29070	1	1158	716	139.4	10.83	1.85	0.54	0.82
41	21.17	240.83	60.1	0	255	1687.3	787.08	1687.2	787.1	16.61	1684.3	785.21	6.51	4.34	6.32	4.27	177.12	0.96	6.86	5099	255	-3.88	13.06	94.44	4335	1	1553	724	161.57	4.34	1.48	0.68	0.88
42	1.18	255	0	255	255	55.85	824.8	55.85	824.8	3.07	55.31	824.26	1.08	1.08	1.22	1.22	0	1	1.53	299.94	255	NaN	NaN	100	255	1	51	760	135	1.08	1	1	1
43	1.18	255	0	255	255	48.26	841.07	48.26	841.07	3.07	47.72	840.53	1.08	1.08	1.22	1.22	0	1	1.53	299.94	255	NaN	NaN	100	255	1	44	775	135	1.08	1	1	1
44	1.18	255	0	255	255	242.4	885.53	242.4	885.53	3.07	241.85	884.99	1.08	1.08	1.22	1.22	0	1	1.53	299.94	255	NaN	NaN	100	255	1	223	816	135	1.08	1	1	1
45	1.18	255	0	255	255	9.22	910.48	9.22	910.48	3.07	8.68	909.94	1.08	1.08	1.22	1.22	0	1	1.53	299.94	255	NaN	NaN	100	255	1	8	839	135	1.08	1	1	1
46	383.46	238.57	62.7	0	255	303.77	917.65	304.18	917.54	82.36	288.49	909.94	31.45	15.18	32.66	14.95	177.96	0.71	32.12	91483	255	-3.55	10.59	93.56	77775	1	266	844	168.31	15.18	2.18	0.46	0.92
47	1.18	255	0	255	255	321.57	920.24	321.57	920.24	3.07	321.03	919.7	1.08	1.08	1.22	1.22	0	1	1.53	299.94	255	NaN	NaN	100	255	1	296	848	135	1.08	1	1	1
48	287	255	0	255	255	836.56	937.33	836.56	937.33	67.44	825.34	928.37	22.78	17.35	22.51	16.24	155.48	0.79	24.37	73186	255	NaN	NaN	100	62220	1	763	857	147.72	17.35	1.39	0.72	0.89
49	1.18	255	0	255	255	824.8	938.68	824.8	938.68	3.07	824.26	938.14	1.08	1.08	1.22	1.22	0	1	1.53	299.94	255	NaN	NaN	100	255	1	760	865	135	1.08	1	1	1
50	226.42	80.79	0	255	255	1038.1	949.26	1038.4	949.28	48.03	1031.4	942.47	14.1	13.01	15.03	11.56	144.04	0.74	16.27	30894	255	-2.46	4.05	88.79	26265	1	953	869	126.87	12.89	1.3	0.77	0.88
51	1.18	255	0	255	255	1037.4	957.11	1037.4	957.11	3.07	1036.8	956.57	1.08	1.08	1.22	1.22	0	1	1.53	299.94	255	NaN	NaN	100	255	1	956	882	135	1.08	1	1	1
52	29.41	255	0	255	255	1035.9	961.37	1035.9	961.37	22.48	1032.5	958.74	8.68	5.42	7.71	4.86	14.9	0.73	9.27	7498.6	255	NaN	NaN	100	6375	1	952	889	20.56	5.42	1.59	0.63	0.81
53	89.39	255	0	255	255	1175.5	963.88	1175.5	963.88	37.93	1169.1	959.83	14.1	8.68	14.66	7.76	179.86	0.78	15.11	22796	255	NaN	NaN	100	19380	1	1078	886	158.96	8.68	1.89	0.53	0.87
54	1.18	255	0	255	255	1167.7	969.7	1167.7	969.7	8.3	1165.9	968.5	3.25	2.17	3.41	2.2	18.43	1	3.91	1499.7	255	NaN	NaN	100	1275	1	1075	895	33.69	2.17	1.55	0.64	0.91
55	5.88	255	0	255	255	56.94	979.89	56.94	979.89	3.07	56.4	979.35	1.08	1.08	1.22	1.22	0	1	1.53	299.94	255	NaN	NaN	100	255	1	52	903	135	1.08	1	1	1
56	1.18	255	0	255	255	58.02	989.65	58.02	989.65	3.07	57.48	989.11	1.08	1.08	1.22	1.22	0	1	1.53	299.94	255	NaN	NaN	100	255	1	53	912	135	1.08	1	1	1
57	1.18	255	0	255	255	73.21	989.65	73.21	989.65	3.07	72.66	989.11	1.08	1.08	1.22	1.22	0	1	1.53	299.94	255	NaN	NaN	100	255	1	67	912	135	1.08	1	1	1
58	1.18	255	0	255	255	461	999	461	999	82.25	447.92	990.19	26.03	18.44	21.47	12	159.39	0.38	26.79	51590	255	NaN	NaN	100	43860	1	414	918	158.63	15.62	1.79	0.56	0.67
59	202.31	255	0	255	255																												

Appendix F

Table F.1: Detailed table showing E-coli removal calculations for drain water experiments.

Run	TSS Removal Efficency	Drainwater Colonies			Average	Volume for plating (ml)	Dilution factor	CFU/ml	Clean Colonies		Eff.	Average	Volume for plating (ml)	Dilution factor	CFU/ml	Cin/Cout	log reduction	Perc red
1	83%	8	9	8.5		0.01	10	8.50E+03	3	1		2	0.01	10	2.00E+03	4.25E+00	0.63	76.47
2	69%	27	68	47.5		0.01	10	4.75E+04	6	36		21	0.01	10	2.10E+04	2.26E+00	0.35	55.79
3	81%	4	9	6.5		1	1	6.50E+00	1	2		1.5	1	1	1.50E+00	4.33E+00	0.64	76.92
4	89%	10	7	8.5		1	1	8.50E+00	2	1		1.5	1	1	1.50E+00	5.67E+00	0.75	82.35
5	85%	9	12	10.5		1	1	1.05E+01	1	1		1	1	1	1.00E+00	1.05E+01	1.02	90.48
6	70%	45	150	97.5		1	1	9.75E+01	3	51		27	1	1	2.70E+01	3.61E+00	0.56	72.31
7	92%	5	7	6		1	1	6.00E+00	2	1		1.5	1	1	1.50E+00	4.00E+00	0.60	75.00
8	85%	5	5	5		1	1	5.00E+00	2	1		1.5	1	1	1.50E+00	3.33E+00	0.52	70.00
9	87%	3	3	3		1	1	3.00E+00	1	1		1	1	1	1.00E+00	3.00E+00	0.48	66.67
10	72%	188	172	180		0.1	10	1.80E+04	12	12		12	0.1	10	1.20E+03	1.50E+01	1.18	93.33
11	94%	63	68	65.5		1	1	6.55E+01	48	49		48.5	1	1	4.85E+01	1.35E+00	0.13	25.95
12	83%	10	30	20		0.1	10	2.00E+03	7	29		18	0.1	10	1.80E+03	1.11E+00	0.05	10.00
13	90%	16	16	16		0.1	10	1.60E+03	5	6		5.5	0.1	10	5.50E+02	2.91E+00	0.46	65.63
14	83%	368	336	352		0.1	10	3.52E+04	7	9		8	0.1	10	8.00E+02	4.40E+01	1.64	97.73
15	88%	324	260	292		0.1	10	2.92E+04	7	6		6.5	0.1	10	6.50E+02	4.49E+01	1.65	97.77

G

Appendix G

Table G.1: Example (drain water run 2) of calculation of TSS removal percentages. The formulas for background calculations is given in Chapter 2.

DAF SEPARATION - Drain Water							
					Total clean effluent (mL)	1860	
					Total canal water consume (mL)	2330	
Date	May 2019				Total concentrate (mL)	2160	
	amount	Unit			Total supernatant (foam) (mL)	0	
White water introduced	1.69	L	L		Total white water introduced (mL)	1690	
Canal Water	2.33	L	L				
Q ratio	42%						
HRT	13	min	minutes				
Original water volume	20		L				
TSS		filter+metal	Vol	After incub.	TSS		
		g	mL	g	g/L		
Effluent	1	0.15	800.00	0.15	0.01		
	2	0.14	800.00	0.16	0.01		
	3	0.00	0.00	0.00	#DIV/0!		
	Average	0.15	500.00	0.16	**0.01**		
	STD	0.00	0.016	0.00	**0.0053**	**48.21%**	
Concentrate	1	0.15	300.00	0.19	0.13		
	2	0.15	300.00	0.19	0.13		
	3	0.00	0.00	0.00	#DIV/0!		
	Average	0.15	200.00	0.19	0.13		
	STD	0.00	0.00	0.00	0.00	**1.10%**	
Canal Water	1	0.14	50.00	0.18	0.65		
	2	0.15	50.00	0.19	0.70		
	3	0.00	0.00	0.00	#DIV/0!		
	Average	0.15	500.00	0.18	**0.68**		
	STD	0.00	0.03	0.01	**0.03**	**5.02%**	
Supernatant	1	0.00	0.00	0.00	#DIV/0!		
	2	0.00	0.00	0.00	#DIV/0!		
	3	0.00	0.00	0.00	#DIV/0!		
	Average	0.00	200.00	0.00	**#DIV/0!**		
	STD	0.00	#DIV/0!	0.00	**#DIV/0!**	**#DIV/0!**	

Total TSS inlet (g)	1.57508			
Total TSS diluted (g/L)	0.065573689			
	TSS	STD	STD	Removal eff.
	g/L	g/L	%	%
Effluent	0.01	0.01	48.21%	83.22%
Concentrate	0.13	0.00	1.10%	-96.22%
Canal Water	0.68	0.03	5.02%	-
Supernatant	#DIV/0!	#DIV/0!	#DIV/0!	-

Appendix H

Please see next page for Table H.1 - Box diagram giving the boundary conditions to optimize significant parameters (time of coagulation, retention time and influent TSS concentration) for canal water experiments done.

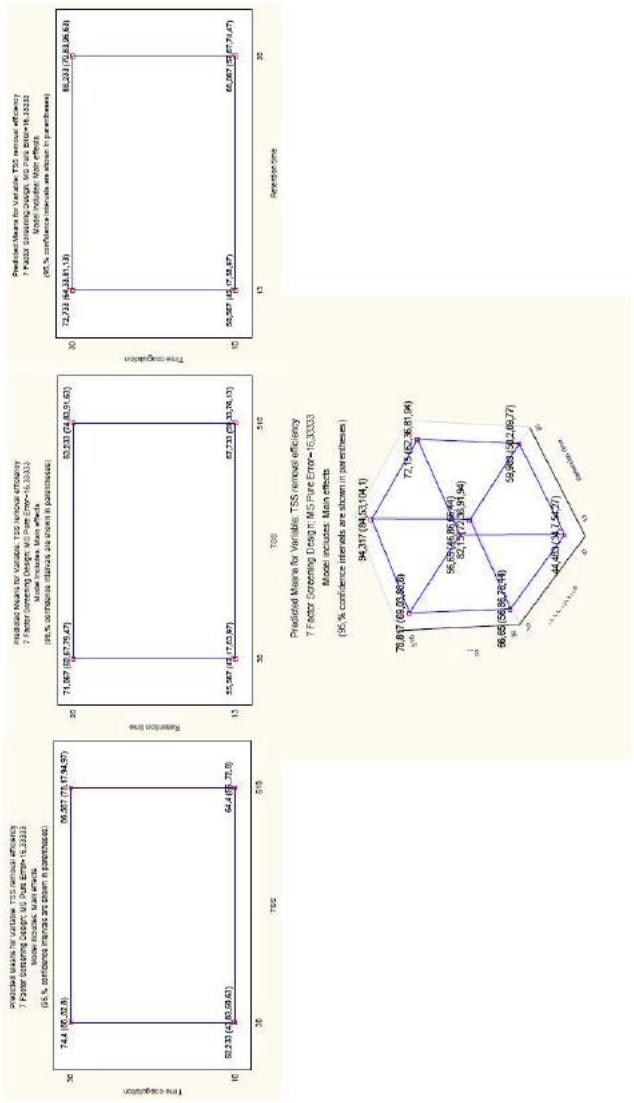

Figure H.1: Box diagram giving the boundary conditions to optimize significant parameters (time of coagulation, retention time and influent TSS concentration) for canal water experiments done.

Appendix I

Flotation techniques/devices	Bubble generation system	Bubble diameter (μm)	References
Electroflotation	Electrolysis of diluted aqueous solutions (H_2 and O_2 bubbles).	20–40[a]	Zabel (1992), Zouboulis et al. (1992a,b)
Gas aphrons	Mechanical agitation or gas aspiration nozzle with circulating surfactant solutions	10–100	Sebba (1962), Jauregi and Varley (1999)
CAF® (cavitation air flotation)	Mechanical agitation (high speed)	40[a]	www.hydrocal.com
Dissolved air flotation	Reduction in pressure of water supersaturated at high pressures	10–100 (40[a])	Edzwald (1995)
ASH (air sparged hydrocyclone), BAF (bubble accelerated flotation)	Centrifugal units with jacketed porous tube	200[a]	Beeby and Nicol (1993), Owen et al. (1999)
Jet flotation	Gas aspiration nozzle to draw air into recycled water in a downcomer	100–600	Jameson and Manlapig (1991), Clayton et al. (1991)
Microcel™ flotation	Injection of water/air mixture through static mixers	400[a]	Yoon and Luttrell (1994), Yoon et al. (1992)
Nozzle flotation	Gas aspiration nozzle to draw air into recycled water	400–800[a]	Bennett (1988)
Column flotation	Aeration of pulp with spargers (porous plate)	1000[a]	Finch and Dobby (1990)
Induced air flotation	Mechanical agitation	700–1500[a]	Bennett (1988)

[a] Mean bubble diameter.

Figure I.1: Methods found in literature to measure bubble size distribution.

Appendix J

Please see next pages for figures giving particle sizes and circularity for canal water and drain water samples, for influent and clean effluent.

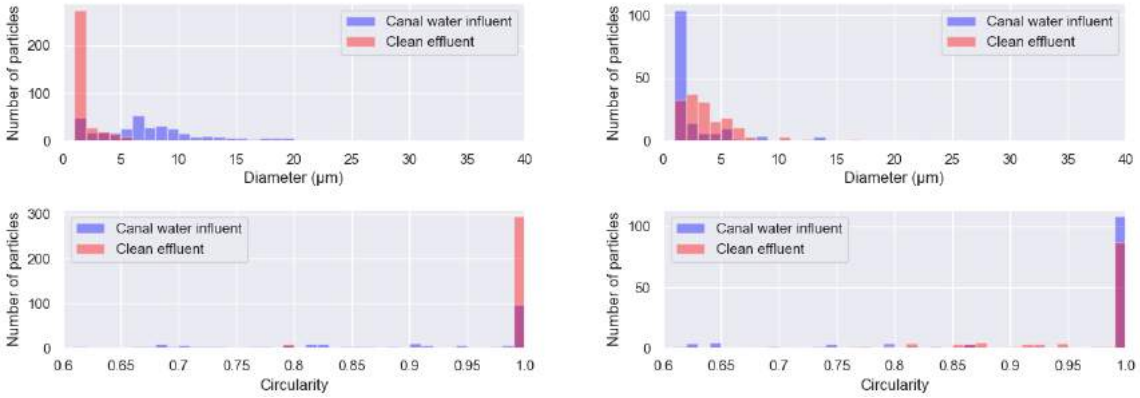

(a) (b)

Figure J.1: Particle diameter and circularity of canal water runs - 1, 2

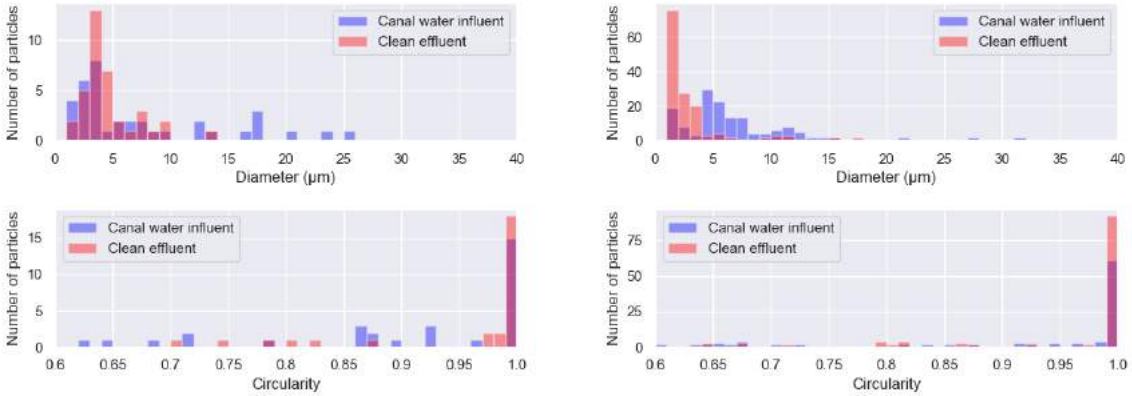

(a) (b)

Figure J.2: Particle diameter and circularity of canal water runs - 3,4

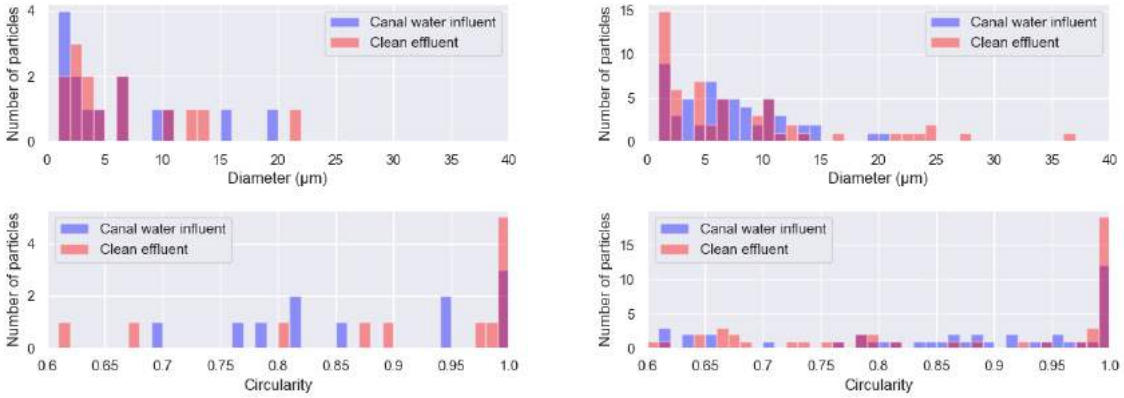

(a) (b)

Figure J.3: Particle diameter and circularity of canal water runs - 5, 6

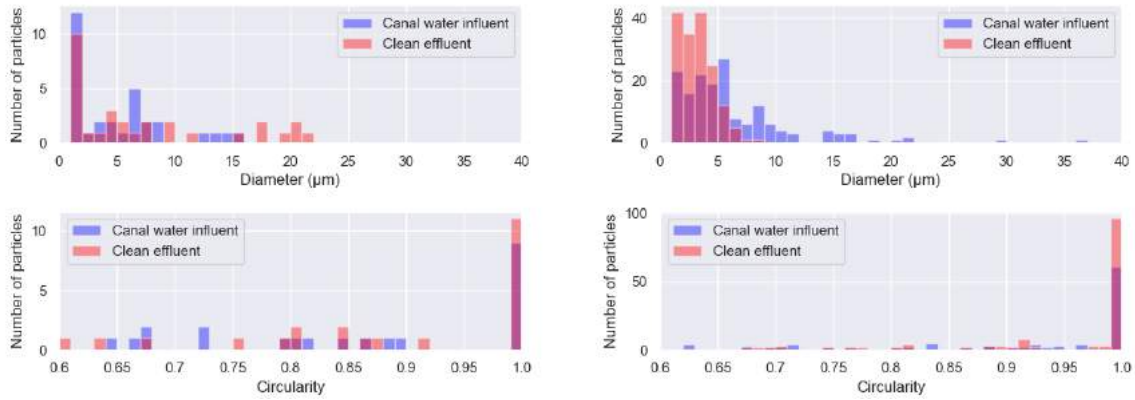

(a) (b)

Figure J.4: Particle diameter and circularity of canal water runs - 7, 8

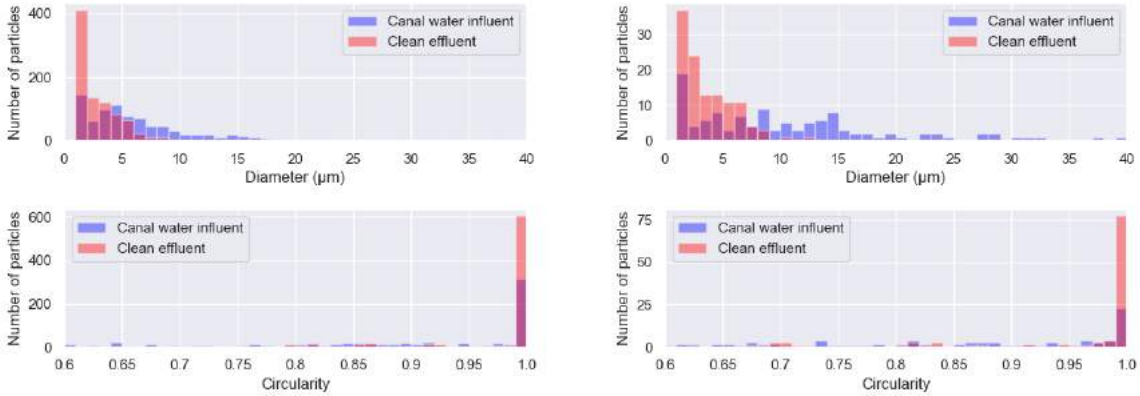

(a) (b)

Figure J.5: Particle diameter and circularity of canal water runs - 9, 10

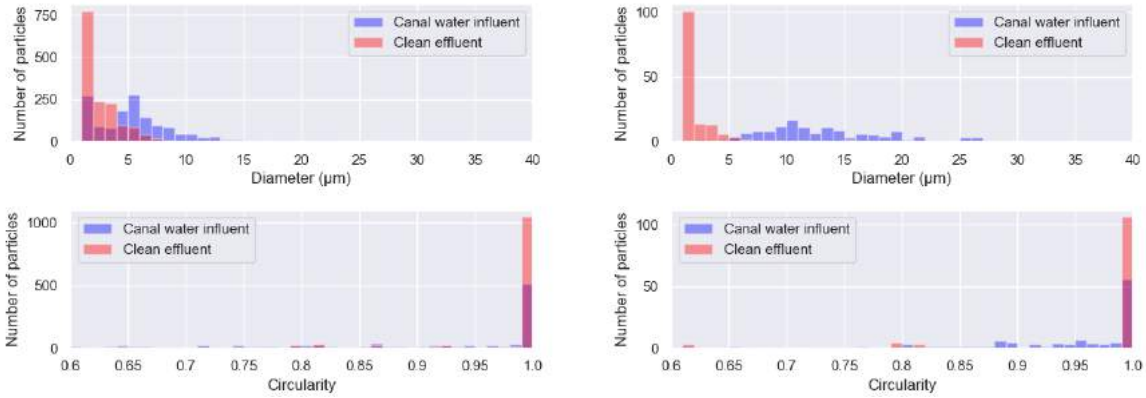

(a) (b)

Figure J.6: Particle diameter and circularity of canal water runs - 11, 12

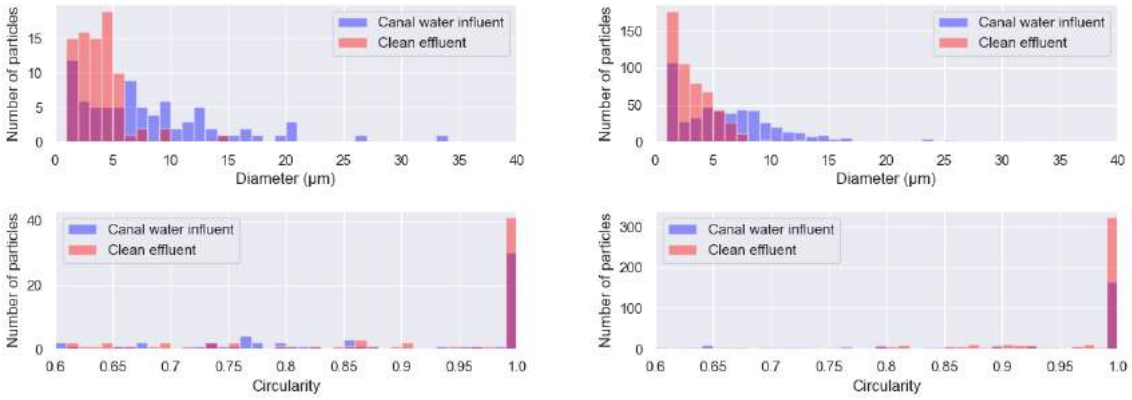

(a) (b)

Figure J.7: Particle diameter and circularity of canal water runs - 13, 14

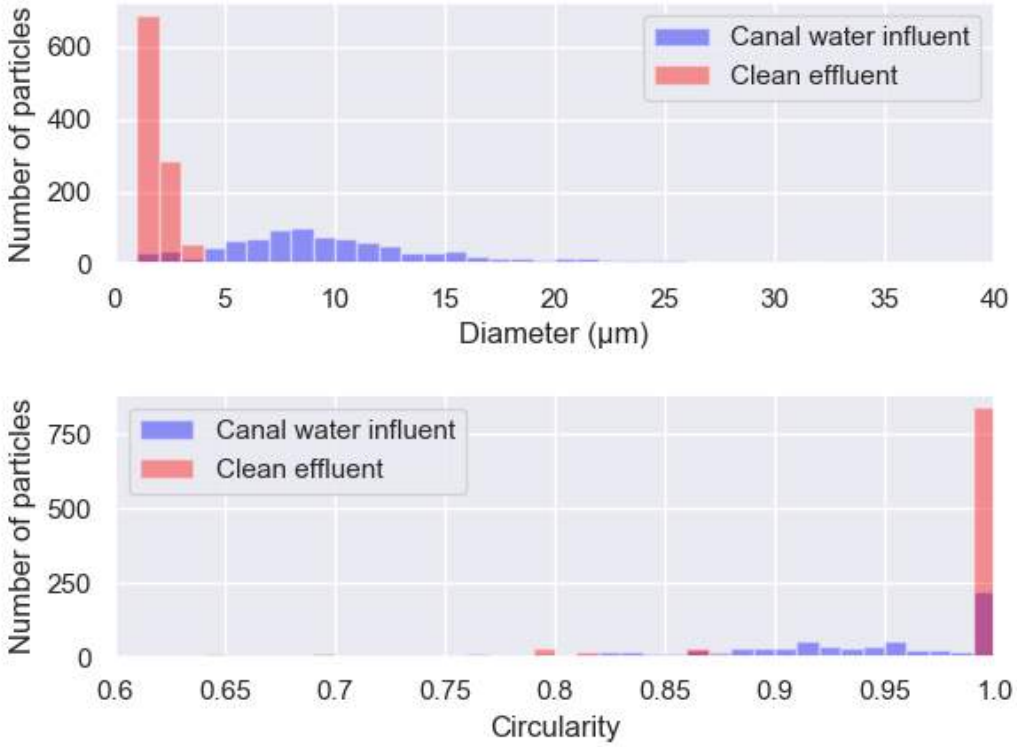

Figure J.8: Particle diameter and circularity of canal water runs - 15.

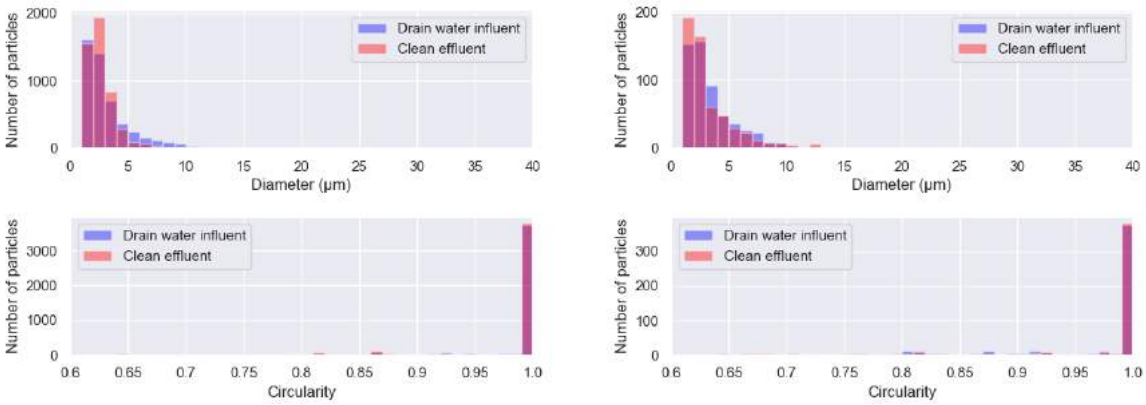

(a) (b)

Figure J.9: Particle diameter and circularity of drain water runs - 2, 3

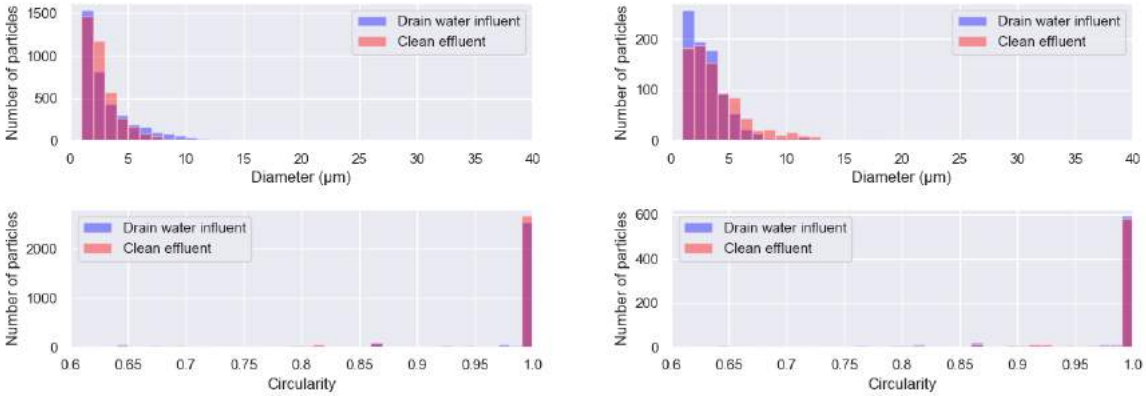

(a) (b)

Figure J.10: Particle diameter and circularity of drain water runs - 5, 6

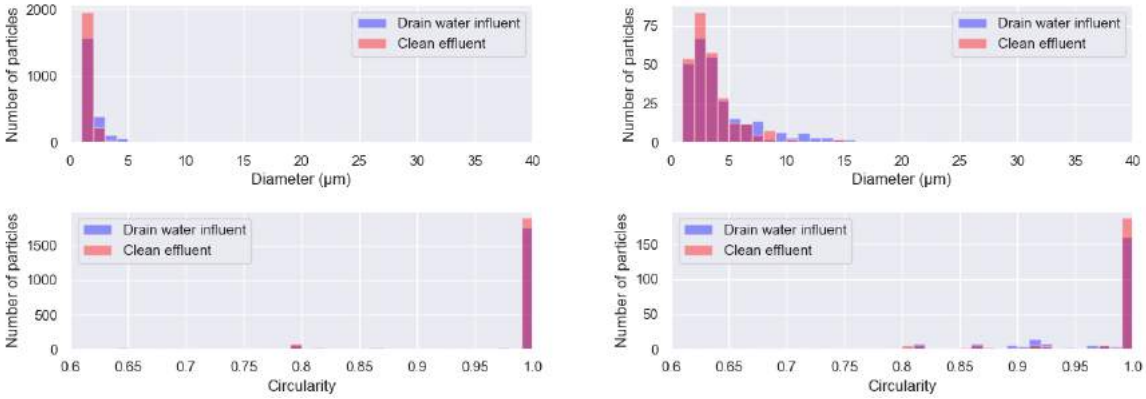

(a) (b)

Figure J.11: Particle diameter and circularity of drain water runs - 7, 8

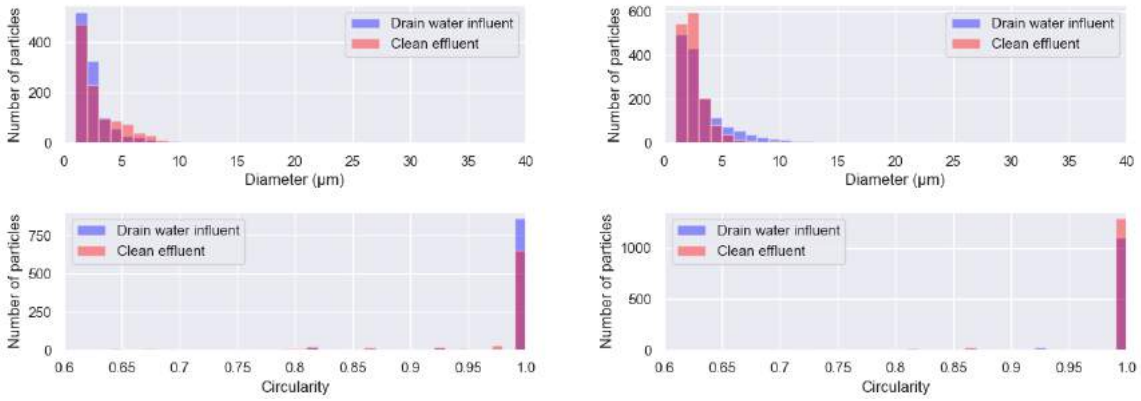

(a) (b)

Figure J.12: Particle diameter and circularity of drain water runs - 9, 10

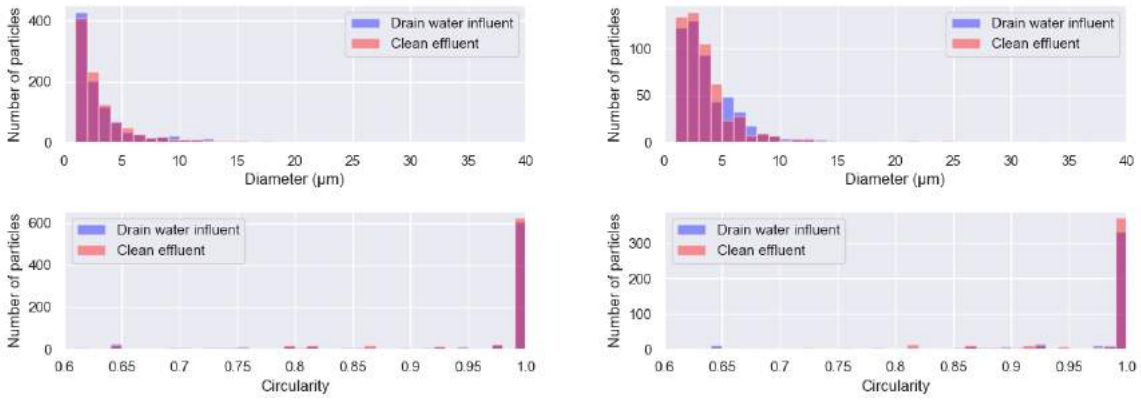

(a) (b)

Figure J.13: Particle diameter and circularity of drain water runs - 14, 15

K

Appendix K

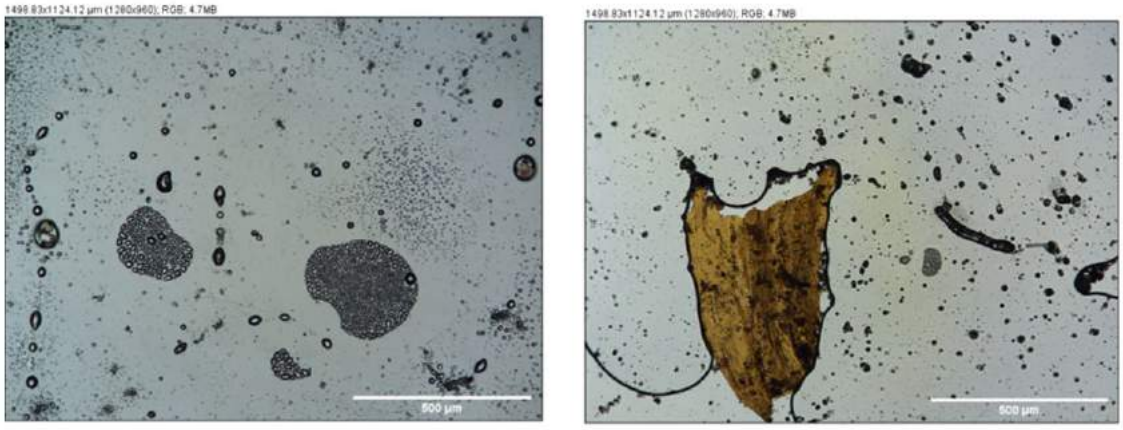

Figure K.1: Particle size anomaly images of drain water captures by the digital microscope.

Appendix L

Sludge-bubble rise velocity is calculates as follows:

$$D_b = \sqrt{\frac{(0.002219(m/s)x10^8 x0.007978(g/cm.s)x18x100}{(0.996(g/cm^3) - 0.00117(g/cm^3))x981(m/s^2)}} = 57.14\mu m \quad \text{(L.1)}$$

The diameter of air bubbles is the same at 57.14 µm.

$$V_p = \frac{((5x10^{-4})^2(\mu m)x(1.02(g/cm^3) - 0.996(g/cm^3))x981(m/s)x}{18x0.007978((g/cm.s)x100)}] = 1.02E10^{-}7m/s \quad \text{(L.2)}$$

Settling velocity of the sludge particles comes out to be be around 5.90E-05 m/s

$$V_{pbb} = V_p + V_{bb} = \frac{\pi}{6}(D_p^3 + D_{bb}^3) = \frac{\pi}{6}(80^3 + 60^3) = 381180m^3 \quad \text{(L.3)}$$

Particle-bubble agglomerate velocity comes out to be be around 381180 m3 . Based on this the spherical particle-bubble floc diameter can be calculated as follows (Benjamin, 2013):

$$D_{pbb} = (\frac{6V_{pbb}}{\pi})^{1/3} = (\frac{6381180}{\pi})^{1/3} = 90m \quad \text{(L.4)}$$

Now, the density of the particle-bubble floc is given as follows (Benjamin, 2013):

$$\rho_{pbb}\frac{\rho_p V_p + \rho_{bb} V_{bb}}{V_{pbb}} = \frac{(1.02x(\pi/6)(80\mu m)^3) + 0.00117(\pi/6)x60(\mu m)^3}{381180\mu m^3)} = 0.7177g/cm^3 \quad \text{(L.5)}$$

This the theoretical density of the particle-bubble floc. Assuming the floc is a spherical particle the rise velocity of the particle-bubble floc can be calculated by Stokes' law (equation 2.9) as follows:

$$V_{rise} = -\frac{(0.996 - 0.0017)(g/cm^3)x981x((cm/s^2)x(90x10^{-4}cm)^2}{18x0.007978(g/cms)x100} = -1.53E-03m/s \quad \text{(L.6)}$$

M

Appendix M

(a)

(b)

Figure M.1: Staring this thesis work began with the annual LOTUS progress meeting (October 2018) in India. Followed by a nice trip to the see the Taj Mahal and the Yamuna River.

(a) (b)

Figure M.2: Beginning phase of the DAF laboratory experiments.The starting of many DAF experiments.

(a) (b)

Figure M.3: Post Lab experiments at TU Delft, reaching the LOTUS site at the Barapullah drain with the DAF equipment.

(a) (b)

Figure M.4: Setting up DAF column at the site. It worked. Phew! Procuring a functioning air compressor was a challenge.

(a) (b)

Figure M.5: Conducting the DAF experiments and finding creative ways to take measurements.

(a)

(b)

Figure M.6: Pipe which pumped the drain water to be used for the experiments and finding new places to take samples at the site lab.

(a)

(b)

Figure M.7: Analysis of the DAF runs in the TERI Lab.

(a)

(b)

Figure M.8: Conducting experiments with anaerobic sludge at the site and PIV experiments. The PIV experiments with just a smart phone were quite challenging however, the final results were promising.

(a)

(b)

Figure M.9: Pathogen experiments conducted at the Site and Lab.

(a) (b)

Figure M.10: Final days at the site. Posters explaining the DAF working near the set up (in English and Hindi).

Bibliography

[1] Adams, C. E., Ford, D. L., and Eckenfelder, W. W. (1981). Development of design and operational criteria for wastewater treatment. In *Development of design and operational criteria for wastewater treatment*. Enviro Press.

[2] Adams, J. (1974). Air flotation. *IAWPR Advanced Study Institute, Birmingham, England*.

[3] Amita Bhaduri (2016). https://www.indiawaterportal.org/articles/once-drain-now-sewer/ on 26th August 2019.

[4] Andreoli, F. C. and Sabogal-Paz, L. P. (2019). Coagulation, flocculation, dissolved air flotation and filtration in the removal of giardia spp. and cryptosporidium spp. from water supply. *Environmental technology*, 40(5):654–663.

[5] Antony, J. (2014). *Design of experiments for engineers and scientists*. Elsevier.

[6] APhA, A. (1998). Wef (american public health association, american water works association, and water environment federation). 1998. *Standard methods for the examination of water and wastewater*, 19.

[7] Ata, S. and Jameson, G. J. (2005). The formation of bubble clusters in flotation cells. *International Journal of Mineral Processing*, 76(1-2):123–139.

[8] Baldursson, S. and Karanis, P. (2011). Waterborne transmission of protozoan parasites: review of worldwide outbreaks–an update 2004–2010. *Water research*, 45(20):6603–6614.

[9] Benjamin, L. (2013). *Water quality engineering : physical/chemical treatment processes*. Hoboken, New Jersey : Wiley.

[10] Biesinger, M., Vining, I., and Shell, G. (1974). Industrial experience with dissolved-air flotation. In *Proc. Ind. Waste Conf.;(United States)*, number CONF-7405111-.

[11] Bonatti, T. R. and Franco, R. M. B. (2016). Real scale environmental monitoring of zoonotic protozoa and helminth eggs in biosolid samples in brazil. *Journal of Parasitic Diseases*, 40(3):633–642.

[12] Bondelind, M., Sasic, S., and Bergdahl, L. (2013). A model to estimate the size of aggregates formed in a dissolved air flotation unit. *Applied Mathematical Modelling*, 37(5):3036–3047.

[13] Bratby, J. and Marais, G. (1975). Saturator performance in dissolved-air (pressure) flotation. *Water Research*, 9(11):929–936.

[14] Briancesco, R. and Bonadonna, L. (2005). An italian study on cryptosporidium and giardia in wastewater, fresh water and treated water. *Environmental Monitoring and Assessment*, 104(1-3):445–457.

[15] Cherian, D. (2004). *Pairing mega events and hydrological systems for urban sustainability: strategy framework for Delhi beyond the Commonwealth Games 2010*. PhD thesis, Massachusetts Institute of Technology.

[16] Chesworth, W. (2007). *Encyclopedia of soil science*. Springer Science & Business Media.

[17] CHROMagar (2009). CHROMagar C.perfringens Instructiond for use, Retrieved from http://www.chromagar.com/food-water-chromagar-c-perfringens–82.html.XW0TpSgzY2w on 27th June 2019.

[18] Coster, M. and Chermant, J.-L. (2001). Image analysis and mathematical morphology for civil engineering materials. *Cement and Concrete Composites*, 23(2-3):133–151.

[19] Dai, X., Boll, J., Hayes, M., and Aston, D. (2004). Adhesion of cryptosporidium parvum and giardia lamblia to solid surfaces: the role of surface charge and hydrophobicity. *Colloids and Surfaces B: Biointerfaces*, 34(4):259–263.

[20] De Nardi, I., Del Nery, V., Amorim, A., Dos Santos, N., and Chimenes, F. (2011). Performances of sbr, chemical–daf and uv disinfection for poultry slaughterhouse wastewater reclamation. *Desalination*, 269(1-3):184–189.

[21] De Renzo, D. J. (1981). *Pollution control technology for industrial wastewater*. Noyes Data Corporation.

[22] De Rijk, S. E., den Blanken, J. G., et al. (1994). Bubble size in flotation thickening. *Water Research*, 28(2):465–473.

[23] Dejaegher, B. and Vander, Y. (2009). The use of experimental design in separation science. *Acta Chromatographica*, 21(2):161–201.

[24] Del Vecchio, R. (1997). Understanding design of experiments: a primer for technologists. hanser.

[25] Eckenfelder, W. W. and O'Connor, D. J. (2013). *Biological waste treatment*. Elsevier.

[26] Economic Times (2017). 10 crore people drinking contaminated water in India, Retrieved from https://economictimes.indiatimes.com/news/politics-and-nation/10-crore-people-drinking-contaminated-water-in-india/articleshow/62191841.cms?from=mdr on 30th June 2019.

[27] Edzwald, J. K. (1995). Principles and applications of dissolved air flotation. *Water Science and Technology*, 31(3-4):1–23.

[28] Edzwald, J. K. (2010). Dissolved air flotation and me. *Water research*, 44(7):2077–2106.

[29] Edzwald, J. K., Tobiason, J. E., Parento, L. M., Kelley, M. B., Kaminski, G. S., Dunn, H. J., and Galant, P. B. (2000). Giardia and cryptosporidium removals by clarification and filtration under challenge conditions. *Journal-American Water Works Association*, 92(12):70–84.

[30] EMD Millipore Corporation (2019). Technical Data Sheet Chromocult Coliform Agar acc. ISO 9308-1, Retrieved from https://www.emdmillipore.com/Web-US-Site/en$_C A$/ − /USD/$ShowDocument-File$?$ProductSKU = MDA_C HEM-110426 DocumentId =$ 201602.248.$ProNetDocumentType = DSLanguage = ENCountry = NFOrigin = PDPon27thJune$2019.

[31] Ferreira, T. and Rasb, W. (2012). Imagej user guide: Ij 1.46 r.

[32] Franzen, A., Skogan, V., and Grutsch, J. (1972). Tertiary treatment of process water. *CHEMICAL ENGINEERING PROGRESS, VOL 68, NO 8, P 65-72, 1972. 7 FIG, 9 TAB, 5 REF.*

[33] Fukushi, K.-i., Matsui, Y., and Tambo, N. (1998). Dissolved air flotation: experiments and kinetic analysis. *Journal of Water Supply: Research and Technology-Aqua*, 47(2):76–86.

[34] Gehr, R. and Henry, J. G. (1983). Polymer dosage control in dissolved air flotation. *Journal of Environmental Engineering*, 109(2):448–465.

[35] Gelinas, S. and Finch, J. (2005). Colorimetric determination of common industrial frothers. *Minerals engineering*, 18(2):263–266.

[36] Gregory, J. (2005). *Particles in water: properties and processes*. CRC Press.

[37] Hague, J., Ta, C., Biggs, M., and Sattary, J. (2001). Small scale model for cfd validation in daf application. *Water science and technology*, 43(8):167–173.

[38] Hall, T., Pressdee, J., Gregory, R., and Murray, K. (1995). Cryptosporidium removal during water treatment using dissolved air flotation. *Water Science and Technology*, 31(3-4):125–135.

[39] Hammer, M. J. (1986). Water and wastewater technology.

[40] Han, M., Park, Y., Lee, J., and Shim, J. (2002). Effect of pressure on bubble size in dissolved air flotation. *Water Science and Technology: Water Supply*, 2(5-6):41–46.

[41] Henry, W. (1803). Iii. experiments on the quantity of gases absorbed by water, at different temperatures, and under different pressures. *Philosophical Transactions of the Royal Society of London*, (93):29–274.

[42] Honkanen, M., Eloranta, H., and Saarenrinne, P. (2010). Digital imaging measurement of dense multiphase flows in industrial processes. *Flow Measurement and Instrumentation*, 21(1):25–32.

[43] Huisman, P., Cramer, W., Van Ee, G., Hooghart, J., Salz, H., and Zuidema, F. (1998). *Water in the Netherlands*. Netherlands Hydrological Society.

[44] Jafarinejad, S. (2017). Activated sludge combined with powdered activated carbon (pact process) for the petroleum industry wastewater treatment: A review. *Chem. Int*, 3:268–277.

[45] Katz, W. J. et al. (1960). Dissolved-air flotation as applied to the treatment of oil-production water and of refinery wastes. In *Drilling and Production Practice*. American Petroleum Institute.

[46] Katz, W. J. and Geinopolos, A. (1967). Sludge thickening by dissolved-air flotation. *Journal (Water Pollution Control Federation)*, pages 946–957.

[47] Khan, M. B., Lee, X. Y., Nisar, H., Ng, C. A., Yeap, K. H., and Malik, A. S. (2015). Digital image processing and analysis for activated sludge wastewater treatment. In *Signal and image analysis for biomedical and life sciences*, pages 227–248. Springer.

[48] Kitchener, J. (1984). The froth flotation process: past, present and future-in brief. In *The Scientific Basis of Flotation*, pages 3–51. Springer.

[49] Kiuri, H. (2001). Development of dissolved air flotation technology from the first generation to the newest (third) one (daf in turbulent flow conditions). *Water Science and Technology*, 43(8):1–7.

[50] Koh, W., Clode, P. L., Monis, P., and Thompson, R. A. (2013). Multiplication of the waterborne pathogen cryptosporidium parvum in an aquatic biofilm system. *Parasites & vectors*, 6(1):270.

[51] Koivunen, J. and Heinonen-Tanski, H. (2008). Dissolved air flotation (daf) for primary and tertiary treatment of municipal wastewaters. *Environmental technology*, 29(1):101–109.

[52] Korich, D., Mead, J., Madore, M., Sinclair, N., and Sterling, C. R. (1990). Effects of ozone, chlorine dioxide, chlorine, and monochloramine on cryptosporidium parvum oocyst viability. *Appl. Environ. Microbiol.*, 56(5):1423–1428.

[53] Krofta, M. and Wang, L. K. (1982). Tertiary treatment of secondary effluent by dissolved air flotation and filtration (sandfloat) system. *Technical report/Lenox Institute of Research (USA)*.

[54] Kwak, D.-H., Jung, H.-J., Kwon, S.-B., Lee, E.-J., Won, C.-H., Lee, J.-W., and Yoo, S.-J. (2009). Rise velocity verification of bubble-floc agglomerates using population balance in the daf process. *Journal of Water Supply: Research and Technology-AQUA*, 58(2):85–94.

[55] Lawler, D. F. (1997). Particle size distributions in treatment processes: theory and practice. *Water Science and Technology*, 36(4):15–23.

[56] Leppinen, D. and Dalziel, S. (2004). Bubble size distribution in dissolved air flotation tanks. *Journal of Water Supply: Research and Technology-AQUA*, 53(8):531–543.

[57] livemint (2019). Which Indian city will run out of water first?, Retrieved from https://www.livemint.com/news/india/which-indian-city-will-run-out-of-water-first-1564920315004.html on 18th September 2019.

[58] Ljunggren, M., Jönsson, L., and la Cour Jansen, J. (2004). Particle visualisation-a tool for determination of rise velocities. *Water science and technology*, 50(12):229–236.

[59] LOTUSHR (2018). LOTUSHR: THE HOLISTIC WATER MANAGEMENT APPROACH, Retrieved from https://lotushr.org/ on 2nd July 2019.

[60] Lundh, M. (2002). *Effects of flow structure on particle separation in dissolved air flotation*. Lund University.

[61] Mahmoudi, M.-R., Ongerth, J. E., and Karanis, P. (2017). Cryptosporidium and cryptosporidiosis: the asian perspective. *International journal of hygiene and environmental health*, 220(7):1098–1109.

[62] Massaldi, H. A., Newman, J., and King, C. J. (1975). Maximum droplet growth when cooling a saturated solution. *Chemical Engineering Science*, 30(5-6):563–566.

[63] McDonald et al. (2014). Water on an urban planet: Urbanization and the reach of urban water infrastructure.

[64] Medema, G., Schets, F., Teunis, P., and Havelaar, A. (1998). Sedimentation of free and attachedcryptosporidium oocysts and giardia cysts in water. *Appl. Environ. Microbiol.*, 64(11):4460–4466.

[65] Mellgren, O. and Shergold, H. (1966). Method for recovering ultrafine mineral particles by extraction with an organic phase. *Trans. Inst. Min. Metall*, 75:C267–C269.

[66] Melo, M., de APereira, O., and de Jesus, R. (2006). Advances in non-conventional flotation for oily water treatment. *FILTRATION-COALVILLE-*, 6(1):31.

[67] Moursy, A. S. and El-Ela, S. E. A. (1982). Treatment of oily refinery wastes using a dissolved air flotation process. *Environment International*, 7(4):267–270.

[68] NDTV (2019). As Chennai Runs Out Of Water, 9 Million Pray For Rain, Retrieved from https://www.ndtv.com/india-news/as-chennai-runs-out-of-water-9-million-pray-for-rain-foreign-media-2060805 on 30th June 2019.

[69] New York Times (2018). Dangerously Low on Water, Cape Town Now Faces 'Day Zero', Retrieved from https://www.nytimes.com/2018/01/30/world/africa/cape-town-day-zero.html on 30th June 2019.

[70] New York Times (2019). A Quarter of Humanity Faces Looming Water Crises, Retrieved from https://www.nytimes.com/interactive/2019/08/06/climate/world-water-stress.html on 18th September 2019.

[71] NIST (2019). What is experimental design retrieved from https://www.itl.nist.gov/div898/handbook/pri/section1/pri11.htm on 7th september 2019.

[72] NITIAayog (2018). Composite water management index.

[73] NURI (2018). Barapullah Nallah,Nizamuddin Urban Renewal Initiative, Aga Khan Development Network Retrieved from http://www.nizamuddin renewal.org/waste-sanitation/barapullahnallah-development.php on 6nd July 2019.

[74] Ødegaard, H. (2001). The use of dissolved air flotation in municipal wastewater treatment. *Water Science and Technology*, 43(8):75–81.

[75] Pearson, S. (1976). Factors influencing oil removal efficiency in dissolved air flotation units. In *Proceedings of 4th annual industrial pollution conference, WWEMA, Philadelphia, PA*.

[76] Pinto Filho, A. and Brandão, C. (2001). Evaluation of flocculation and dissolved air flotation as an advanced wastewater treatment. *Water science and technology*, 43(8):83–90.

[77] Plummer, J. D., Edzwald, J. K., and Kelley, M. B. (1995). Removing cryptosporidium by dissolved-air flotation. *Journal-American Water Works Association*, 87(9):85–95.

[78] Ramirez, E. (1979). Comparative physicochemical study of industrial waste-water treatment by electrolytic dispersed air and dissolved air flotation technologies. In *Proceedings of Purdue industrial waste conference*, volume 34, page 699.

[79] Rezakazemi, M., Khajeh, A., and Mesbah, M. (2018). Membrane filtration of wastewater from gas and oil production. *Environmental chemistry letters*, 16(2):367–388.

[80] Rodrigues, R. and Rubio, J. (2003). New basis for measuring the size distribution of bubbles. *Minerals Engineering*, 16(8):757–765.

[81] Rodrigues, R. T. and Rubio, J. (2007). Daf–dissolved air flotation: Potential applications in the mining and mineral processing industry. *International Journal of Mineral Processing*, 82(1):1–13.

[82] Rohlich, G. A. (1954). Application of air flotation to refinery waste waters. *Industrial & Engineering Chemistry*, 46(2):304–308.

[83] Roy, R. K. (2001). *Design of experiments using the Taguchi approach: 16 steps to product and process improvement*. John Wiley & Sons.

[84] Rubio, J., Souza, M., and Smith, R. (2002). Overview of flotation as a wastewater treatment technique. *Minerals engineering*, 15(3):139–155.

[85] Sahu, P. K., Ramisetti, N. R., Cecchi, T., Swain, S., Patro, C. S., and Panda, J. (2018). An overview of experimental designs in hplc method development and validation. *Journal of pharmaceutical and biomedical analysis*, 147:590–611.

[86] Santos, P. R. d. and Daniel, L. A. (2017a). Dissolved air flotation as a potential treatment process to remove giardia cysts from anaerobically treated sewage. *Environmental technology*, 38(19):2392–2399.

[87] Santos, P. R. d. and Daniel, L. A. (2017b). Occurrence and removal of giardia spp. cysts and cryptosporidium spp. oocysts from a municipal wastewater treatment plant in brazil. *Environmental technology*, 38(10):1245–1254.

[88] Sato, Y., Murakami, Y., Hirose, T., Yamamoto, H., and Uryu, Y. (1979). Removal of emulsified oil particles by dissolved air flotation. *Journal of chemical engineering of Japan*, 12(6):454–459.

[89] Schügerl, K. (2000). Recovery of proteins and microorganisms from cultivation media by foam flotation. In *New Products and New Areas of Bioprocess Engineering*, pages 191–233. Springer.

[90] Shammas, N. K. (2005). Coagulation and flocculation. In *Physicochemical treatment processes*, pages 103–139. Springer.

[91] Shammas, N. K. (2010). Flotation–filtration system for wastewater reuse. In *Flotation Technology*, pages 347–362. Springer.

[92] Shammas, N. K. and Bennett, G. F. (2010). Principles of air flotation technology. In *Flotation Technology*, pages 1–47. Springer.

[93] Shammas, N. K., Wang, L. K., and Hahn, H. H. (2010). Fundamentals of wastewater flotation. In *Flotation Technology*, pages 121–164. Springer.

[94] Shannon, W. and Buisson, D. (1980). Dissolved air flotation in hot water. *Water Research*, 14(7):759–765.

[95] SMITH, R. W. (1989). Flotation of algae, bacteria and other microorganisms. *Mineral Procesing and Extractive Metallurgy Review*, 4(3-4):277–299.

[96] Stumm, W. and O'Melia, C. R. (1968). Stoichiometry of coagulation. *Journal-American Water Works Association*, 60(5):514–539.

[97] T K Gadhok (2014). Risks in Delhi: Environmental concerns, Retrieved from https://www.geospatialworld.net/article/risks-in-delhi-environmental-concerns/.

[98] Tchobanoglous, G., Burton, F. L., Stensel, H. D., et al. (2005). *Metcalf & Eddy wastewater engineering: treatment and reuse*. International Edition. McGrawHill.

[99] Thielicke, W. (2014). *The flapping flight of birds: Analysis and application*. University of Groningen.

[100] Tsai, J.-C., Kumar, M., Chen, S.-Y., and Lin, J.-G. (2007). Nano-bubble flotation technology with coagulation process for the cost-effective treatment of chemical mechanical polishing wastewater. *Separation and Purification Technology*, 58(1):61–67.

[101] USGC (2016). United States Geological Survey (USGC) water science school, Retrieved from https://water.usgs.gov/edu/qa-chemical-cloudy.htmll.

[102] Vigneswaran, S. (2009). *Waste Water Treatment Technologies-Volume I*. EOLSS Publications.

[103] Vlyssides, A. G., Mai, S. T., and Barampouti, E. M. P. (2004). Bubble size distribution formed by depressurizing air-saturated water. *Industrial & engineering chemistry research*, 43(11):2775–2780.

[104] Vrablik, E. (1960). Fundamental principles of dissolved-air flotation of industrial wastes. In *Proceedings of the 14th Purdure Industrial Wastes Conference*.

[105] Wang, L. K. (2006). Adsorptive bubble separation and dispersed air flotation. In *Advanced physicochemical treatment processes*, pages 81–122. Springer.

[106] Wang, L. K., Fahey, E. M., and Wu, Z. (2005). Dissolved air flotation. In *Physicochemical treatment processes*, pages 431–500. Springer.

[107] Wang, L. K., Shammas, N. K., Selke, W. A., and Aulenbach, D. B. (2007). Flotation thickening. In *Biosolids Treatment Processes*, pages 71–100. Springer.

[108] Wiesner, M. R. and Mazounie, P. (1989). Raw water characteristics and the selection of treatment configurations for particle removal. *Journal-American Water Works Association*, 81(5):80–89.

[109] Wikipedia contributors (2019). Calcium hydroxide — Wikipedia, the free encyclopedia. [Online; accessed 24-October-2019].

[110] Woodward, F., Hall, M. W., Sproul, O. J., and Ghosh, M. M. (1977). New concepts in treatment of poultry processing wastes. *Water Res*, 11:873.

[111] WorldBank (2018). Water scarce cities: Thriving in a finite world.

[112] WWAP (2012). Global physical and economic water scarcity, world water development report 4. world water assessment programme (wwap).

[113] WWAP (2019). The united nations world water development report 2019: Leaving no one behind.